CHARLES UNIVERSITY IN PRAGUE

Study programme: Organic chemistry

Ing. Gábor Benkovics

SELECTIVELY SUBSTITUTED CYCLODEXTRINS FOR ANALYTICAL AND PHARMACEUTICAL APPLICATIONS

Ph.D. thesis

Supervisors: doc. RNDr. Jindřich Jindřich, CSc.; Éva Fenyvesi, Ph.D.

Consultant: Milo Malanga, Ph.D.

Prague 2017

Statement:

I declare, that I worked up this PhD thesis individually, under the supervision of doc. RNDr. Jindřich Jindřich, CSc., and that all the literature sources have been cited properly. I am aware of the fact, that potential use of the results published in this work, outside of the Charles University in Prague, is possible only with the official permission of the University. Neither this work, nor any of its substantial parts have ever been used for acquiring of another academic degree.

In Prague, 1. 10. 2017.

Prohlášení:

Prohlašuji, že jsem závěrečnou práci zpracoval samostatně, a že jsem uvedl všechny použité informační zdroje a literaturu. Tato práce ani její podstatná část nebyla předložena k získání jiného nebo stejného akademického titulu.

V Praze, 1. 10. 2017.

Selectively substituted cyclodextrins for analytical and pharmaceutical applications

Abstract

This thesis is focused on the selective modification of cyclodextrins, and its primary aim is the preparation and characterization of mono- and persubstituted derivatives of cyclodextrins in a regioselective and straightforward manner. The work is divided into two main parts describing synthetic strategies and applications of modified cyclodextrins with one or several substituents, respectively.

The first section deals with the introduction of a single chromophoric moiety on the cyclodextrin scaffold such as cinnamyl, rhodaminyl, fluoresceinyl and eosinyl groups.

The complete set of monocinnamyl-α-cyclodextrin regioisomers has been prepared by direct alkylation, and the self-assembling properties of the corresponding regioisomers were thoroughly investigated by dynamic light scattering and NMR experiments. These investigations revealed that the different isomers (mono-6-*O*-, mono-2-*O*- and mono-3-*O*-cinnamyl-α-cyclodextrin) form distinct supramolecular species through intermolecular association. A fast method for the unambiguous identification of the pure regioisomers has also been developed based on a series of 2D NMR measurements.

Xanthene-modified β-cyclodextrins, other representatives of monosubstituted cyclodextrins, have been synthesized. A new synthetic strategy for the green and mild coupling reaction between mono(6-deoxy-6-amino)-β-cyclodextrin and the xanthene dyes has been developed. Spectroscopic investigations showed that fluorescein- and rhodamine B-appended β-cyclodextrin can be used as pH-sensitive fluorescent sensors, while the eosin Y-tagged β-cyclodextrin can be used for the photogeneration of singlet-oxygen and applicable in photodynamic therapy. Similarly to the cinnamylated derivatives xanthene-cyclodextrins also showed a tendency to self-associate and this phenomenon clearly influences their photophysical properties. For this reason, a great emphasis was placed on the study of the supramolecular behavior of xanthene-modified β-cyclodextrins.

The second part of the thesis is discussing the perfunctionalization of β- and γ-cyclodextrin with methyl and carboxymethyl groups. The developed synthetic strategy is based on primary-side selective protection, secondary-side methylation and deprotection-carboxymethylation of the primary side, resulting in two-faced derivatives fully methylated on their secondary side and carboxymethylated on their primary side. The prepared derivatives were exploited as chiral selectors in capillary electrophoresis for the enantioseparation of pharmacologically significant molecules, and they represent the first single-isomer carboxymethylated cyclodextrins applied in this field.

Keywords: Cyclodextrins, Monosubstitution, Persubstitution, Regioselectivity, Supramolecular aggregates, Fluorophore labeling, Chiral separation, Photodynamic therapy, Capillary electrophoresis

Selektivně susbstituované cyklodextriny pro analytické a farmaceutické aplikace

Abstrakt

Tato práce se zabývá selektivní modifikací cyklodextrinů. Jejím hlavním cílem je příprava a charakterizace mono- a persubstituovaných derivátů cyklodextrinu syntetizovaných regioselektivně a přímočaře. Práce je tedy rozdělena na dvě hlavní části popisující syntetické přístupy a aplikace modifikovaných cyklodextrinů jednak s jedním substituentem, jednak s více substituenty.

První část představuje cyklodextrinové skelety s jednou chromoforní skupinou, jako je cinammylová, rhodaminylová, fluoresceinylová a eosinylová funkční skupina.

Kompletní série regioisomerů monocinammylových derivátů α-CD byla připravena pomocí přímé alkylace a jejich samoskladné vlastnosti byly následně podrobně zkoumány pomocí metod dynamického rozptylu světla a NMR. Tento výzkum odhalil, že jednotlivé regioisomery (mono-6-*O*-, mono-2-*O*- a mono-3-*O*-cinnamyl-α-cyklodextriny) jsou schopny tvořit rozdílná supramolekulární uskupení pomocí intermolekulárních asociací. Byla vyvinuta rychlá metoda pro jednoznačnou identifikaci čistých regioisomerů na základě série změřených 2D spekter.

Byly syntetizovány deriváty β-cyklodextrinu s xantinovým skeletem, představující další zástupce monosubstituovaných cyklodextrinů. Byly vyvinuty nové syntetické strategie pro spojení mono-6-deoxy-6-amino-β-cyklodextrinu s xantinovými barvivy za mírných podmínek a podmínek „green chemistry“. Spektroskopická měření odhalila, že deriváty β-cyklodextrinu s fluorereseinem a rhodaminem B mohou být používány jako fluorescentní senzory využívající změny pH, zatímco eosin Y-β-cyklodextrin může být využit pro fotopřípravu singletového kyslíku a aplikován ve fotodynamické terapii. Podobně jako cinammylové deriváty, také cyklodextriny s xantinovým skeletem vykazovaly tendenci ke samoskladbě a tento jev přímo ovlivňuje jejich fotofyzikální vlastnosti. Z toho důvodu je v práci velký důraz kladen na studium supramolekulárních vlastností modifikovaných β-cyklodextrinů s xantinovým zbytkem.

Druhá část této práce diskutuje perfunkcionalizace β- a γ-cyklodextrinů methylovými a karboxylovými funkčními skupinami. Vyvinutá syntetická strategie je založena na selektivním chránění primární strany, methylací sekundárního okraje cyklodextrinu a odchraňující karboxymethylaci primárního okraje, což vede k derivátům s methylovými funkčními skupinami na sekundárním okraji a karboxylovými skupinami na primární straně cyklodextrinu. Připravené deriváty byly následně použity jako chirální selektory v kapilární elektroforéze pro separace enantiomerů farmakologicky významných molekul a představují první persubstituované isomerně čisté cyklodextriny s karboxymethylovými skupinami použité v této oblasti.

Klíčová slova: Cyklodextriny, Supramolekulární agregáty, Monosubstituce, Persubstituce, Regioselektivita, Fluorescenční značení, Chirální separace, Fotodynamická terapie, Kapilární elektroforéza

Table of contents

Table of contents 7
1. Introduction 9
2. Objective 11
3. Theoretical overview 12
3.1 Properties of CDs 12
3.1.1 Inclusion phenomenon 14
3.1.1.1 Chiral separations exploiting the inclusion phenomenon 18
3.2 Chemically modified CDs 20
3.2.1 Monosubstitution 21
3.2.1.1 Primary-side monosubstitution 22
3.2.1.2 Secondary-side monosubstitution 23
3.2.2 Persubstitution 24
3.3 Supramolecular aggregates based on monosubstituted CDs 25
3.4 Fluorophore-tagged CDs 27
3.4.1 Optical imaging of drug delivery systems: fluorophore-tagged CDs crossing barriers 33
3.4.2 Fluorophore-tagged CDs as phototherapeutics 36
3.5 Persubstituted anionic CDs as chiral selectors for capillary electrophoresis 38
4. Results and discussion 41
4.1 Synthesis of monocinnamyl-α-CDs 41
4.2 Supramolecular characterization of regioisomers of monocinnamyl-α-CD 45
4.3 Synthesis of xanthene-modified β-CDs 54
4.3.1 Rhodamine B-appended β-CD 55
4.3.2 Fluorescein-appended β-CD 59
4.3.3 Eosin-appended β-CDs 62
4.4 Spectroscopic and supramolecular characterization of xanthene-modified β-CDs 64
4.4.1 IR and UV-Vis spectroscopic characterization of rhodamine B-appended β-CD 64
4.4.2 UV-Vis spectroscopic characterization of fluorescein-appended β-CD 66
4.4.3 Aggregation behavior of Eo-β-CD conjugates 67
4.4.4 Spectroscopic and photophysical properties of Eo-β-CD conjugates 68
4.5 Synthesis of per(2,3-di-O-methyl-6-O-carboxymethyl)-CDs 70
4.6 Characterization and application of per(2,3-di-O-methyl-6-O-carboxymethyl)-CDs in chiral capillary electrophoresis 74
5. Conclusions 80
6. Experimental part 81
6.1 Details of analytical measurements 81
6.2 Reagents and chemicals 84
6.3 Synthesis of compounds 85
6.3.1 Synthesis of monosubstituted cinnamyl-α-cyclodextrins 85
6.3.2 Synthesis of monosubstituted β-CD scaffolds for fluorophore labeling 88
6.3.3 Synthesis of xanthene-modified β-CDs 91

6.3.4 Synthesis of persubstituted CDs 97
7. Acknowledgements 107
8. References 108
9. List of author's publications 114
10. List of abbreviations 118

1. Introduction

Cyclodextrins (CDs) are cyclic oligosaccharides of natural origin, composed of glucose units linked by α-1,4-glycosidic bonds. The first reference about their existence was reported by Villiers in the 19th century[1], but for a long period, they were considered only as curiosities for fundamental academic research, having no potential in industrial applications. This view has changed only in the middle of the 20th century when after developing reliable methods for their enzymatic production and isolation from starch the three native CDs became available. Freudenberg, Cramer, and Plieninger were the first who realized the potentialities in industrial utilization of these oligosaccharides. They filed the first patent on the applications of CDs in drug formulations[2]. This work laid down the foundations of CD technology, by pointing out the beneficial properties of CDs, spanning from stabilization of fragile, easily oxidizable substances through solubility enhancements to the reduction of a loss of highly volatile compounds.

Despite the promising properties of CDs, misleading results about their acute toxicity hampered their widespread utilization in pharmaceutical industry, cosmetics and food industry. Only in the 1980s when adequate toxicological studies proved that the previously observed toxicity originated from the complexed impurities and not from the CDs itself, a new period in CD chemistry could start, hallmarked by large-scale production and application of CDs in almost all segments of industry[3]. The demand for CDs continuously increased and through biotechnological advancements, their production rate could reach several metric tons annually.

As CDs became available at a relatively low price and high purity, different synthetic methodologies were developed for their chemical derivatization[4]. The main goal of the functionalization was to further improve their properties, mainly their complex forming ability, water solubility or spectroscopic characteristics. Random functionalization processes with methyl-, 2-hydroxyalkyl- or sulfoalkyl-groups generated derivatives with improved solubility and enhanced encapsulation capacities. Furthermore, the hydroxypropylation and sulfobutylation processes ameliorated the hemolytic and renal toxic concentration threshold of parent CDs. As a matter of fact, 2-hydroxypropyl-β-CD (HP-β-CD) and sulfobutylether-β-CD (SBE-β-CD) became approved excipients extensively used in drug formulations to increase the active pharmaceutical ingredient's (API's) solubility or bioavailability. HP-β-CD and

SBE-β-CD showed that the molecular encapsulation phenomenon can be industrially utilized not only with native CDs but also with their derivatized counterparts.

The successful application of HP-β-CD and SBE-β-CD accelerated research on CD derivatization, and several synthetic methodologies became available for the precise stereochemical control of the substitution. Selectively substituted derivatives, also called single-isomer CD derivatives (SIDs) have been prepared and applied first in separation sciences and in chemosensing respectively, where the isomeric purity of CDs is of vital importance. Not only analytical sciences but also pharmaceutical applications benefited from selectively substituted CDs: Sugammadex, a currently approved drug marketed under the trade name Bridion®, became the first selectively modified CD in drug formulations. The API-Sugammadex is a SID of γ-CD tailored to form strong inclusion complexes with aminosteroid type neuromuscular blocking agents. Due to the selective encapsulation phenomenon, it can reverse the effect of aminosteroids, thus it can be applied to speed up the post-operative care of the patient[5].

The case of Sugammadex is the real success story of CD technology, and it indicates that we live in an era where CD derivatives are being rediscovered as APIs[6]. In this new period of CD chemistry, the SIDs are a hot topic for several reasons:

- Being chemically well-defined substances, SIDs allow to perform reproducible binding, pharmacokinetic and toxicity studies of drug/CD complexes and as a consequence, they provide a more straightforward advance from the proof-of-concept stage to the clinical tests and eventually the market.
- SIDs are required as reference materials for the characterization of randomly substituted CDs.
- Because the position and the number of substituents influence complexation ability of CDs, SIDs can help to understand better the performance of randomly substituted CDs.
- SIDs circumvent the problem with low batch-to-batch reproducibility, which is a common problem in the case of randomly substituted CDs.
- In separation sciences, SIDs provide a comprehensive theoretical framework of the separation of the components and allow to identify the variables to predict successful separations.
- SIDs allow an accurate study of the host-guest interaction at a molecular level.

The demand for SIDs initiates organic chemists to investigate further possible synthetic routes and to find the most practical way towards these chemically modified sugars. Synthesis of SIDs, in most of the cases, requires a series of protection and deprotection steps to assure derivatization on the selected positions or preparative separation techniques for the isolation of the targeted derivative. The increased number of chemical transformations and purification steps consequently increases their value with respect to the randomly substituted CDs.

Development of selectively substituted CDs gives a difficult task also to analytical chemists since throughout the development of new synthetic protocols *ad-hoc* developed analytical methods are needed to distinguish between the desired product and the unwanted by-products.

2. Objective

The main goal of this thesis was to develop synthetic strategies for the selective mono- and persubstitution of the CD scaffold. Parallel to the synthetic work, a great emphasis was placed on the development of analytical methods for the unambiguous identification and characterization of the newly prepared compounds and synthesis intermediates.

The synthetic work is divided into the following main parts:

- selective monosubstitution of α-CD;
- selective monosubstitution of β-CD;
- selective persubstitution of β-CD;
- selective persubstitution of γ-CD.

The analytical investigations, aiming the determination of the properties of the prepared compounds, can be summarized in the following points:

- characterization of the aggregation behavior of monocinnamyl-α-CDs (Cin-α-CDs);
- spectroscopic characterization of xanthene-modified β-CDs;
- characterization of the aggregation behavior of xanthene-modified β-CDs;
- NMR and HPLC characterization of per(2,3-di-*O*-methyl-6-*O*-carboxymethyl)-CDs and their synthesis intermediates.

Finally, practical utilizations of the newly prepared CD derivatives were proposed in various fields of analytical and pharmaceutical chemistry. These applications can be categorized into the following areas:

- application of Cin-α-CDs as pseudostationary phases in CE;

- application of fluorescein- and rhodamine B-appended β-CDs as fluorescent chemosensors;
- application of eosin-appended β-CDs as photosensitizers in photodynamic therapy;
- application of per(2,3-di-*O*-methyl-6-*O*-carboxymethyl)-β- and -γ-CDs as chiral resolving agents for capillary electrophoresis (CE).

3. Theoretical overview

3.1 Properties of CDs

CDs are macrocyclic oligosaccharides consisting of mutually linked α-D-glucopyranose units. The connectivities between the subunits are α-1,4-glycosidic bonds; therefore CDs are not reducing sugars. The shape of the macrocycle is not a perfect ring but rather resembles a truncated hollow cone with a narrower and a wider side. As a consequence of the $^4C_1$ conformation of the glucopyranose units, all the secondary hydroxyl groups of the glucose subunits are located on the wider edge (secondary side), and all the primary hydroxyl groups are situated on the narrower side (primary side) of the cone. The most studied and from the practical point of view most interesting CDs are named as α-, β- and γ-CD and are formed by 6, 7 and 8 glucose subunits respectively (Figure 1).

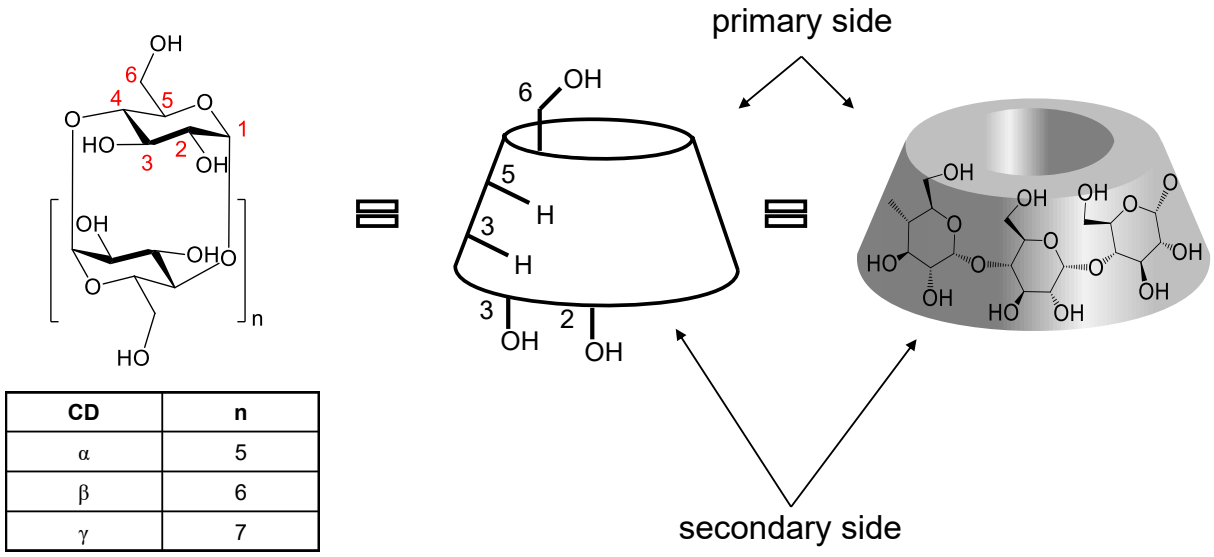

CD	n
α	5
β	6
γ	7

Figure 1. The molecular structures of CDs with example of glucose atom numbering (1-6) and schematic representation showing the geometry and the 3D structure of the molecule.

The number of glucose units defines the diameter of the cavity ranging from 0.47 nm for α-CD, through 0.60 nm for β-CD to 0.83 nm for the γ-CD (Table 1). CDs have one set of primary hydroxyl groups on the primary side and two sets of secondary hydroxyl groups located on the secondary side of the macrocycle. The large number of hydroxyl groups makes the outer surface hydrophilic and it is responsible for the water solubility of CDs. Intramolecular hydrogen bonds on the secondary side between the adjacent glucose units have a great impact on the physico-chemical properties of CDs. The structure of β-CD allows a perfect orbital overlap for the hydrogen bond formation between the *C*-2 hydroxyl group of glucose unit and the *C*-3 hydroxyl group of the adjacent glucose unit (for the glucose atom labeling see Figure 1)[4]. In total 7 hydrogen bonds can form a complete secondary ring, which makes β-CD the most rigid and least water-soluble among the native CDs. In the molecule of α-CD, the hydrogen bond wreath formation is not complete because one glucopyranose moiety is distorted. In the case of γ-CD, the bigger size allows more flexibility and non-planarity which prevents the formation of the complete hydrogen bond belt. Due to these reasons α- and γ-CD are much more flexible molecules, and their water solubility overcomes the solubility of β-CD by around tenfold (Table 1).

Table 1. Important physico-chemical properties of native cyclodextrins[4].

	α-CD	β-CD	γ-CD
Number of glucose units	6	7	8
Molecular weight ($g \cdot mol^{-1}$)	972	1035	1297
Cavity diameter (nm)	0.47-0.53	0.60-0.65	0.75-0.83
Height of the torus (nm)	0.79±0.01	0.79±0.01	0.79±0.01
Outer diameter (nm)	1.46	1.54	1.75
Cavity volume (nm^3)	1.74	2.62	4.27
Approx. cavity volume in 1 g CD (mL)	0.1	0.14	0.20
Aqueous solubility (mg/mL) at 25 °C	145	18.5	232
Crystal water, wt %	10.2	13.2-14.5	8.13-17.7
pK_a at 25 °C (by potentiometry)	12.33	12.20	12.08

Conversely to the exterior, the interior of all CDs is rather lipophilic, because only the unpolarized methine groups and the glycosidic ether oxygen atoms are directed inwards the cavity.

3.1.1 Inclusion phenomenon

Due to their hydrophobic cavity, CDs are able to interact with a great variety of ionic and neutral species. This type of supramolecular relationship is referred to as host-guest interaction, where the CD is the host and the encapsulated molecule is the guest entity. For the successful formation of the host-guest complex, several criteria have to be fulfilled, such as steric requirements (dimensional fit), charge, polarity, energetic properties of the host and the guest. The driving forces leading to the inclusion complexation include the electrostatic interaction, van der Waals interaction, hydrophobic interaction, hydrogen bonding, and charge–transfer interaction. Usually, it is found that van der Waals interaction and hydrophobic interaction constitutthe major driving forces for complexation, whereas electrostatic interaction and hydrogen bonding can significantly affect the conformation of a particular inclusion complex[7]. Inclusion complex formation in aqueous solution is a thermodynamically favored, reversible process, which can be characterized by the association constant (K_{ass}), also referred to as stability constant, binding constant or complexation constant (Equation 1). K_{ass} describes the equilibrium between the complexed and uncomplexed species in solution, and it can be used to quantify the strength of the host-guest interaction[8].

$$[CD] + [guest] \rightleftharpoons [complex]$$

$$K_{ass} = \frac{[complex]}{[CD]\ [guest]} \quad (1)$$

K_{ass} is a function of several parameters, and it varies between native CDs significantly. Due to dimensional fit, it can be generalized, that α-CD forms complexes with high K_{ass} values with molecules having an aliphatic chain (e.g. decanol), β-CD with smaller aromatic compounds (e.g., toluene, naphthalenesufonate), and γ-CD includes preferentially larger molecules with fused ring systems (e.g., pyrene, fullerene).

The most common pharmaceutical application of CDs is the improvement of solubility, stability, and bioavailability of the API which requires temporary encapsulation and therefore a medium K_{ass} between the host and the guest. CD-drug interaction has to be strong enough to keep the targeted guest molecule in molecularly dispersed and therefore in a dissolved form, but low enough to allow the dissociation of the complex and the release of the encapsulated drug when it is required.

In other pharmaceutical applications, a selective, irreversible trapping of the API is the goal, which obviously needs extremely strong interaction, therefore remarkably high K_{ass} values.

Applications such as separation methods, catalysis or chemosensing make use of molecular recognition ability of CDs, where selective binding of one species from a pool of structurally similar homologs is the key factor. It is therefore evident that for the successful utilization of CDs in any of the applications mentioned above it is pivotal to understand the inclusion process fully and to characterize the formed host-guest complex. Complexation alters the physico-chemical properties of the guest and the host as well, which can be used to determine the K_{ass} value. Inclusion complexes can be isolated as crystalline species and studied in solid form with techniques such as thermogravimetry[9], infrared spectroscopy[10], X-ray powder diffraction[11] or single crystal X-ray analysis[12].

The majority of industrially important applications, however, require the characterization of CD complexes in solution. Most methods for determining K_{ass} values in the liquid phase are based on titrating changes in the physico-chemical properties of the guest molecule with the CD and then analyzing the concentration dependencies. Changes in the measured experiment observables are plotted against the CD concentration, and K_{ass} can be calculated by graphical methods (linearization) which produce a linear relationship between the given physico-chemical properties and the K_{ass} value. The most common linearization methods for this purpose are the Benesi-Hildebrand method[13] and the Rose-Drago method[14].

These graphical methods can be used for bimolecular processes where the stoichiometry between the host and the guest is strictly 1:1. In CD chemistry, however, there are plenty of examples where highly ordered inclusion complexes are formed, such as ternary complexes between two guests and one CD; sandwich-type complexes in which two CDs encapsulate the same guest; or polymer-like structures (pseudorotaxanes, supramolecular polymers, etc.) with a deviation from the 1:1 stoichiometry. For these systems with higher stoichiometries, non-linear curve fitting methods with appropriate computational algorithms have to be used to obtain accurate data for the K_{ass}[15].

Recently, UV/Vis, fluorescent, circular dichroism, and NMR spectroscopy are the most frequently used analytical tools for these purposes, while isothermal titration calorimetry (ITC) and CE are gaining attention as complementary techniques to provide information on the K_{ass} values and on other parameters of the complexation process in solution.

In UV/Vis spectroscopy, the absorption maxima of the included guest are changed upon complexation. Hypsochromic and bathochromic shifts can be observed, and the

enhanced absorption is often a reported effect of the complex formation. The increase in UV/Vis absorption can be attributed to the fact, that the included chromophore experiences a more lipophilic environment when it is moved from aqueous solution to the CD cavity. K_{ass} determination by UV/Vis spectroscopy is based on titration of the guest solution (with constant concentration) by the solution of CD. Changes in the absorbance maxima are plotted against the CD concentration, and K_{ass} can be calculated by above mentioned graphical or curve fitting methods.

NMR spectroscopy is another widely used technique to characterize the guest binding and to quantify the strength of the interaction. The principles are the guest induced chemical shift changes of CDs internal protons which in most of the cases are caused by the shielding tensor of the included species. Due to ring anisotropies, aromatic compounds provide strong shielding effects upon complexation to CD cavity. These effects on CDs internal protons can be subjected to quantitative calculations. The shielding effect of the CD macrocycle on the guest is less pronounced; nevertheless, it can be large enough to be used for NMR titrations.

Shielding exerted by the CD cavity can be useful in cases when the guest itself has only weak shielding tensors (aliphatic compounds) and generates only weak shifts on the CD protons. Complexation induced chemical shift changes can be quantified, either on the spectrum of guest or host by using titration experiments, resulting in the K_{ass} value. The standard NMR titration protocol is usually performed by measuring one of the CDs internal proton chemical-shift change upon different guest concentrations. The obtained shifts are then fitted by a nonlinear least-square fitting which gives the apparent K_{ass} value.

The great advantage of NMR titration is that it provides several independent signals for the evaluation of K_{ass}; furthermore, at the same time, it gives an insight into the conformation of the supramolecular complexes. By analyzing the differences in chemical shift changes between *H*-3 and *H*-5 or *H*-6 protons the direction of inclusion or the extent of penetration can be revealed, since *H*-3 protons are located closer to the secondary rim, while *H*-5 and *H*-6 protons are situated closer to the primary rim. If, for example, the guest inclusion is only partial from the secondary side, *H*-3 protons are the most affected ones by the anisotropic effect of the guest, on the other hand, if the penetration takes place from the narrower primary side, *H*-6 and *H*-5 protons experience the largest shielding effect.

Besides the analysis of chemical shift changes, advanced 2D NMR techniques based on nuclear overhauser effect (NOE), such as nuclear Overhauser effect spectroscopy (NOESY) or rotational nuclear overhauser effect spectroscopy (ROESY) can afford further structural information. Intermolecular NOE correlations between CDs internal protons and the

appropriate guest protons are considered as unambiguous evidence of the formation of the supramolecular complex[16].

ITC can be used to follow the thermodynamic changes in solution. Since guest binding or guest release from the CD cavity is always accompanied by heat release or heat absorption, ITC is suitable for monitoring CD-guest interactions in a liquid phase. The greatest advantage of this technique is the very accurate determination of the K_{ass}; furthermore, it provides all thermodynamic parameters of the inclusion process ($\Delta G°$, $\Delta H°$, and $\Delta S°$) within one experiment. These benefits, together with the minute needed concentrations and volumes of both components, make ITC the most frequently used technique for studying the binding thermodynamics of CD-based systems[17, 18].

Chromatographic and electrophoretic methods can also be applied as indirect methods to follow and quantify the inclusion process in solution. The basic principle is the alteration of the guest molecules retention time (liquid chromatography) or migration time (electrophoresis) upon complexation. In the case of CE, association constants are calculated from the relationship between ligand concentration and the measured electrophoretic mobility of the guest. The experiment is traditionally carried out, by running the sample first in the background electrolyte (BGE) (without CD added). The effective electrophoretic mobility (μ_{eff}) of a charged molecule is a function of the charge-to-size ratio and the viscosity of the electrophoresis media. In practical terms, the effective electrophoretic mobility can be obtained from (Equation 2)

$$\mu_{eff} = \frac{l_c l_d}{U} \cdot \left(\frac{1}{t} - \frac{1}{t_0}\right) \quad (2)$$

where l_c and l_d, are the total capillary length and the capillary length to the detector, U is the run voltage, and t and t_0 are the measured and free migration time of the molecule[19]. The electroosmotic flow (EOF) represents the migration velocity of neutral species in the system, a flow that affects all the analytes that are within the capillary. This can be considered as a benchmark for each experiment. Obviously, according to changes in the BGE (e.g., increase in viscosity due to CD addition), the migration time of the neutral species may change as well. By relating the migration time of the guest to that of the EOF, these effects are compensated during the calculations simply by subtracting the observed guest mobility from the EOF mobility (Equation 3)

$$\mu_{eff} = \mu_{EOF} - \mu_{Guest} \quad (3)$$

After determining the μ_{eff} of the guest, measurements are carried out in BGEs containing an increasing concentration of the studied CD. The presence of the CD affects the migration velocity of the guest in case the complexation takes place. The increasing concentrations of the CDs result in the alteration of migration times of the guest peaks. In general, the more stable complex is formed with the CD, the more the migration time of the free guest is influenced. The effective mobility of the guest is influenced by the concentration of CD, as the following equation shows:

$$\mu_{eff} = \frac{\mu_{free} + \mu_{complex} K_{ass}[CD]}{1 + K_{ass}[CD]} \quad (4)$$

where μ_{eff} is the effective guest mobility at the actual CD concentration while μ_{free} and $\mu_{complex}$ are the effective mobility of the free and complexed ligand. Based on equation (4), the stability constants can be determined using x-reciprocal method[20]. The experimental mobility differences are calculated first by the subtraction of the μ_{eff} value obtained at 0 mM CD concentration ($\mu_{eff\ noCD}$) from actual μ_{eff} values at each CD levels (practically: $\mu_{eff} - \mu_{eff\ noCD}$). For the calculation $(\mu_{eff} - \mu_{eff\ noCD})/[CD]$ is plotted as a function of $(\mu_{eff} - \mu_{eff\ noCD})$. The negative of the slope equals to the K_{ass} value. Due to the high sample throughput, possible automatization and the minute concentrations and volumes needed for the measurements, CE is an ideal technique for the initial screenings where a large number of CD derivatives have to be tested for the corresponding analyte to find the optimal K_{ass} value for the drug formulation or enantioseparation.

3.1.1.1 Chiral separations exploiting the inclusion phenomenon

Enantiomeric purity and characterization of the enantiomers' biological activity are crucial requirements for novel chiral drug candidates. For this purpose, enantioselective total syntheses and enantioselective analytical methods are necessary. CE has been widely used for chiral separation due to its high efficiency, rapid analysis time, high resolution, small sample volume requirement, and minute solvent consumption[21]. Applying CDs and their derivatives as chiral selectors is one of the most commonly used methods in chiral capillary electrophoresis (CCE)[22].

Chiral recognition using CDs is based on the different interaction affinity between the chiral selector and the analyte enantiomers which leads to the formation of diastereomeric complexes. This is possible because CDs are inherently chiral molecules with multiple

stereogenic centers. If the K_{ass} values of the enantiomers with the applied CD selector are different, then enantioseparation in CCE can be obtained. The complex formation is driven mainly by the host-guest inclusion phenomenon, but the inclusion alone is not enough for chiral recognition: interactions between substituents on the asymmetric center of the analyte and the hydroxyl or other functional groups on the CD rim are responsible for chiral recognition. A combination of these oriented interactions with the inclusion process and with other weak forces, such as hydrophobic interaction, hydrogen bonding, van der Waals interaction and dipole-dipole interaction results in a selectivity-structure correlation, and forms the basis for chiral separation by CDs. Chiral selectivity is influenced by the size and shape of the CD, as well as the fit of the enantiomer into the cavity and its interactions with the functional groups present on the rims of the CD[23].

Synthetic modifications of the native CDs can provide a large variety of CD selectors decorated with various substituents to achieve the desired enantiorecognition properties. The complexity of the interactions between the selector and the analyte makes it particularly difficult to predict the success of the enantioseparation. Until now, the consensus is that no general scheme of the enantiomeric discrimination of CDs has resulted from studies, i.e., how to design CD modifications to improve effectiveness for resolution of enantiomers[24]. On the other hand, the use of SID structures for enantioresolution has been stressed as a mandatory condition for several reasons:

- to eliminate the drawback of several isomers in randomly substituted CDs resulting in ill-defined complex mixtures
- to provide a comprehensive theoretical framework on the enantiomer migration in electrophoresis
- to get a better understanding into the insight of the enantiorecognition process at the molecular level by analytical NMR techniques

Despite the numerous randomly substituted CD derivatives investigated in the past decades, only few research groups are involved in the application of SIDs for chiral separations[24,25,26]. Consequently, a great need still exists for further effort in synthetic chemistry aiming at the development of novel CDs with improved chiral recognition ability towards a large pool of racemic analytes with shorter separation time and greater analysis accuracy.

3.2 Chemically modified CDs

CDs are modified for a variety of reasons, among which the most important are

- to increase the solubility of native CD in a desired solvent,
- to enhance the extent of guest complexation,
- to achieve specific binding behavior,
- to introduce a chromophore unit into the structure.

The strategy for modification depends on the purpose of the final product.

The first applied CD derivatives and also the most widely used ones up to date are different randomly substituted derivatives with varying degree of substitution (DS, the number of substituents attached to a CD molecule). Randomly methylated β-CD (RAMEB), HP-β-CD, 2-hydroxypropyl-*γ*-CD (HP-*γ*-CD), and SBE-β-CD are commercially available and industrially produced in ton amounts annually. These products are not single chemical entities, but mixtures of variously substituted isomers and homologs. All of them show higher aqueous solubility than their unmodified analogs; therefore they are utilized in many drug formulations as solubility enhancers.

On the other hand, analytical applications such as separation methods or chemosensing, but also some specific pharmaceutical applications require well-characterized selectively substituted CD derivatives and very often SIDs. Due to the numerous functional groups present on the molecule and due to their symmetrical nature the selective modification of native CDs remains a very challenging task. The preparation of SIDs usually involves multiple synthetic steps or extensive purification procedures to recover pure single-isomer compound.

CDs possess three different types of hydroxyl groups (*OH*-2, *OH*-3, and *OH*-6) exhibiting different reactivities. *OH*-6 groups are primary hydroxyls; therefore they are less hindered, more basic and more nucleophilic than the others. They can react with electrophiles, even if they are sterically hindered, using only a weak base[27]. The hydrogen bond wreath between secondary hydroxyl groups and the proximity of the electron-withdrawing anomeric acetal function reinforces the acidity of the *OH*-2 hydroxyls; hence they become more acidic than the others (pK_a=12.2)[28]. *OH*-2 groups can be selectively deprotonated in anhydrous basic conditions; nevertheless, selectivity between the positions *OH*-2 and *OH*-3 cannot be achieved if the conditions used are too basic or if the electrophile is too strong. Hydroxyls *OH*-3 are less reactive, sterically more hindered and can only be selectively modified after

protection of the other positions or by using complexing electrophiles oriented towards position *C*-3.

These differences of reactivity between the three types of hydroxyl functions can be exploited in selective functionalization strategies.

3.2.1 Monosubstitution

Monosubstituted CDs are CD derivatives having only one hydroxyl group modified with a functional group. The preparation of these compounds in most of the cases is based on the use of the reagent in limiting amount. However, due to the very similar reactivity of hydroxyl groups, oversubstitution during the reaction cannot be avoided, making chromatographic or crystallization steps essential for the preparation of pure monofunctionalized CDs. Alternative approaches use sterically hindered reagents, preventing the approach of the second molecule of reagent, to ensure higher yields for the monosubstituted compounds[29]. The three different hydroxyl groups on the glucose subunits offer three different sites on the CD molecule where the monofunctionalization can occur. As a consequence, monosubstituted CDs can be mixtures of three regioisomers (Figure 2).

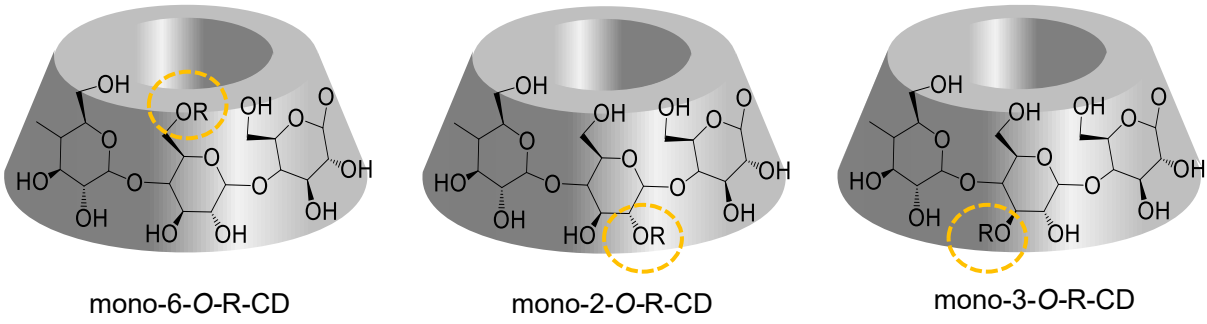

Figure 2. Schematic representation of the three possible regioisomers of a monosubstituted CD.

The number of known monosubstituted CD derivatives is enormous because for a long time monosubstitution has been the almost exclusive reaction to prepare selectively modified CDs in a practical manner. From the synthetic point of view, the most important derivatives are those versatile intermediates that can be effectively transformed according to the requirements of the specific application. The modification of a monosubstituted CD with a suitable functional group is an easier process than the optimization of a new monosubstitution reaction on a native CD[30].

3.2.1.1 Primary-side monosubstitution

Monotosylation of the primary rim is the most widely used method to access *C*-6 monofunctionalized CDs. Tosyl chloride (TsCl) reacts with α-, β- and γ-CD in pyridine and gives the *C*-6 monosubstituted product in about 30% yield (for β-CD)[31,32]. The *C*-6 regioselectivity is attributed to the inclusion of pyridine into the CD cavity, in such way that it activates only the hydroxyl groups of the primary side. Several alternative methods have been developed with the aim to further improve the yield of monotosylation or to replace the pyridine with more user-friendly solvent[33]. No matter which strategy is applied, total conversion of starting material to the monosubstituted product cannot be achieved, and a mixture of overtosylated products and the unreacted starting CD is formed. The separation of the targeted monosulfonated compound is achieved through recrystallization from warm water for the β-derivative and through chromatography in the case of α- and γ-CD.

Many nucleophiles can react with tosylated CDs, to give the corresponding *C*-6 monofunctionalized CDs. However, alkaline bases cannot be used as nucleophiles due to the intramolecular substitution, resulting in a mono-3,6-anhydro product[34]. Sodium azide in *N,N*-dimethylformamide (DMF) on the other hand reacts with mono-6-*O*-tosyl-CDs to give the CD monoazides with high yields. CD monoazides are valuable precursors since they can be used as starting materials in azide-alkyne click reactions; furthermore, they can be readily reduced to mono(6-amino-6-deoxy)-CDs (NH_2-β-CD) opening the way towards the preparation of amine, thioureido or amide-linked CD scaffolds[35]. A variety of other nucleophiles can react with mono-6-*O*-tosyl-CDs, such as iodide, dithiol, hydroxylamine, alkylamine or polyalkylamine to afford iodo-[36], thio-[37], hydroxylamino-[38] or alkylamino-CDs[39] monosubstituted at position *C*-6.

Moreover, the tosyl function can be oxidized to aldehyde using a non-nucleophilic base in dimethyl sulfoxide (DMSO)[40]. Monoaldehyde CDs can be further oxidized selectively to afford the corresponding carboxylic acid derivatives[41]. An alternative strategy to overcome the difficulties connected with the preparation of mono-6-*O*-tosyl-CD intermediate is the preparation of 6-monoaldehyde-CD directly with Dess-Martin periodinane in a fairly good 85% yield, which is considered as the most efficient reaction to date used for selective monofunctionalization of CDs[29].

3.2.1.2 Secondary-side monosubstitution

To selectively modify the wider annuli, the higher acidity of secondary hydroxyl groups over the primary ones is exploited. Above pH 10 secondary alkoxides can be modified without any reaction occurring on the primary side. Due to the very similar reactivity of 2-*O*- and 3-*O*- alcoholates this strategy in most of the cases does not give regioselectivity and as a consequence a mixture of the two, secondary side-substituted products is formed (2-*O*- and 3-*O*-substituted derivatives). To isolate the two isomers, the reaction mixture is usually subjected to multistep chromatographic purification. First, the mixture of monosubstituted CDs is separated from the disubstituted and starting CDs, then the monosubstituted fraction is peracetylated (usually with pyridine/Ac_2O), and the pure monosubstituted isomers are separated as peracetates on silica gel with the use of chloroform ($CHCl_3$)/MeOH elution mixtures[42]. On the other hand, if the attached substituent is bulky and hydrophobic enough, the peracetylation step can be avoided and a single chromatographic step on reversed-phase silica gel using H_2O/MeOH[43], or H_2O/acetonitrile (ACN)[44] elution mixtures results in isolation of the pure regioisomers.

The use of supramolecular inclusion complexes is another very elegant approach towards monofunctionalized CDs. It benefits from the highly stereoselective orientation of the CD cavity. If the electrophilic reagent forms a complex with CD, then the orientation of the reagent within the complex introduces an additional factor in determining the nature of the product[45]. If the complex is very strong, then the formation of the predominant product will be dictated by the orientation of the reagent within the complex.

A representative example of the inclusion induced regioselectivity is the preparation of mono-2-*O*-tosyl-β-CD. For the regioselective synthesis of this compound, the property of β-CD to complex *m*-nitrophenyl tosylate is taken advantage of to direct the tosyl group to the secondary side. This avoids the natural tendency of CD to react on its primary side and predominantly gives CDs substituted at the 2-*O*-position. To favor the complexation of the reagents to the CD cavity, most of the inclusion assisted modifications are carried out in an aqueous environment, however, in some cases, high regioselectivity can also be achieved in organic solvents, as it was recently reported for the preparation of mono-2-*O*-lauryl-β-CD[46].

Hydroxyl groups in position *C*-3 are the least reactive; therefore, they are the most difficult to substitute regioselectively. Monocinnamylation of β-CD belongs to the few reported procedures giving 100% 3-*O* regioselectivity. The formation of only one regioisomer out of the 3 possible ones is attributed to a highly regioselective complexation and orientation

of the alkylating reagent by the β-CD cavity. This methodology is of relevant synthetic importance, since it gives access to a variety of 3-*O*-monofunctionalized β-CDs as the double bond of the cinnamyl moiety can be transformed to aldehyde or carboxymethyl (CM) functions through oxidative processes[47].

Complexation with Cu (II) ions can also be used to induce regioselectivity on the secondary side. The strategy is based on the use of bulky electrophilic reagents, such as benzyl bromide and a temporary complexation of some of the secondary hydroxyl groups. Complex formation occurs on adjacent glucopyranose units in aqueous sodium hydroxide (two Cu (II) ions form the complex with the secondary side of β-CD) and it significantly affects the reactivity of CD alcohol functions. With bulky alkylating agents this methodology gives preference to 3-*O* monosubstitution[48].

3.2.2 Persubstitution

In persubstitued CDs, each glucose unit is equally modified. The most simple representatives of this class of compounds are the per-2,3,6-tri-*O*-alkyl-CDs where all the glucose positions are modified with the same substituent. These uniformly persubstituted compounds can be obtained quantitatively using the alkyl or benzyl halide and sodium hydride in anhydrous organic solvents[49].

The preparation of persubstituted CDs carrying non-identical substituents in the 2-, 3- and 6-positions is a more challenging task and takes advantage of the different reactivity of CD's hydroxyl groups. *OH*-2 groups are the most acidic and *OH*-6 hydroxyls are the most basic ones[50]. However, this difference in acidity can be exploited for selective modification only till a certain extent. As the number of functionalized positions increases, the steric hindrance on the secondary rim makes the alkoxides less reactive. The electrophile can then react with the hydroxyls of the primary rim, resulting in non-selective modification therefore in a large number of regioisomeric products.

To avoid this scenario, for the preparation of selectively persubstituted CDs, the primary hydroxyls are usually protected before the manipulation on the secondary rim. The primary hydroxyls are better nucleophiles than the secondary ones, so they can be selectively modified using a weak base. Furthermore, it has been shown that bases, such as pyridine or imidazole, activate the primary hydroxyl groups of CDs, rendering them susceptible to electrophilic attack. The most frequently used protocol for the selective protection of the primary rim is based on the use of *tert*-butyldimethylsilyl chloride (TBDMSiCl) in DMF with

imidazole as a base or in pyridine and gives access to CDs persilylated on their primary rim[51,55]. The resulting per(6-*O*-*tert*-butyldimethylsilyl)-CDs (TBDMSi-CD) have been widely used for the subsequent mono-[53,54,55,56], hemi- [57,58,59,60], or perfunctionalization [61,62,63,64] of the secondary face.

Silyl ether protection is fully compatible with strong basic conditions, necessary for the complete substitution of the secondary side by protecting groups (allyl, benzyl or acetyl groups) or by alkylating agents (preparation of per-2,3-*O*-alkylated-CDs). After the secondary side derivatization, TBDMSi groups can be easily removed using tetra-*n*-butylammonium fluoride (TBAF) or by acid hydrolysis, which generates two-faced CDs with a polar primary side and with a fully protected, therefore apolar secondary side. These amphiphilic CDs open the way towards various functionalization exclusively on the primary side. This strategy based on selective protection and deprotection of the two distinct faces of CDs has been exploited in the synthesis of series of SIDs carrying sulfato-[65], carboxymethyl-[66,67] or amino-functions[68] on their primary side.

Another approach for the synthesis of per-6-substituted CD derivatives is based on the selective reaction of halogens and triphenylphosphine with CD in a Vilsmeier-Haack-type reaction. The resulting per(6-deoxy-6-halogeno)-CD can be converted *via* azido derivative to per(6-deoxy-6-amino)-CD[69]. Heptakis(6-deoxy-6-bromo)-β-CD has been used as a precursor for the synthesis of per-6-substituted cationic β-CDs[70], while octakis(6-deoxy-6-halogeno)-γ-CDs are the key intermediates in the synthesis of Sugammadex[5]. Furthermore, per-6-halogenated CDs can be directly converted to per-6-deoxy-CDs when treated with $NaBH_4$ in DMSO[71] or to per-3,6-anhydro-CDs[72] under strong basic conditions. The latter ones are especially interesting molecules, having all the glucose units in an inverted $^1C_4$ conformation and their oxygen atoms inside the cavity. Anhydro CDs, therefore, can be considered as inside-out CDs with strong affinity towards metal cations or ammonium ions.

Per(6-deoxy-6-halogeno)-CDs are an important class of compounds which can be used for the selective functionalization of the primary face. Together with per-6-*O*-silylated CDs, they are the cornerstones of the selective persubstitution of CDs.

3.3 Supramolecular aggregates based on monosubstituted CDs

Supramolecular polymers (SPs) are aggregates of monomer units held together by non-covalent interactions, such as electrostatic interactions, coordination bonds, hydrogen bonds, hydrophobic interactions and host-guest interactions[73]. Their formation is spontaneous and

reversible by self-assembly of the monomer units. Because of this special non-covalent intermolecular bonding, the formation and of the SP is under thermodynamic equilibrium, which means that the polymer growth or the destruction of the polymer chain can be adjusted by external stimuli. This reversibility makes decomposition SPs promising functional materials and gives them the potential to be easily processed, recycled or applied as self-healing materials. Recently, much attention has been focused on the preparation and application of SPs and the most promising systems have already found their fields of application ranging from cosmetics, printing, personal care to plastic industry[74].

CDs have been used as the host component for the construction of various interesting supramolecular structures such as pseudorotaxanes, rotaxanes, supramolecular dimers, oligomers and even polymers[75]. Modification of the parent CD molecule with an apolar substituent, which can form the inclusion complex with the CD's cavity results in a conjugate with the ability to self-associate into supramolecular assemblies in polar solvents. The formation of these structures is based mainly on the intermolecular host-guest interactions between the hydrophobic interior of the CD in one conjugate and the apolar substituent of another conjugate.

Earlier studies, however, pointed out that the size matching between the covalently attached guest part and between the CD's cavity is not the only requirement for the effective SP formation. In the case of mono-6-*O*-benzoyl-β-CD, for example, the direct attachment of the phenyl moiety to the CD rim did not result in intermolecular complex formation[76]. On the other hand, too long and flexible spacers between the host and the guest moiety favored the self-inclusion process of the guest part to the parent CD's cavity[77]. These findings showed that a compromise in the flexibility and in the length of the spacer has to be found for efficient formation of intermolecular complexes. With this aim cinnamoyl (Cio) moieties have been conjugated with α- and β-CD through amide and ester linkages by the group of Harada[44,78].

These monosubstituted derivatives formed various supramolecular assemblies (dimers, cyclic oligomers, linear polymers) in water depending on the position of the Cio moiety on the CD rim. It was also experimentally proven that the cavity of the CD shows distinguishable inclusion affinities towards different substrates, even to homologs and isomers. Self-sorting complex formation ability was described for the two regioisomers of monocinnamoyl-α-CD (Cio-α-CD). While the 2-Cio-α-CD isomer itself formed an insoluble double threaded supramolecular dimer in water, the 3-Cio-α-CD itself formed a soluble supramolecular oligomer in the same solvent. The mixture of the two regioisomers led to a formation of the self-sorting oligomeric system, where only the heterosupramolecular interactions between the

two isomers were present, but the homosupramolecular interactions between the same species were missing. This work clearly demonstrates that the intermolecular complex formation is a regioselective process where the CD cavity can differentiate between the positional isomers which results in different aggregation behavior of the regioisomers[44].

3.4 Fluorophore-tagged CDs

CDs due to their carbohydrate nature do not absorb light in the UV-Vis region (200-800 nm), but they can be converted into spectroscopically active compounds *via* modification with a chromophore unit. Among the chromophores, the group of fluorophores can provide high sensitivity in analytical applications (chemosensing) and low detection limit in optical imaging methods (fluorescent microscopy). Fluorophore-tagged CDs, therefore, combine interesting spectroscopic properties with promising supramolecular features which make these conjugates widely applicable in various pharmaceutical fields as fluorophore-labeled drug delivery systems, in different phototherapies or fluorescent detection of biologically relevant compounds.

The first fluorophore-tagged CDs were prepared more than 30 years ago with the aim to mimic photochemical processes of photosynthesis and to study the inclusion process using spectroscopic techniques[79,80]. With the increased interest in CD-containing drug formulations and CD-based drug delivery systems, fluorophore-appended CDs became important from another perspective as well. With their aid and with the help of sophisticated fluorescent imaging techniques it is possible to visualize and understand processes which CDs undergo in biological media. For this purpose, different labeling strategies have been developed throughout the years, which ensure the stability of fluorophore-CD conjugates against enzymatic degradation and therefore the reliability of the visualization process. Although the covalently attached fluorophore unit influences the properties of the CD core, the preparation of fluorescent CD derivatives generates potential tools for the visualization of the microenvironment and structural details in living cells and for studying the localization and movement of molecules in biological media. Furthermore, current trends in phototherapeutic applications show that fluorescent CDs can be successfully used to tackle resistance mechanisms in bacterial infections and cancer, which predicts a bright future for these colorful sugar molecules[81].

In the case of fluorophore-tagged CDs, the high DS is not a strict requirement as for imaging purposes low DS values (DS $\leq$ 1) are sufficient. Fluorescently-labeled CD

derivatives used for visualization (having DS < 1) are usually composite materials consisting of both unmodified CDs and CDs substituted with the fluorophore tag. On the other hand, applications such as chemosensing and photodynamic therapy (PDT), require well-defined systems in which all CD units are appended with a fluorophore, having, therefore, DS = 1. These derivatives are single-isomers, monosubstituted by the fluorophore unit. As discussed in section 3.2.1, monosubstituted CDs have three possible regioisomers, depending on the position of the substituent on the CD ring (2-*O*, 3-*O* and 6-*O* substituted derivatives). Several studies pointed out that the site of attachment of the fluorophore unit has an important impact on the spectroscopic and supramolecular behavior of the conjugate, therefore, the isomeric purity of fluorophore-appended CDs is of high importance in most of the applications[82,83,84]. In order to ensure isomeric purity, the fluorophore tagging is usually carried out through a multistep synthetic procedure. A suitable approach is to pre-modify the CD ring in a regioselective manner with an effective leaving group (i.e., tosyl or halides), which is then replaced by a nucleophile fluorophore molecule or by an azido moiety serving as anchoring group for the fluorescent tagging. In this second scenario, the fluorophore is connected to the CD scaffold through stable amide, thioureido or triazole linkages.

As the separation of 2-*O* and 3-*O* substituted products are laborious and time-consuming, the majority of the fluorophore-tagged CDs are primary-side substituted derivatives prepared from mono-6-*O* sulfonated intermediates. After the successful conjugation of the fluorophore with the CD unit, special attention has to be taken on the quantification of the free dye-related impurities and also on the stability of the linkage between the tag and the CD. The presence of residual dye-related impurities and the eventual cleavage of the tag from the conjugate during the application might lead to false positive and false negative results in the biological experiments.

Among the fluorescent dyes, the group of fluorophores based on xanthene scaffolds is the most popular. Widely used representatives of this class of fluorophores are fluorescein (Flu), rhodamine B (Rho) and the eosins (Figure 3) which have been applied as chemosensors[85] and have been exploited in various areas such as cell biology, microscopy, biotechnology and ophthalmology due to their versatile photophysical properties. However, the chemical modification of this evergreen class of dyes is still an ongoing process[86,87]. Flu is the most frequently used fluorescent probe in biological applications and in particular for labeling of amino acids, proteins, and enzymes[88]. Rhodamine derivatives are robust dyes that find application as fluorophores for microscopy, in cell sorting and colorimetric enzymatic

tests[89]. Eosin derivatives are known for their photobactericidal activity and are commonly used photosensitizing agents in PDT[90,91].

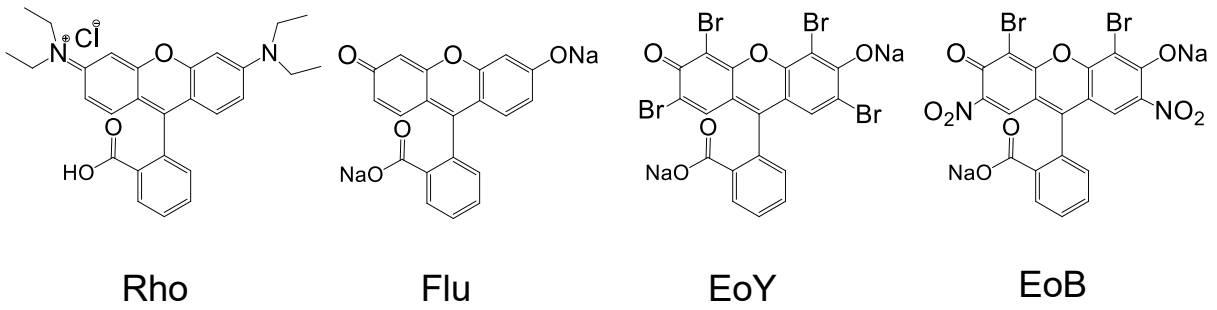

Figure 3. Structures of fluorescent xanthene dyes. Rhodamine B·HCl (Rho), fluorescein disodium salt (Flu), eosin Y disodium salt (EoY) and eosin B disodium salt (EoB).

The first attempt to exploit xanthene dye modification on CDs was performed to construct chemosensors with an additional property compared to aryl-CDs, the first CD-based fluorescent chemosensors. Flu is a xanthene dye derivative which can exist in cationic, anionic and neutral forms depending on the pH of the environment. Wang and co-workers prepared mono-6-*O*-fluoresceinyl-β-CD and demonstrated that the ionization state of the Flu moiety has a great impact on the inclusion of guest molecules[92]. As expected, this charge-changeable receptor differentiated guests based on electrostatic interactions. The binding of adamantane carboxylic acid to the cationic form of the host was larger by three orders of magnitudes compared to the anionic one. Interestingly the fluorescent conjugate showed also ability in discriminating uncharged guests. The anionic form bound the tested uncharged guests weaker than the neutral form did, while the cationic form generated complexes of the highest stability. These results indicated that charge effects might play a major role in binding of uncharged guests as well. Furthermore, these experimental observations confirmed the molecular orbital calculations of Kitagawa *et al*. showing that the complexation of a neutral polar guest into the CD cavity generates an electrostatic potential gradient with a positive potential on the primary side and negative potential on the secondary rim[93]. This gradient is further increased when a positive charge (cationic form of Flu) is located on the primary rim and decreased when the primary rim carries a negatively charged substituent (negative form of Flu). The preparation of mono-6-*O*-fluoresceinyl-β-CD applied in the work of Wang and co-workers consisted of ester formation between mono-6-*O*-tosyl-β-CD (Ts-β-CD) and Flu sodium salt in water[92]. Three years later the mono-6-*O*-fluoresceinyl-γ-CD conjugate was also

prepared and applied as a charge-changeable receptor for detecting terpenoids and bile acids[94]. The synthesis of the γ-derivative was also based on ester formation between the fluorophore and the CD scaffold, but in this case, mono(6-deoxy-6-iodo)-γ-CD was used as a precursor and DMF and anhydrous conditions were used for the successful ester formation. Mono-6-*O*-fluoresceinyl-γ-CD also showed pH tunable complexation properties, but its molecular recognition abilities were very different from that of the β-CD analog. Although it should reveal interesting sensing abilities towards aliphatic compounds, to the best of our knowledge, the α-member of this Flu-CD family has never been prepared.

Xanthene dyes as Flu or Rho are the most frequently used fluorescent probes in optical imaging of biological substrates; therefore, synthetic strategies for xanthene dye labeling of CDs were highly demanded to investigate the biological aspects of CD-based drug delivery. In the aforementioned Flu-appended CD chemosensors, however, the Flu moiety was attached to the CD cavity through an ester bond which precludes any biomedical application of these conjugates. In biological media, the biodegradability of the ester linkage would result in the cleavage of the conjugate and would consequently lead to false positive results in fluorescent microscopic or spectroscopic investigations. To circumvent this scenario, a more stable and resistant linkage against enzymatic degradation was required for xanthene-dye-CD conjugation. First Harada's group prepared stable rhodamine-α–CD conjugates with the purpose of visualizing CD-based rotaxanes (threaded CD molecules on axle molecule) immobilized on glass surface[95]. The synthetic strategy towards the rhodamine-labeled α-CD was based on the amide formation between the carboxyl function of the Rho and the amino moiety of mono(6-deoxy-6-amino)-α-CD by using coupling conditions *N,N′*-dicyclohexylcarbodiimide (DCC), *N*-hydroxybenzotriazole (HOBt) in anhydrous DMF. Similar approach was used by Hasegawa and co-workers for the conjugation of Rho dye with β-CD through a shorter ethylenediamine (EDA) and a longer and more flexible tetraethylenepentaamine (TEPA) linker[96]. Both derivatives were prepared from a pre-modified CD, monosubstituted by the aminonalkylamino moiety at the position *C*-6 and from Rho by using the coupling agent 1-ethyl-3-diaminopropyl-carbodiimide (EDC). The compounds obtained were used as pH sensitive probes to visualize cellular compartments with acidic property. The pH sensitivity was connected to the Rho moiety, due to its cyclization from amide form into a spirolactam form. This structural conversion between an opened and closed structure is a reversible process and is characteristic for xanthene dyes linked through an amidic bond[97]. In the case of Rho-TEPA-β-CD conjugate, this phenomenon resulted in remarkable changes in UV absorbance. At acidic pH, the opened amide form

showed absorbance at 576 nm while in basic conditions the spirolactam form did not show any significant UV absorption above 400 nm, which can be used to visualize acidic environments by fluorescence (Figure 4). This sensing ability of the Rho-TEPA-β-CD conjugate combined with its aqueous solubility and low cytotoxicity on HeLa cells made possible its application in the biological field. To the best of our knowledge, the work of Hasegawa and co-workers is the first example of Rho-linked CDs examined in biological matrices[96].

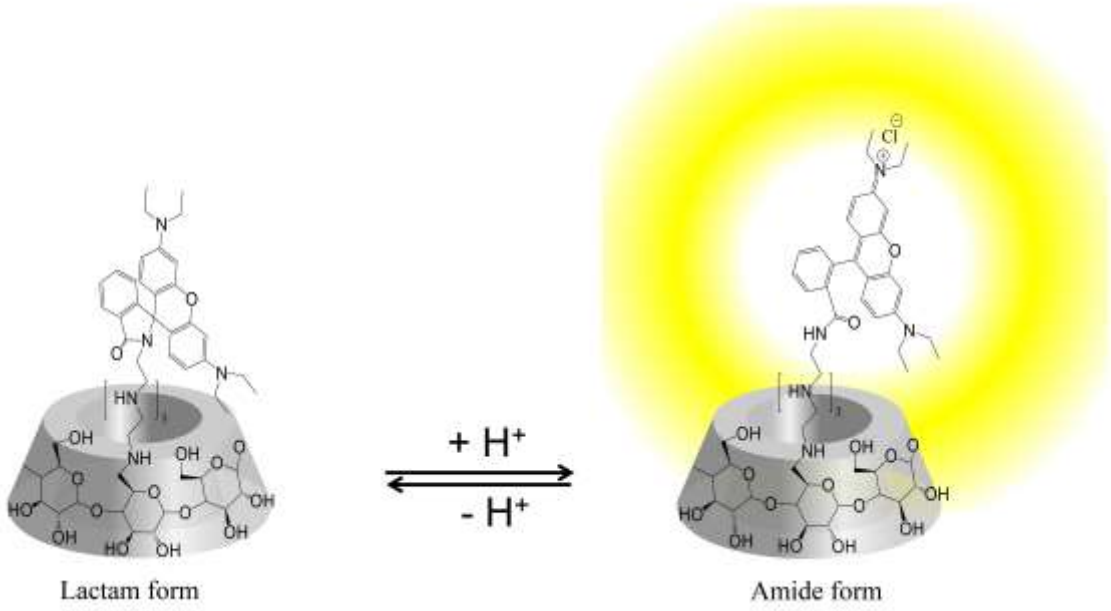

Figure 4. The structural conversion of lactam and amide form of rhodamine B linked to β-CD scaffold through an amide bond at different pH conditions[96].

Positively charged CDs are known to interact strongly with deoxyribonucleic acid (DNA) and to encapsulate it into spherical nanoparticles[98]. As a consequence, CD derivatives tailored for these purposes can be used as nonviral vectors in gene therapy applications. Visualization and better understanding of the DNA internalization with these CD-based transfection agents called for a strategy for the fluorescent labeling of positively charged CDs. It is well known that isothiocyanate compounds promptly react with amino functions in alkaline solutions and this is the main reason for their wide use as labeling agents. Mourtzis and co-workers used for the first time this type of chemistry to append fluorescein isothiocyanate (FITC) onto per(6-deoxy-6-guanidinoalkylamino)- and per(6-deoxy-6-aminoalkylamino)-β- and γ-CDs[99]. The enzymatically stable thioureido bond between the

probe and the CD core allowed these derivatives to be used for studying the DNA transfection process on HeLa cells by fluorescent microscopy. Although the focus point of these investigations was not the synthesis of pure fluorescent CD derivatives, but rather the biological visualization, the synthetic procedure is detailed and reproducible. Furthermore, this study represents the first *in-vitro* investigation of fluorophore-modified CDs. One year after Mourtzis work, the same strategy was chosen by the group of Wenz to prepare FITC-tagged NH_2-β-CD[100]. Threading this conjugate together with unmodified α-CD onto polymeric backbone afforded a polyrotaxene which could be visualized by fluorescence microscopy and atomic force microscopy. At this point, it is worth to mention that both pioneering research groups in the field of rotaxane molecules – the group of Harada and the group of Wenz - used xanthene-dye-appended CDs to get more information about rotaxane structures[95,100]. This means that although indirectly, fluorophore-tagged CDs also contributed to the development of mechanically bound structures – the Nobel-prize awarded molecules of 2016.

The approach of CD – xanthene-dye conjugation through thioureido linkage was not only extended to various positively and negatively charged, alkylated, hydroxyalkylated CD monomers, but also to polymeric CD scaffolds by CycloLab Cyclodextrin Research and Development Laboratory. The synthetic strategy is based on the versatility of mono(6-deoxy-6-azido)-β-CD (N_3-β-CD) intermediate. The azido moiety is usually stable under the reaction conditions used for the hydroxyl groups functionalization. After the hydroxyl modification, the azido group can be readily converted to amino function, allowing the selective reaction with isothiocyanate-modified xanthene dyes. Amino-modified[101], carboxymethylated[102], hydroxypropylated[102], phosphorylated[103], randomly methylated[104] β-CDs tagged with rhodamine B isothiocyanate (RBITC) or FITC at position *C*-6 became commercially available and boosted extensive research in biological and photochemical fields. Although the substitution pattern of these derivatives is random, the fluorescent probe in all the cases is located at the position *C*-6, due to the common intermediate N_3-β-CD. As the azido group stands the harsh alkaline conditions required for the cross-linking of several CD units, this approach is suitable also for the preparation of fluorescently labeled water-soluble epichlorohydrin-branched CD polymers[105]. Although xanthene dye tagging of CDs using thioureido chemistry is a versatile method in terms of CDs, it is limited from the viewpoint of xanthene dyes. Introduction of the isothiocyanate group onto the xanthene structure is not a straightforward process due to the formation of numerous positional isomers. Purification processes make the pure isothiocyanate-modified xanthene dyes very expensive and hardly

available from commercial sources. These limitations called for further exploitations of the amide bond formation between amino-functionalized CDs and the xanthene dyes since the carboxyl group is a common function in most of the commercially available xanthene dye derivatives. A green coupling method has been recently developed for Rho and Flu tagging of NH_2-β-CD using 4-(4,6-dimethoxy-1,3,5-triazin-2-yl)-4-methyl morpholinium chloride (DMT-MM) as coupling agent under mild reaction conditions[106]. Since this strategy did not require the isothiocyanate-premodified dyes, it could be easily extended for eosin B (EoB) and eosin Y (EoY) conjugation of NH_2-β-CD[107], which demonstrates the versatility of this synthetic route.

3.4.1 Optical imaging of drug delivery systems: fluorophore-tagged CDs crossing barriers

The fact that modified CDs are able to interact with a wide range of biomolecules changed the beliefs about their pharmaceutical application. As these molecules cannot be considered only latent participants of the drug delivery process, their pharmacokinetic profile, from the administration until the excretion, must be deeply investigated. Native CDs have been used in pharmaceutical industry for decades, and several mechanisms of action have been established during the years based on relevant biochemical investigations and on *in-silico* studies as well. According to the most accepted theories, native CDs transport their complexed cargo until the outer surface of the cell membrane, where the inclusion complex dissociates, and the free drug enters the cell, while the CD carrier after certain amount of time leaves the extracellular environment[108]. The three commonly used CDs, α-, β- and γ-CD do not enter, neither bind nor insert into the plasma membrane, therefore they are rapidly excreted from the body. Recently published results from computational investigations also proved that an inclusion complex of a model guest molecule with β-CD faces too large energy barrier to penetrate through biological membranes[109]. These models, however, cannot be simply extended to the chemically modified CDs. Methylated β-CDs, for instance, are known to complex and extract cholesterol from the cell membranes; therefore, they do not act only as drop-and-leave molecular vehicles for guest molecule[110]. After the dissociation of their host-guest complex, the 'empty' CD certainly alters the cellular environment by complexing cholesterol. The disruption of cholesterol-rich membrane rafts may alter the integrity of the cell barriers, can increase their permeability and modify the absorption of bioactive molecules with consequences that are difficult to predict.

These data raise many important questions about CDs:

- Are methylated CDs able to complex also the intracellular cholesterol, or do they interact only with the outer membrane lipids?

- Are CDs able to enter cells? If they are able to enter, which cell organelle is their primary target?

- What is the mechanism of their internalization?

Due to the availability of fluorophore-tagged CDs discussed in section 3.4, many research groups tried to answer these questions. Hasegawa and co-workers investigated the possibility of selective staining of acidic cell compartments of living HeLa cells with Rho-TEPA-β-CD[96]. This conjugate, being fluorescent only at low pH values (when it is present in the amide form), was localized with a fluorescent microscope in lysosomes, while the unconjugated Rho did not give any selective staining. These data strongly suggested the Rho-TEPA-β-CD internalization; furthermore, they showed that this derivative can be used as a selective marker of acidic cell compartments. The authors of this study assumed that the accumulation of Rho-TEPA-β-CD in lysosomes was the result of endocytosis, but this hypothesis was not further investigated. The internalization process of FITC-labeled CD derivatives carrying multiple positive charges was also studied on HeLa cells[99]. The per(6-deoxy-6-guanidinoalkylamino)- and per(6-deoxy-6-aminoalkylamino) derivatives of β- and γ-CD entered the cytoplasm, as revealed by confocal microscopy. Interestingly the guanidinoalkylamino derivatives internalized faster than the aminoalkylamino derivatives, while the FITC/β-CD inclusion complex or the FITC-labeled mono-NH_2-β-CD used in the control experiments showed no internalization. These findings clearly demonstrated the importance of the high local density of positive charges for the cellular entry. Due to the structural similarity of guanidinoalkylamino-CDs to the well-known hepta-arginine cell-penetrating peptides, the authors proposed that these cationic CDs also use a passive transfer mechanism through the lipid bilayer for entering the cells. However, because of the cholesterol complexing ability of CDs, the contribution of additional membrane relaxation processes to the internalization could not be excluded.

During the development of effective CD based transfection agents, Diaz-Moscoso studied another per-6-multicationic-CD, equipped with long fatty acid chains on the secondary side[111]. This amphiphilic system was able to compact DNA into stable nanoparticles. The uptake mechanism of these nanoparticles (CDplexes) by Vero cells was

studied in the presence of selective endocytic pathway inhibitors (chlorpromazine, genistein, dynasore and methylated β-CD). Furthermore, to achieve a deep insight into the transfection process, the intracellular trafficking was investigated by using an *ad-hoc* prepared lissamine-rhodamine-labeled amphiphilic β-CD. Confocal microscopy data revealed that the labeled CDplexes were internalized within 40 minutes and were accumulated in the proximity of the cell nucleus. The study on selective endocytic pathway inhibition showed that CDplex internalization is a complex process involving both clathrin-dependent and clathrin-independent endocytosis. Another important observation of this work was that CDplexes were not detected inside the cellular membrane, which rules out their irreversible interaction with the membrane lipids and the previously hypothesized internalization mechanism due to cholesterol depletion.

To further address the influence of cholesterol extraction on the cellular uptake of CDs, Plazzo *et al.* studied FITC-tagged methylated-β-CD (FITC-Me-β-CD) uptake by HeLa cells[112]. At first, the ability of FITC-Me-β-CD to bind cholesterol was demonstrated using spin-labeled cholesterol and electron paramagnetic resonance measurements; then, a series of confocal microscopy experiments were conducted to follow the cellular uptake and the distribution of FITC-Me-β-CD under different conditions. The fluorescence intensity of FITC-Me-β-CD inside the cell membranes turned out to be dependent on incubation time, the concentration of FITC-Me-β-CD used for incubation, and on the temperature. Furthermore, FITC-Me-β-CD was colocalized in vesicles with a marker for clathrin-dependent endocytosis (Tf texas red), and its internalization was effectively inhibited with chlorpromazine and rottlerin, which indicates that FITC-Me-β-CD enters HeLa cells through receptor-mediated endocytosis. Cholesterol pre-loaded FITC-Me-β-CD's internalization was also studied in this work, and it showed no differences compared to the uptake of 'empty' FITC-Me-β-CD. This is an additional proof that cholesterol binding is not affecting the cellular uptake of CDs significantly. The cell penetration effect of FITC-Me-β-CD was further examined on intestinal epithelial CaCo-2 cells by Fenyvesi and co-workers, with flow cytometry, confocal microscopy, and transepithelial permeability measurements and demonstrated that methylated CDs can also enter intestinal epithelial cells by endocytotic mechanism[113].

As it can be seen from the reported examples, CD derivatives do not only increase the solubility of poorly soluble drugs and act as permeation enhancers but are also able to enter cells thus improving the drug bioavailability. This contribution of the CD endocytosis to the drug delivery process can be directly demonstrated by visualizing the absorption of fluorescent drug molecules complexed in fluorophore-tagged CD carriers. This approach was

used recently by Reti-Nagy *et al*. who studied the role of CD endocytosis on the drug delivery of paclitaxel[114]. This study was performed on intestinal Caco-2 cells, and the effect of FITC-labeled HP-β-CD, RBITC-labeled Me-β-CD, and FITC-labeled epichlorohydrin-crosslinked β-CD polymer was investigated. Similarly to the results of the previous works, the internalization of all the three types of labeled CD carriers was confirmed by fluorescent microscopy. Surprisingly, rottlerin, a selective inhibitor of macropinocytosis, could not inhibit RBITC-Me-β-CD internalization, while in a previous work of the same research group the same inhibitor decreased the endocytosis of FITC-Me-β-CD[113]. These results indicate that slight changes in the fluorescent label on the same CD scaffold can lead to different internalization mechanism. This finding leads to the question if the behavior of the labeled CDs allows to draw conclusions on the behavior of the nonlabeled CD. The FITC labeled β-CD polymer had no impact on paclitaxel uptake, but, on the other hand, FITC-HP-β-CD and RBITC-Me-β-CD were found to have a positive impact on it. Moreover, the contribution of CD internalization on drug absorption was proved at a cellular level as well, since intracellular colocalization of the fluorescent paclitaxel derivative (Flutax-1) and the RBITC-Me-β-CD could be identified.

3.4.2 Fluorophore-tagged CDs as phototherapeutics

CDs have been greatly developed during the last thirty years as carriers of "conventional" drugs[115,116]. However, the use of CDs as suitable vehicles for photoactivable therapeutic compounds has been only recently object of attention[117]. Due to their hydrophobic cavity, natural CDs can host a variety of photosensitive agents by supramolecular interactions[118,119]. Nevertheless, in most cases, the low binding constants between unmodified CDs and guest molecules represent a major drawback of these systems as bio-carriers, making the modification of the CD structure strictly necessary in view of actual applications[120]. Modification of the CDs molecular scaffold through functionalization of the primary or secondary hydroxyl groups with suitable photoresponsive units allows to obtain multifunctional nanocarriers with intriguing properties while, at the same time, maintaining the macrocycle's capacity for guests encapsulation[99,121].

Reactive Oxygen Species (ROS) are produced by biological processes for the correct metabolic functionality. Their concentration is controlled by a complex metabolic balance, whose dysfunction can generate high concentrations of ROS, which result in toxic effects, as

observed in a number of inflammatory diseases. The cytotoxicity of ROS can be however used against bacterial and tumor pathologies in a new treatment modality, called PDT.

PDT takes advantage of the effects arising from the appropriate combination of visible light with a photosensitizer (PS) in the presence of molecular oxygen[122,123]. The excited PS transfers the energy of its long-lived excited triplet state to nearby molecular oxygen. This process results, in general, in the *in situ* production of singlet oxygen ($^1O_2$) which is the foremost mediator of cytotoxic reactions in the cells[124]. One of the biggest advantages of PDT is that this approach does not suffer multi-drug resistance problems, which is an alarming threat to current anticancer and antibiotic therapies. PDTs efficacy against multidrug-resistant pathogens and tumor cells comes from the multitarget character of the formed toxic species. $^1O_2$ can cause irreversible cellular damages leading to cell death, but the cell response to PDT depends mainly on the experimental conditions, such as the PS dose and the subcellular localization of the PS. The first of these conditions can be easily controlled with the intensity and the location of the light irradiation, while the latter one is a specificity of the applied PS.

Porphyrins, phthalocyanines, and xanthene dyes are well-known and widely used PS agents by virtue of their high quantum yields, long lifetimes of their excited state, minimal dark toxicity and strong absorption in the visible region, all important prerequisites of a successful PDT application. However, many promising photosensitizing systems are hampered by their intrinsic low aqueous solubility and by aggregation phenomena that compromise their efficacy. These parameters are very critical for the photodynamic effect, as low solubility affects bio-distribution, cellular uptake and $^1O_2$ production of the PS. Furthermore, aggregation processes can deactivate the excited electronic states of PSs and cause further loss of photoreactivity.

CD technology offers a great opportunity to face solubility and aggregation problems. By developing well-determined methods for selective modification of CDs, in recent years the covalent conjugation of porphyrins[125], phtalocyanines[126] and xanthene dye derivatives[127] with CD scaffolds have attracted considerable interest in PDT. This approach not only improves the PSs amphiphilicity and biocompatibility, but in the cases where the conjugated dye does not occupy the CD cavity, also offers an additional binding-site for a co-drug, enabling thereby the application of these systems in combined phototherapies. This methodology was followed by Kralova *et al*. and also by Lourenco *et al.* during the development of porphyrin-appended β- and γ-CDs and porphyrin-linked bis-β-CD[125,126]. These host molecules were able to accommodate cytotoxic drugs such as doxorubicin and paclitaxel which allows the attack on tumor cells from two different perspectives: through conventional chemotherapy due to the

cytostatic effects of the complexed drug and through the photodynamic effect of the covalently linked porphyrin. Furthermore, the porphyrin moiety turned out to be an efficient targeting unit for tumor tissues which makes these systems very attractive in multimodal cancer therapy.

3.5 Persubstituted anionic CDs as chiral selectors for capillary electrophoresis

CDs are the most commonly used chiral resolving agents in CE because of their high separation efficiency and reasonable selectivity without interfering with analyte detection[129,130]. However, the application of native CDs in CE has some limitations. Low aqueous solubility is a major problem especially in the case of β-CD as the optimal CD concentration necessary for the enantiomer recognition may exceed the solubility limit.

Semisynthetic CD derivatives bearing ionizable functional groups possess enhanced water solubility and also self-electrophoretic mobility. The self-mobility of charged CDs makes the enantioseparation of uncharged enantiomers possible, and it is also advantageous in the case of charged analytes because of the strong ionic interaction between the oppositely charged species. All these advantages led to the development of a wide range of different ionic CD derivatives. The most successful representatives (such as sulfated, carboxymethylated and sulfobutylated) became commercially available as randomly substituted derivatives[131,132]. Despite the ease of their preparation and their extensive application in CCE, randomly substituted CDs are mixtures of positional isomers and variously substituted homologs. In such a mixture, each entity has its own unique binding characteristics for a given enantiomer pair. Therefore, chiral separations with these products suffer from a low batch-to-batch reproducibility and the outcome of the separation cannot be predicted.

To have a better control over the molecular recognition processes and to achieve more predictable separations, SIDs have been synthesized and characterized[25,133,134,135,136]. Their typical representatives, frequently applied in CCE are the monosubstituted CDs and the persubstituted CDs. The application of persubstituted anionic SIDs for chiral separation was introduced by Vigh and co-workers[133]. This group prepared and characterized various families of structurally well-defined sulfated CDs with high isomeric purity. In the first generation of these sulfated SIDs, position *O*-6 was persubstituted with sulfo groups while the remaining *O*-2 and *O*-3 positions of the glucopyranose units were bearing identical alkyl or acetyl substituents or they were unmodified, bearing hydroxyl groups in both positions[25,133,134]. The

first generation was followed by the second generation of sulfated SIDs where the *O*-6 positions were bearing the sulfo groups, but the *O*-2 and *O*-3 positions were differently substituted[135]. In the most recent work of the Vigh group in this field, the synthesis and the novel CE use of a completely original class of sulfated CDs was reported[136]. In this study, the sulfo groups were located exclusively on the *O*-2 positions, while the remaining *O*-3 and *O*-6 positions were non-identically persubstituted with methyl and acetyl groups, respectively. These structurally related classes of SIDs allowed systematic studies comparing the effect of the substituents and the impact of their location in the enantiorecognition process. The fact that the development of these chiral selectors is still ongoing even 20 years after their introduction, clearly shows their synthetic versatility and demonstrates that sulfated SIDs have a central role in enantioresolutions. Till nowadays these compounds have been the only persubstituted negatively charged SIDs used in CCE. Several review articles[129,137,138] pointed out the unambiguous superiority of these selectors over the corresponding randomly substituted CDs. A clear advantage of this class of compounds originates from their strong ionic character. These molecules being permanently negatively charged assure a strong interaction with cationic analytes at any pH. This simplifies the development of CCE methods since the separation selectivity can be determined as a function of the concentration of the chiral selector and the pH of the BGE (CHARM-model)[139].

The strong ionic interaction between the sulfated SIDs and the cationic analytes is an unquestionable advantage which helps to predict and understand the enantioseparation process. Despite of the great advantages of strong ionic SIDs, Cucinotta *et al.* proposed an alternative approach for the development of an ideal chiral selector[138]. Their argument was based on the theory of Wren and Rowe stating that the experimental conditions maximizing the difference in the formation degree of diastereoisomeric complexes are preferred over those maximizing the degree of formation of both diastereomeric complexes[140]. This approach justifies the development of other types of SID selectors besides the strong anionic SIDs. In this aspect, a chiral selector with a well-defined structure and with an additional tunable ionization state would be a promising tool in CCE. The comparison of the enantioselectivity of the proposed weak anionic SIDs at various pH values would provide experimental evidence for the necessity of strong ionic interaction between the selector and the analyte. If high selectivities are found even in the case of an uncharged selector, the role of ionic interaction in the enantioselectivity should be reconsidered[141].

Carboxymethyl (CM) SIDs are ideal candidates for this purpose since the presence and magnitude of their negative charge are pH-dependent. Rezanka *et al.* described the

preparation of monosubstituted CM SIDs and their application in CCE[26]. Since in the case of monosubstituted CDs three regioisomers may exist, carrying the substituent at the position *O*-2, *O*-3 or *O*-6, respectively, Rezanka *et al.* focused on the impact of the position of the CM group on the enantioselectivity of the chiral selector. They prepared a complete set of regioisomers of monosubstituted CM-CDs and compared the enantioselectivities of the regioisomers. Although with these monosubstituted CM-CDs it was unambiguously proven that the position of the functional group plays an important role, these selectors could not offer a wide variability in ionization state; therefore, they cannot be considered the best candidates to study the influence of the selector's ionization state on the enantioseparation.

Depending on the pH of the BGE these compounds can carry a single negative charge or can be electroneutral at low pH values. Persubstituted CM SIDs, on the other hand, would provide a wide range of differently dissociated forms depending on the pH of the BGE; therefore, they are more versatile tools for a better understanding on the influence of electrostatic interactions in the enantiorecognition process.

The first synthesis of CD derivative persubstituted by CM functions on its primary side and by methyl groups on its *O*-2 and *O*-3 positions was reported by DeGrado and Akerfeldt[142]. The preparation consisted of 5 reaction steps and a final purification of the product by high-performance liquid chromatography (HPLC), therefore not suitable for multi-gram preparations. The synthesis of this percarboxymethylated β-CD derivative was improved by Kraus *et al.*[66], furthermore it was also extended to the α-CD without the need of HPLC purification. A few years later, Culha and co-workers utilized the procedure of Kraus for the preparation of the β-CD derivative with the aim to compare its enantiomer separation selectivity with the commercially available sulfated analog and with randomly carboxymethylated β-CD. The initial electrophoresis study showed promising results, but the synthesis in Culha's case did not result in a single-isomer compound but in a mixture of homologs, variously substituted on the primary side[143]. More recently Idriss *et al.* reinvestigated the β-analog as an MRI contrast agent exploiting the chelating ability[144]. Moreover, the γ-member of this family of compounds shows a structural similarity to the molecule of Sugammadex; therefore its complexation ability towards aminosteroidical muscle relaxing agents might have a potential applicability[145].

These compounds are typical representatives of persubstituted CM SIDs, but their application as chiral resolving agents has not been described to date. One of the objectives of this thesis has been to prepare persubstituted CM-CDs: the sodium salt of octakis(2,3-di-*O*-methyl-6-*O*-carboxymethyl)-γ-CD (ODMCM-γ-CD) and the sodium salt of heptakis(2,3-di-

O-methyl-6-*O*-carboxymethyl)-β-CD (HDMCM-β-CD), to elaborate their application as chiral resolving agents and to investigate the effect of their ionization state on the enantioseparation of various analytes.

4. Results and discussion

4.1 Synthesis of monocinnamyl-α-CDs

The strategy towards supramolecular polymers (SPs) – polymeric structures whose monomeric units hold together via highly directional and reversible non-covalent interactions - was based on the preparation of monocinnamyl-α-CDs (Cin-α-CDs), where the rigid double bond in the cinnamyl moiety should prevent the self-inclusion of the phenyl ring into the CD cavity and favor the formation of intermolecular complexes in polar solvents. Inspired by the previous results concerning the ability of Cio-α-CDs to form supramolecular polymeric structures[44], the aim was to prepare pure regioisomers of cinnamyl-appended α-CD, to test and compare their ability to form supramolecular architectures and to investigate their application as additives to the BGE in capillary separation techniques. As this analytical application requires chemically stable entities, the preparation of the cinnamyl conjugates was based on ether linkages instead of labile ester bonds. The family of Cin-α-CDs was synthesized according to this strategy. The complete set of peracetylated regioisomers of Cin-α-CD was previously prepared and characterized, but attempts to separate the unmodified 2-*O*- **(1a)** and 3-*O*-Cin-α-CD **(1b)** regioisomers were unsuccessful[38]. In order to isolate the single regioisomers using the reported procedures, exhaustive per-*O*-acetylation of the regioisomers mixture, chromatographic separation of the per-*O*-acetylated derivatives and the de-*O*-acetylation of regioisomers must be performed. These three reactions make the large-scale preparation of the single regioisomers expensive and time-consuming. Instead of using a series of protection and deprotection steps, a direct synthetic approach was selected for the preparation of the Cin-*α*-CD regioisomers. In more detail, the synthesis of 6-*O*-Cin-α-CD **(2)** was adapted from a reported procedure[42]. Native α-CD was reacted with cinnamyl bromide at 0 °C in aqueous alkaline solution. Under these strongly basic conditions the deprotonation of all the hydroxy groups results in an electrophilic attack at position 6, because it is the most accessible one. After preparative direct-phase chromatographic purification, the 6-*O*-Cin-*α*-CD regioisomer was isolated in 5% yield. 2-*O*-Cin-α-CD and 3-*O*-Cin-α-CD were synthesized by using DMSO as a solvent, NaH as a base and cinnamyl-bromide as an

alkylating agent. The reaction resulted in a mixture of unreacted α-CD, monosubstituted α-CDs, and disubstituted α-CDs. From this mixture, 2-*O*-Cin-α-CD and 3-*O*-Cin-α-CD were isolated in a single preparative reversed-phase chromatographic cycle by using H_2O/MeOH step gradient elution. This procedure allowed the preparation of the complete set of Cin-α-CD regioisomers in suitable amounts for the detailed characterization of their aggregation ability and for their application in CE. The monosubstituted products were characterized by ESI-mass spectrometry (MS), ^{1}H NMR and ^{13}C NMR spectroscopy and the three positional isomers were unambiguously distinguished and characterized by cross-linking the data of ^{1}H NMR, ^{13}C NMR, correlation spectroscopy NMR (COSY), total correlated spectroscopy NMR (TOCSY), distortionless enhanced polarization transfer edited heteronuclear single quantum correlation NMR (DEPT-edited-HSQC) and heteronuclear multiple bond coherence NMR (HMBC). As an example, the elucidation of the 2-*O*-Cin-α-CD regioisomer is discussed here. The allylic proton signals can be detected in a separated region of the ^{1}H-proton spectrum around 4.47 ppm (see proton A in Figure 5).

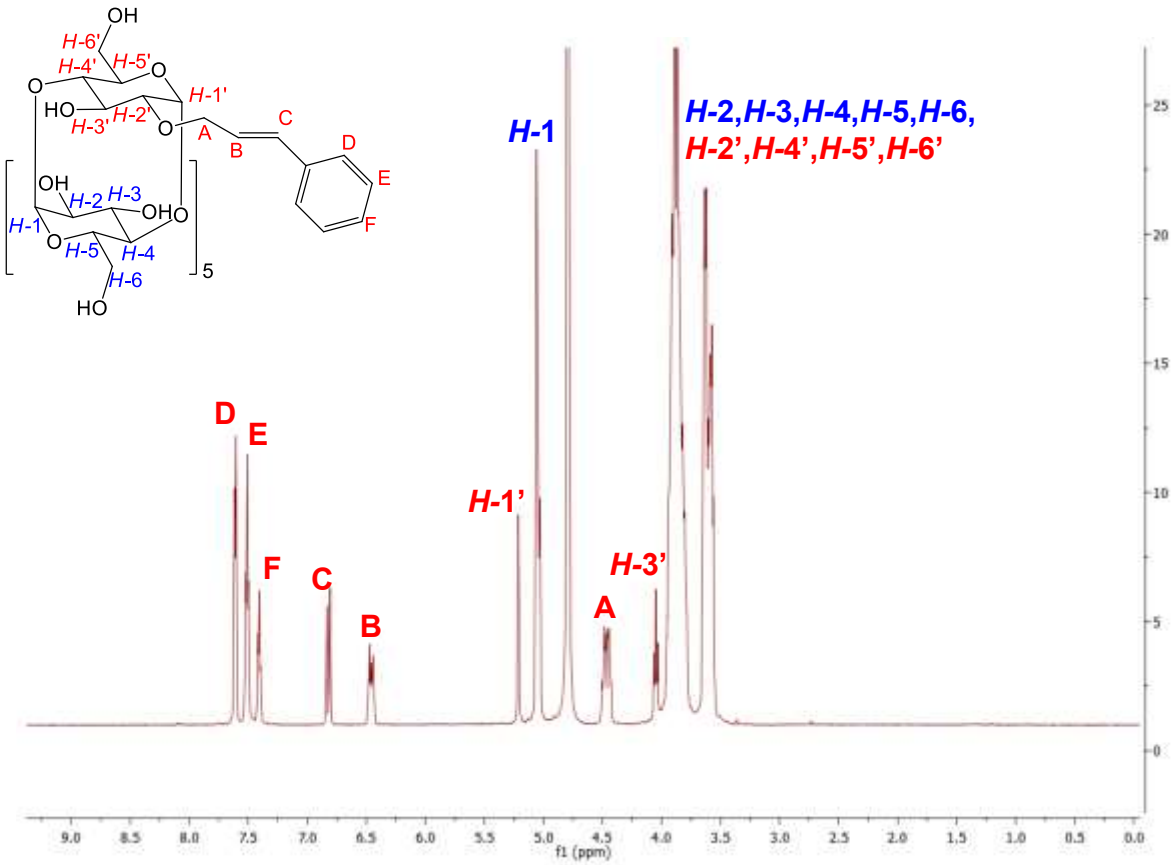

Figure 5. ^{1}H NMR spectrum of 2-*O*-Cin-α-CD **(1a)** in D_2O (600 MHz, 25 °C).

These frequencies can also be easily identified in the DEPT-edited-HSQC spectrum of the compound (see A in Figure 6b). The DEPT-edited-HSQC spectrum clearly shows that the compound is unsubstituted at the *O*-6 position, since the characteristic resonances of the two magnetically non-equivalent protons (*H*-6a and *H*-6b), typical for primary-side monosubstituted CD[146], are not detectable in the spectrum (Figure 6b). Another sign of the unsubstituted primary side can be observed solely by looking at the ^{13}C NMR spectrum. Earlier works of Rezanka et al. pointed out that if a monosubstituted CD bears its substitutent on its primary side, it shows a significaly downfield shifted signal of the substituted *C*-6' atom[30]. As no such signal can be observed here, the substitution must occur on the secondary side and as a consequence, the compound is *O*-2 or *O*-3 monosubstituted (the monosubstitution has been effectively proven by MS). Analyzing the HMBC spectrum (Figure 6c), cross-peaks between the allylic protons A (4.47 ppm) and a CD-related carbon at 81.38 ppm can be detected (see the black circle in Figure 6c). This carbon resonance (81.38 ppm) can either belong to *C*-2' or *C*-3' of the glucose unit bearing the cinnamyl substituent (otherwise the cross-peak would not be present in the HMBC spectrum). The frequency of this carbon (and of the correlated proton at 3.57 ppm) can be also detected in the DEPT-edited HSQC spectrum (see *C*-2' in Figure 6b). Finally, the COSY spectrum clarifies that the carbon at 81.38 ppm corresponds to the *C*-2' since the cross-peak with the anomeric resonance can be detected (see the black circles in Figure 6d). This set of data proves unambiguously that the compound is the 2-*O*-Cin-α-CD.

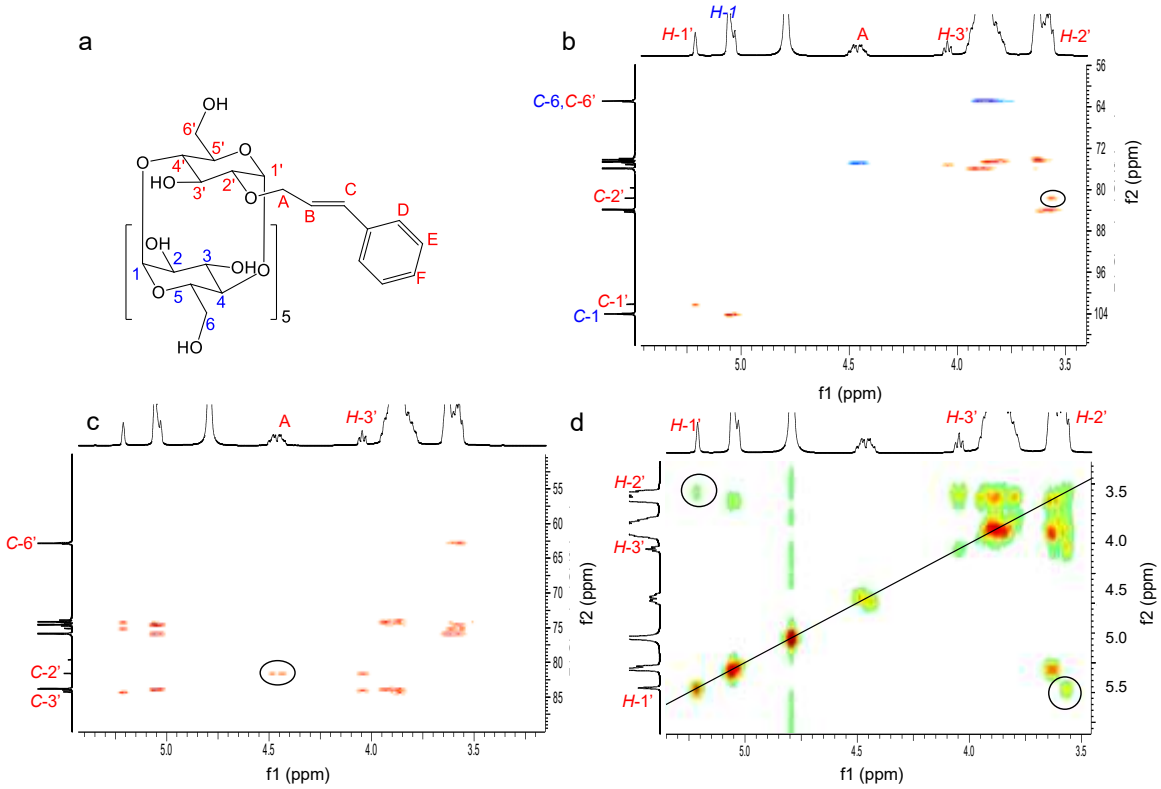

Figure 6. 2D NMR spectra (D_2O, 600 MHz, 25 °C) used for structure elucidation of 2-*O*-Cin-α-CD: a) structure of 2-*O*-Cin-α-CD with atom labeling of the glucose units b) part of DEPT-edited HSQC spectrum of 2-*O*-Cin-α-CD c) part of the HMBC spectrum of 2-*O*-Cin-α-CD d) part of the COSY spectrum of 2-*O*-Cin-α-CD.

A schematic representation of the spectral evidences used for the identification of the cinnamyl position is shown in Figure 7.

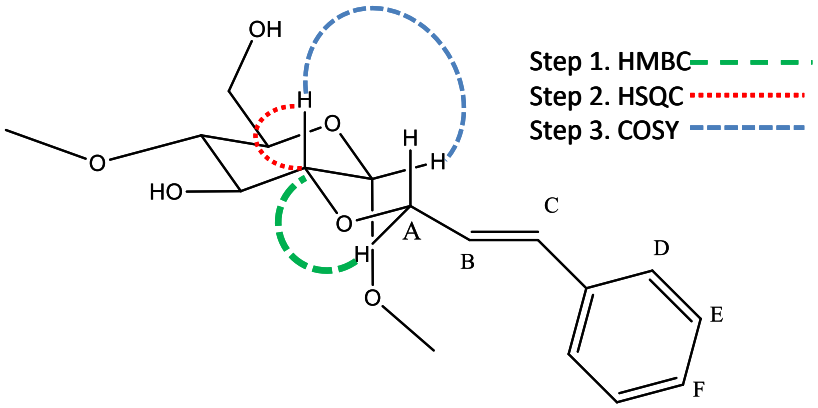

Figure 7. Example of elucidation of 2D NMR spectra of 2-*O*-Cin-α-CD.

4.2 Supramolecular characterization of regioisomers of monocinnamyl-α-CD

6-*O*-Cin-α-CD was found to be sparingly soluble in water (<5 mg/mL at 25°C) which precluded the in-depth study of the aggregation behavior of this isomer. On the other hand, both 2-*O*-Cin-α-CD and 3-*O*-Cin-α-CD are well soluble in water, therefore, the supramolecular structures of these secondary-side substituted regioisomers were first investigated in D_2O solutions. When the cinnamyl moiety is included in the CD cavity thus forming intermolecular complexes or self-included intramolecular species, the 2D ROESY spectrum shows this interaction as NOE cross-peaks between the inner hydrogens (*H*-3 and *H*-5) of the CD cavity and the aromatic or double bond hydrogens of the cinnamyl moiety.

In the spectra of both regioisomers, intense correlations were observed between the phenyl protons (7.2-7.5 ppm) and the protons of the CD cavity (3.6-4.1 ppm) (red circles in Figure 8) proving that the phenyl part is located in the CD cavity.

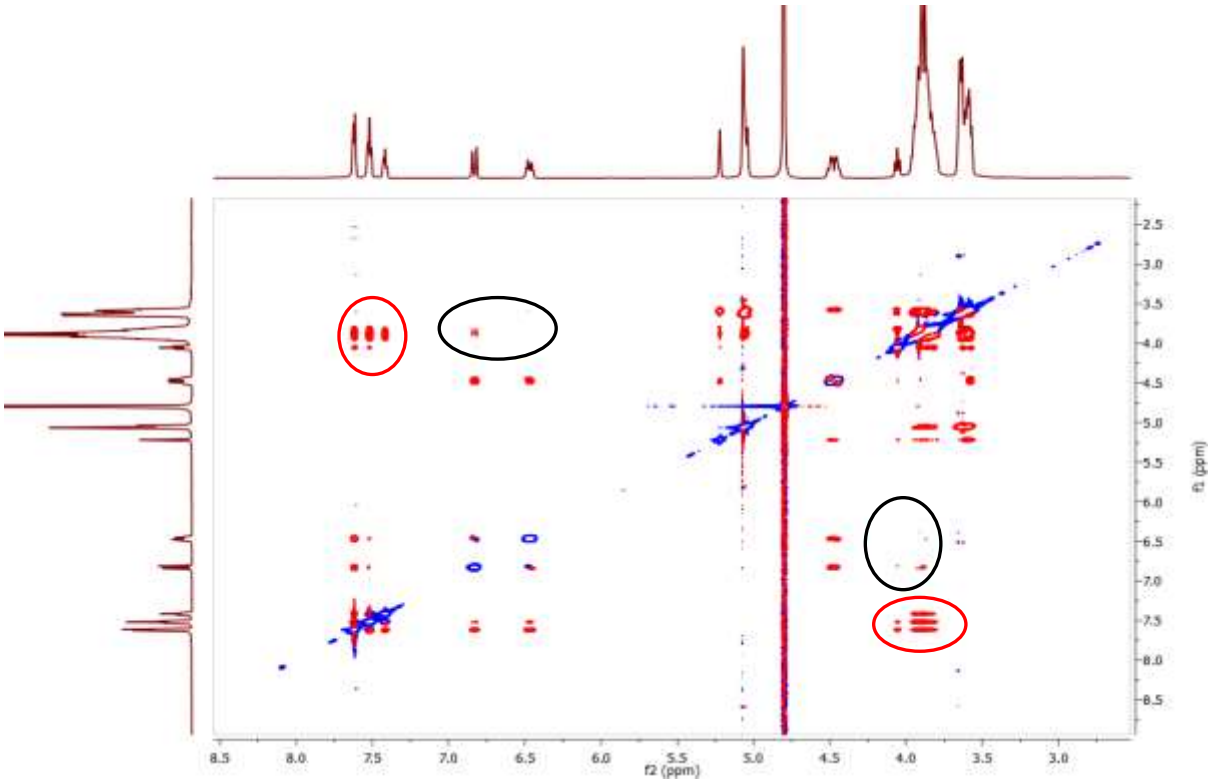

Figure 8. 2D ROESY spectrum of 2-*O*-Cin-α-CD in D_2O at 25 °C at 24 mM concentration (600 MHz).

These correlations were observed for both inner proton region at 3.6-3.8 ppm for protons *H*-5 (red dashed line in Figure 9) and 3.8-4.1 for protons *H*-3 (black dashed line in Figure 9) indicating, that the cinnamyl part penetrated deeply into the CD cavity. Less intense cross-correlation was found for the two protons from the double bond region of the cinnamyl moiety (6.2-6.7 ppm) (black circles in Figure 8), but their presence indicates that the double bond is also situated in the proximity of the cavity and therefore contributing to the host-guest interaction.

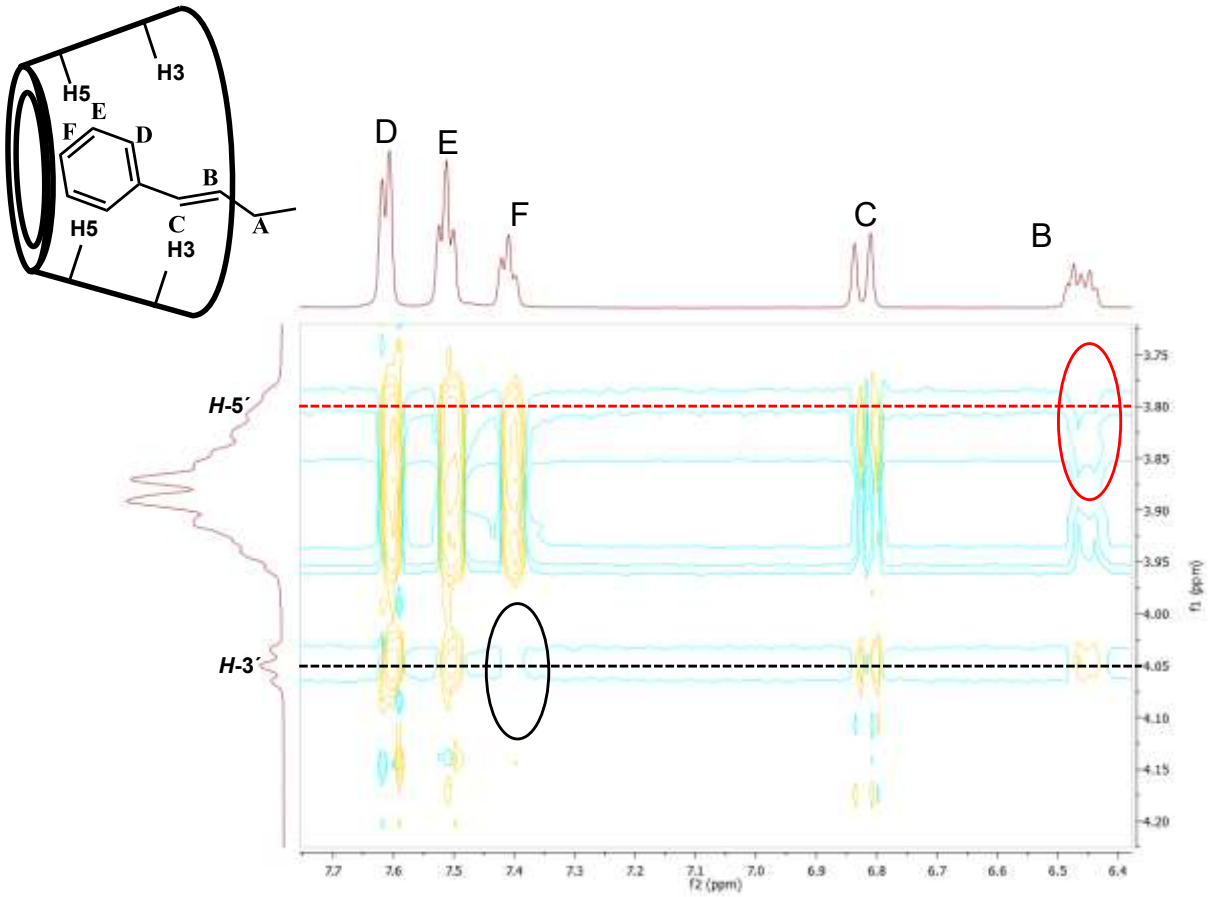

Figure 9. Expansion of the 2D ROESY spectrum of 2-*O*-Cin-α-CD indicating the geometric arrangement (D_2O, 600 MHz, 25 °C).

More detailed study of the ROESY spectra (see Figure 9) provided relevant information about the mode of the host-guest interaction. Important differences can be observed between the interactions of the two double bond protons (B and C in Figure 9) with the cavity. In the 2D ROESY spectra of both regioisomers, proton C interacts with both cavity protons (*H*-3 and *H*-5), indicating that proton C penetrated into the cavity. On the other hand, proton B shows interaction only with *H*-3, but there is no interaction with *H*-5 (red circle in Figure 9), suggesting that the linker in the host-guest complex is closer to the wider rim of the CD. Aromatic protons D, E and F also interact differently with the two inner protons of the

cavity. While protons D and E show cross-correlation with both protons *H*-3 and *H*-5, proton F interacts only with *H*-5, but it does not interact with proton *H*-3 (black circle in Fig. 9). These observations altogether leave us with only one possible mode of interaction, which is the inclusion of the cinnamyl moiety to the cavity from the secondary side (the side close to the *H*-3 protons) and not from the primary side (the side close to the *H*-5 protons) of the CD's cavity. The 2D ROESY spectra of the two studied regioisomer are comparable, showing that in both cases the cinnamyl group is located inside the CD cavity and in both molecules this inclusion phenomenon takes place from the secondary side of the CD cavity.

To further investigate the supramolecular structures and the effect of different external stimuli on the size distribution of the supramolecular assemblies, a series of dynamic light scattering (DLS) experiments was performed. As the first parameter, the effect of different solvents on the size distribution was tested. In aqueous solution both regioisomers formed large aggregates with a hydrodynamic diameter (D_h) up to 700 nm and the size of the aggregates formed by 2-*O*-Cin-α-CD or 3-*O*-Cin-α-CD were comparable (see Record 1 in Figure 10 and Figure 11).

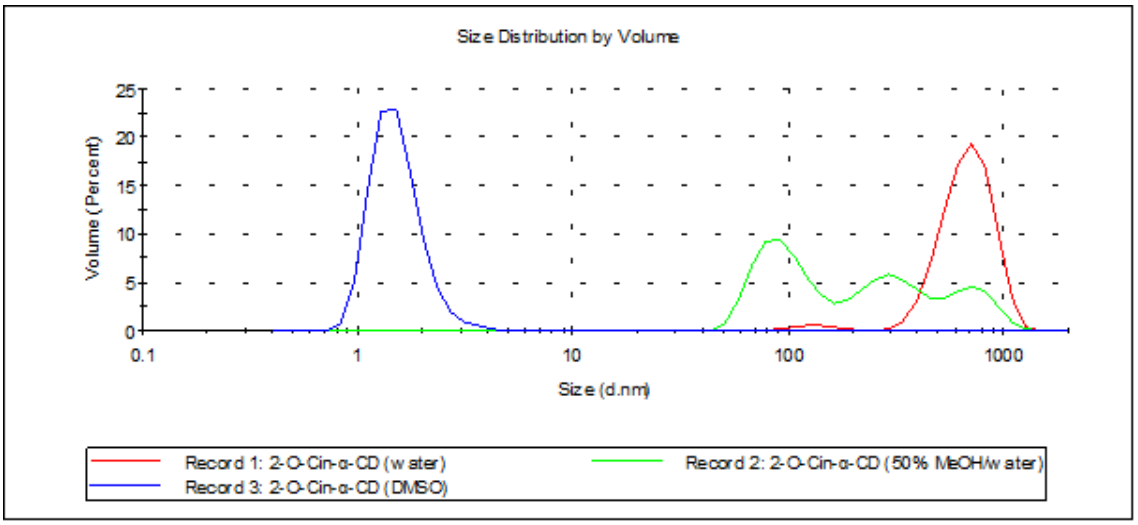

Figure 10. Effect of solvent on the size distribution of aggregates formed by 2-*O*-Cin-α-CD at 25 °C (the applied concentrations are 10 mg/mL (9.2 mM)).

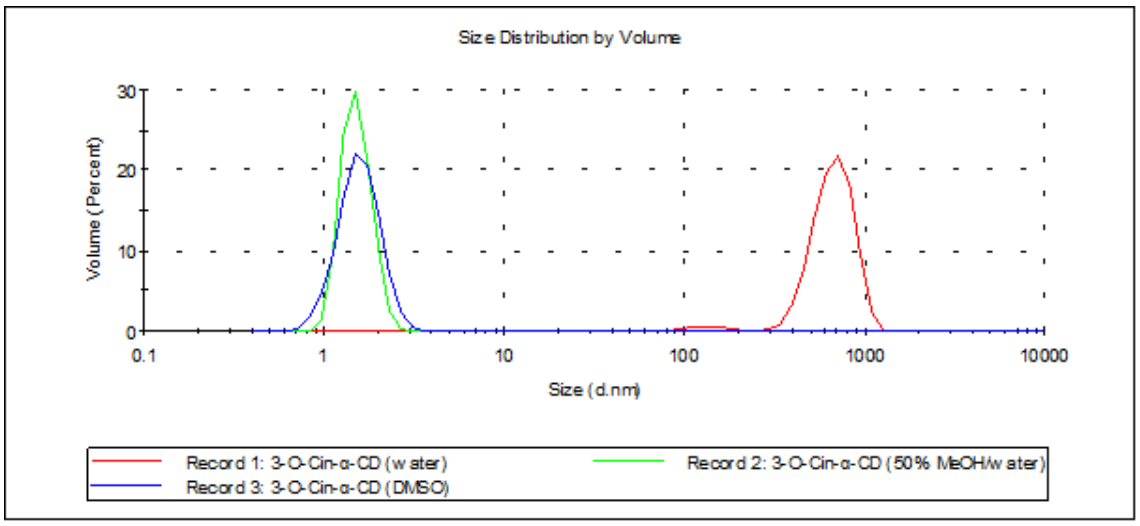

Figure 11. Effect of solvent on the size distribution of aggregates formed by 3-*O*-Cin-α-CD at 25 °C (the applied concentrations are 10 mg/mL (9.2 mM)).

In DMSO, no aggregation was observed for either of the derivatives (see Record 3 in Figure 10 and Figure 11). The two regioisomers were present in molecularly dispersed form with a D_h around 1.25 nm, which corresponds to the size of the unmodified, non-aggregated α-CD[147]. These results are in agreement with the results obtained by NMR experiments, where no chemical shift changes were observed upon dilution in DMSO-d_6 also indicating the absence of the intermolecular interactions. Different aggregate sizes were observed for the two regioisomers in 50% MeOH solution (Record 2 in Figure 10 and Figure 11). 2-*O*-Cin-α-CD was present in the form of aggregates with a very broad size distribution ranging from 100 nm to 700 nm, while 3-*O*-Cin-α-CD was found in a disaggregated form (D_h = 1.25 nm).

The temperature also influenced the size of the aggregates formed by the two regioisomers differently (Figure 12). Monotonous decay in size distribution was observed for the aggregates formed by the 2-*O*-isomer in water when the temperature was gradually elevated, although large aggregates with a D_h of 400 nm were still present at 75 °C. On the other hand, the aggregates formed by the 3-*O*-isomer in water were much more labile, and they completely disaggregated as the temperature reached 50 °C. From these results, it was concluded that the temperature could be used as an external stimulus to adjust the size distribution in water and to study its impact on the separation efficiency in separation techniques. The temperature caused disaggregation is a reversible process – cooling back the solutions to room temperature caused a formation of large particles with D_h comparable to the size of the initial particles.

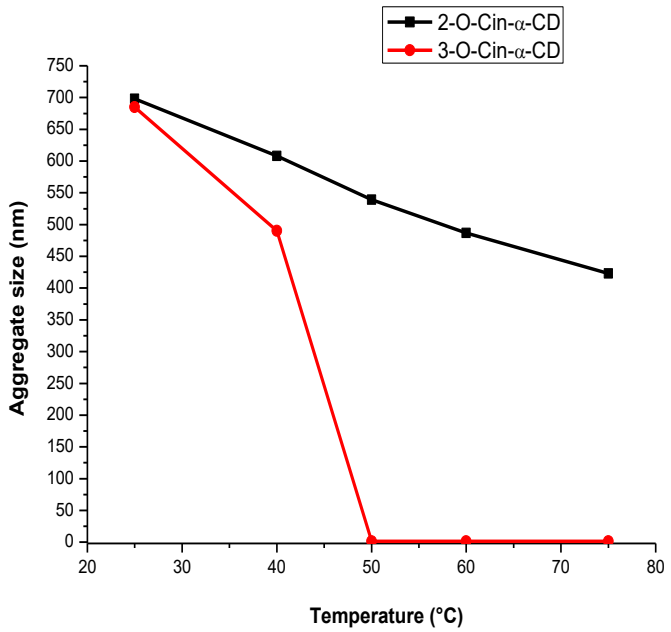

Figure 12. Aggregate sizes (diameter) of 2-*O*-Cin-α-CD (black) and 3-*O*-Cin-α-CD (red) in water at various temperatures (the applied concentrations are 10 mg/mL (9.2 mM)).

To demonstrate that in the case of the Cin-α-CD regioisomers the main force, which initializes the aggregate formation, is the host-guest interaction between the monomer units, another series of DLS experiment was set up to measure the aggregate size distribution after the successive addition of potential competitive host or guest molecules. This experiment aimed to prove that the size of the supramolecular assembly can be modulated by the addition of suitable chain growth inhibitors, which are able to displace the cinnamyl moiety from the neighboring CD cavity, or to shield the cinnamyl moiety from the cavity of the adjacent Cin-α-CD. Based on the previous observation that elevated temperature resulted in partial or complete disaggregation depending on the type of the regioisomer the following experiment was performed:

The aqueous solutions (10 mg/mL) of mono-2-*O*-Cin-α-CD and mono-3-*O*-Cin-α-CD were equilibrated separately at 75 °C temperature, stirred in a closed vial for 12 hours and then the system was perturbed with an addition of the inhibitor in a 10-fold molar excess respect to the Cin-α-CD. The solutions were cooled back to room temperature, and the size distributions of the formed aggregates were measured. In Figure 13, a schematic representation of the experiment setup is shown.

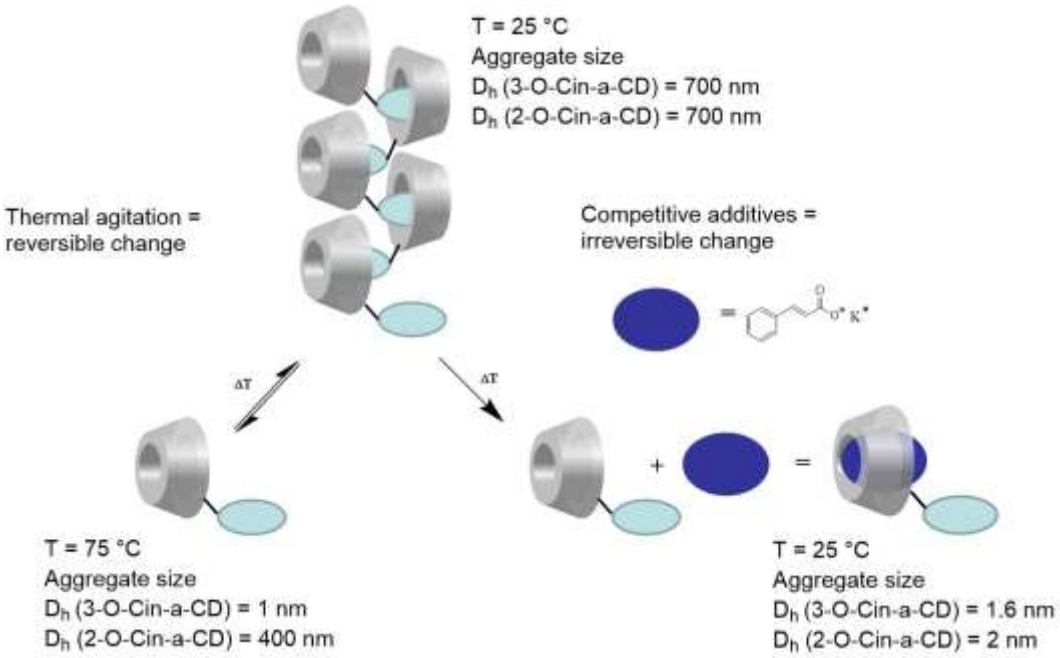

Figure 13. Schematic representation of the DLS and NMR experiments proving the host-guest nature of the aggregate formation.

As shown in Figure 14, the addition of unmodified α-CD as competitive host molecule to the aqueous solution of the 3-*O*-isomer did not decrease significantly the aggregate size distribution, which indicates that α-CD was not able to inhibit the intermolecular interactions between the molecules of 3-*O*-Cin-α-CD. Potassium adamantane-1-carboxylate (AdCOOK) was more effective chain growth inhibitor as it decreased the aggregate size from 700 nm to 400 nm. Potassium-cinnamate (CioOK) as a competitive guest molecule was able to completely displace the cinnamyl part of 3-*O*-Cin-α-CD from the adjacent CD cavity which resulted in decomposition of the host-guest complexes; therefore, a significant decrease in the D_h of the aggregates (from 700 nm to 1.6 nm) were registered (Figure 14).

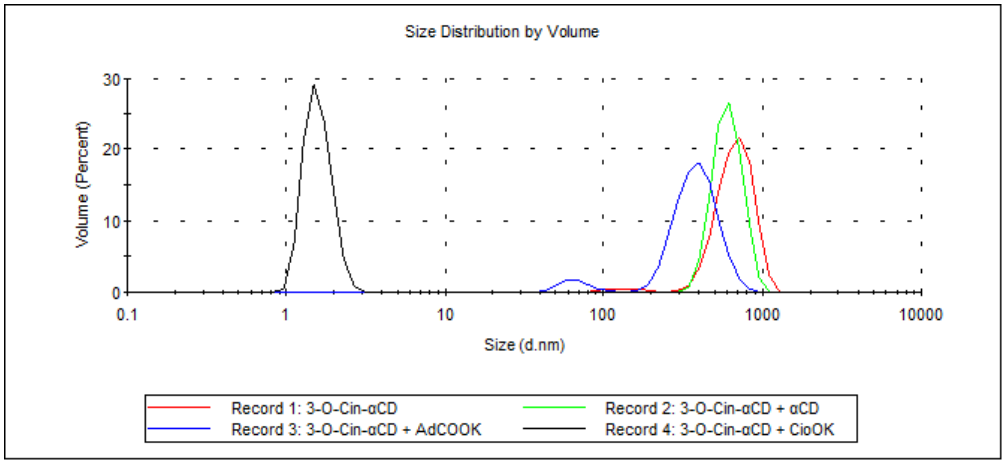

Figure 14. The effect of competitive additives on the size distribution of aggregates formed by 3-*O*-Cin-α-CD at 25 °C (the applied concentrations of the mono-3-*O*-Cin-α-CD are 10 mg/mL (9.2 mM)).

The observed difference between the efficiency of the chain growth inhibition of AdCOOK and CioOK can be explained by the different size of the two competitive guest molecules. Due to the high isostericity of CioOK with the cinnamyl substituent of Cin-α-CDs CioOK can accommodate the CD cavity, which results in a complete collapse of the supramolecular aggregates. On the other hand, AdCOOK as a guest molecule is apparently too bulky (fits perfectly to the larger cavity of β-CD, but only partialy to the cavity of α-CD); therefore, the displacement of the cinnamyl moieties in the intermolecular complexes and the caused disaggregation is only partial (from 700 nm to 400 nm). The 2-*O*-isomer showed similar behavior upon addition of chain inhibitors as 3-*O*-Cin-α-CD, which indicates that in the case of both regioisomers the main force of the aggregation is the intermolecular host-guest interaction. The disrupted aggregates were stable at room temperature and did not show any aggregation in time. Hence it was concluded that the disaggregation caused by competitive additives is an irreversible process. Because CioOK as competitive additive showed remarkable changes in the aggregation behavior of Cin-α-CDs, its interaction with both regioisomers was further investigated by 1D and 2D NMR experiments to get a deeper insight into the disaggregation process. ROESY and ^{1}H NMR spectra of both regioisomers were recorded in the presence of CioOK (5-fold molar excess) in D_2O after equilibrating the solutions at 75 °C and cooling back to 25 °C just before the measurements.

Instead of the previously observed NOE cross-correlations in the ROESY spectra of both Cin-α-CD isomers, new cross-peaks appeared showing interaction only between potassium cinnamate and between the inner hydrogens of the CD cavity (Figure 15). The disappeared cross-peaks between the protons of the cinnamyl part of Cin-α-CDs (black dashed line in Figure 15) and between the CD cavity protons indicate that the cinnamyl moiety was effectively displaced by the additive.

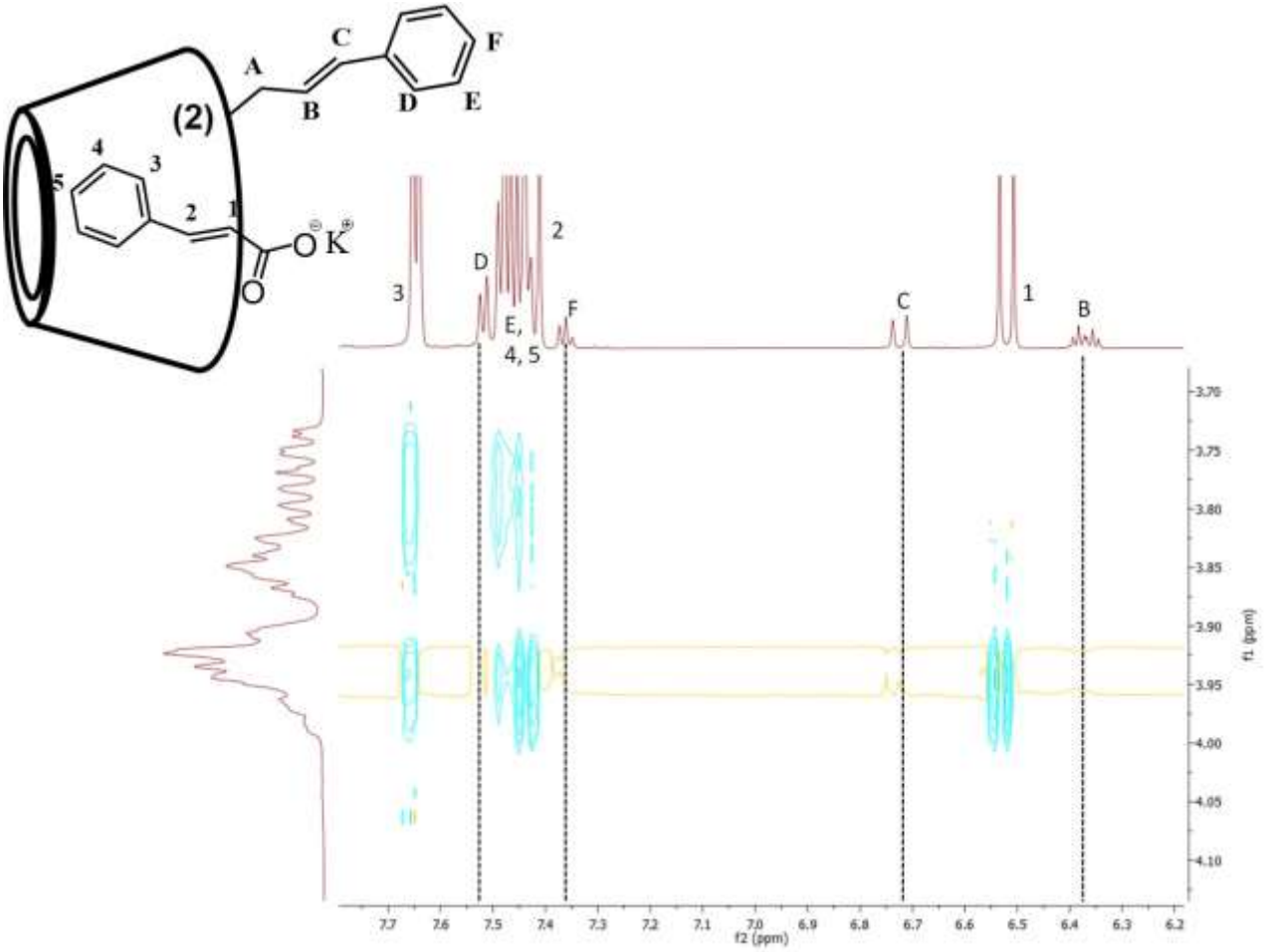

Figure 15. Expansion of the 2D ROESY spectrum of 2-*O*-Cin-α-CD in the presence of CioOK as competitive guest molecule (D_2O, 600 MHz, 25 °C).

This phenomenon can also be observed in the ^{1}H NMR spectrum of both isomers (Figure 16). If the chemical shifts of aromatic or double bond protons of the given regioisomer are compared before and after the addition of the competitive guest molecule, significant changes in chemical shifts can be detected, which indicates that the cinnamyl part of the molecule is located in the different chemical environment after the addition of the competitive guest. These results are in good agreement with the data obtained from DLS experiments and further confirmed the hypothesis that the observed disaggregation by CioOK is caused by the formation of a host-guest complex between Cin-α-CDs and CioOK.

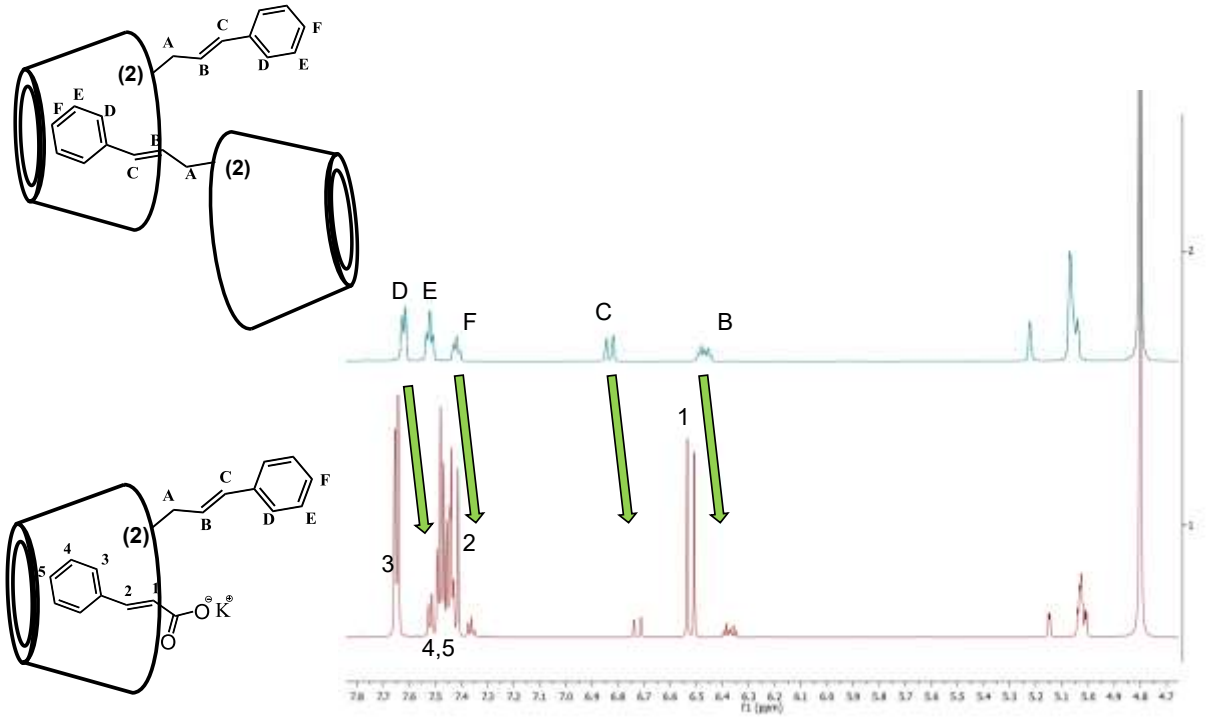

Figure 16. ^{1}H NMR spectrum of 2-*O*-Cin-α-CD before (up) and after (down) the addition of CioOK in 5-fold molar excess (D_2O, 600 MHz, 25 °C).

The results indicate that the size of these structures can be modulated by external stimuli, such as solvent composition, temperature or addition of guest molecules. Furthermore, it was shown that by using a suitable additive – potassium cinnamate as a competitive guest molecule, the formation of supramolecular aggregate can be irreversibly inhibited. These properties of CD-based supramolecular aggregates together with the high aqueous solubility and inherent chirality of the monomer species (and therefore the entire aggregate) promises great advantages as a new chiral selector for capillary separation techniques.

4.3 Synthesis of xanthene-modified β-CDs

The generalized reaction scheme for the xanthene-appended β-CD derivative is depicted in Figure 17.

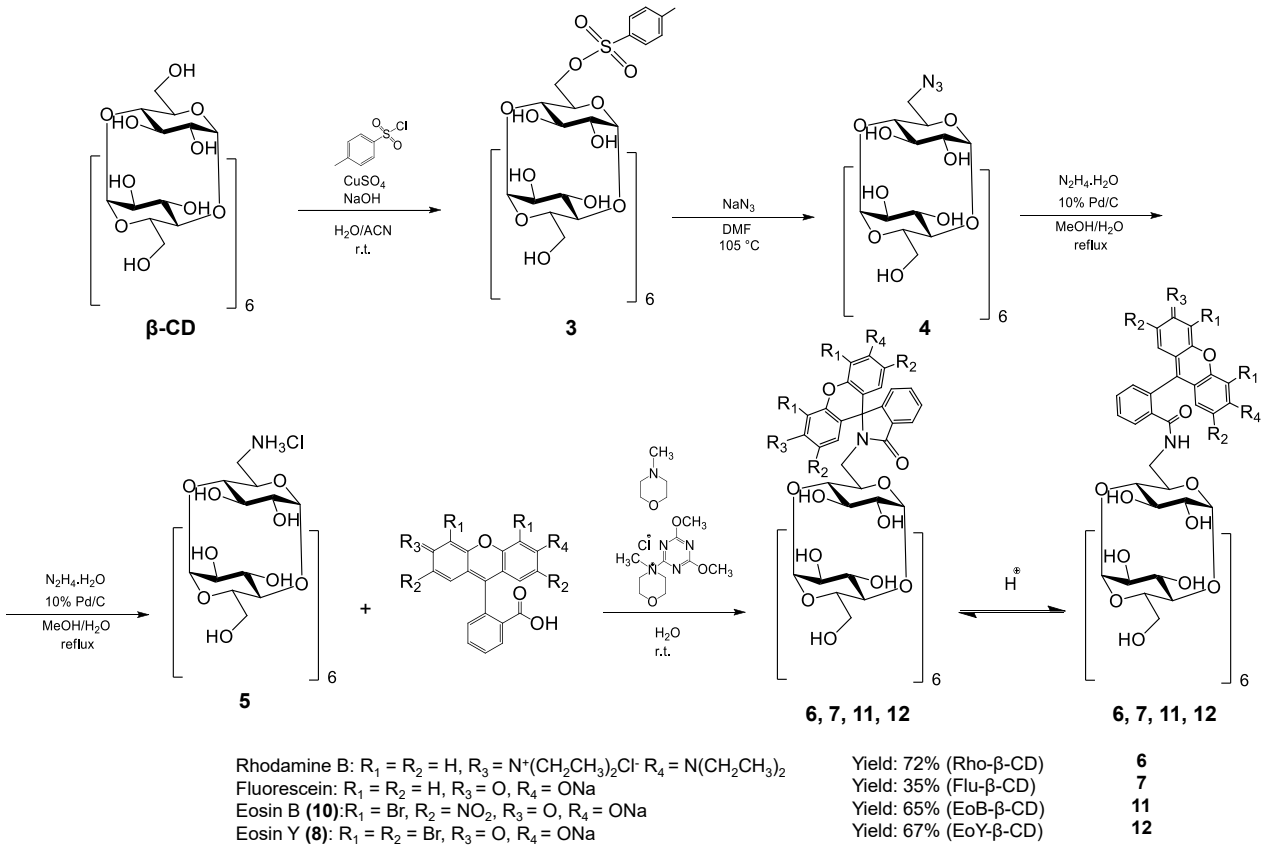

Figure 17. Reaction scheme for the synthesis of xanthene-modified β-CDs.

The synthetic route starts with monofunctionalization of β-CD at position 6 through described procedures (compounds **3, 4** and **5**)[33,35]. The strategy for the fluorophore labeling is based on the condensation reaction between the amino function of NH_3-Cl-β-CD **(5)** and the carboxyl moiety of the xanthene dye promoted by the coupling agent DMT-MM-Cl. It is accepted that the carboxylic acid has to be deprotonated to generate an activated ester with DMT-MM-Cl[148]. The activated species undergoes attack by the amine, thus generating the desired amide bond. The xanthene dyes, the NH_3Cl-β-CD, and the coupling agent are soluble in water, thus allowing for a homogenous reaction that occurs at room temperature. Since β-CDs modified with amines are usually stored in the HCl salt form (to avoid decomposition),

during the reaction, an additional base such as *N*-methylmorpholine (NMM) or NaOH is required. If amine-bearing CDs are used as free bases, the use of the additional base can be omitted. The work-up of the reactions simply consists of the selective precipitation of the target compound with acetone and removal of the unreacted dye by filtration. The purity of the starting dye is a crucial parameter for the outcome of the reaction since it will greatly affect the crude composition and consequently the purification process. If the purity of the starting dye is satisfactory, selective precipitation/filtration are the only steps required for obtaining a fluorescent-appended β-CD derivative of acceptable purity (>90%, based on thin layer chromatography (TLC) analysis). If the starting fluorophore is a mixture of fluorescent (but not clearly identified) dyes, then column chromatography is needed to achieve the desired purity.

4.3.1 Rhodamine B-appended β-CD

Rhodamine B (Rho) in HCl form was sourced in good purity, allowing for a clean formation of the product with a very low amount of Rho-related by-products (not detectable by TLC), a minute amount of two β-CD-related by-products (ByP) (see ByP_1-, ByP_2-β-CD in TLC-5 in Figure 18, the sum of the two being less than 5% based on the intensity of the spots on TLC-5), and some unreacted NH_2-β-CD (less than 5% based on the intensity of the spots on TLC-5 in Figure 18). The reaction was completed in a couple of hours, at room temperature, in an aqueous environment.

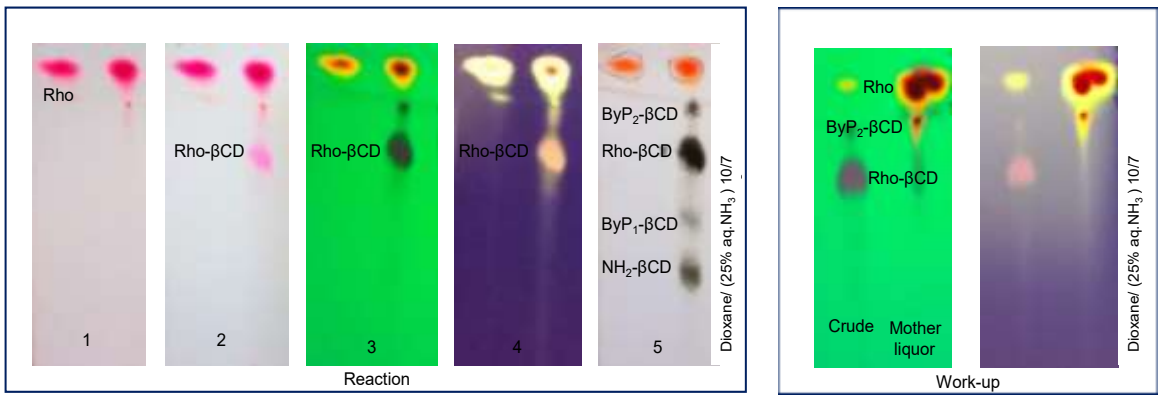

Figure 18. TLC plate at different development stages for monitoring the composition of Rho-β-CD **(6)** crude (left panel: immediately after the removal from the developing chamber (1), after heating (2), under UV excitation at 254 nm (3), under UV excitation at 366 nm (4), and finally, after charring (5) and TLC for evaluating the effectiveness of the work-up (right panel: under UV excitation at 254 nm (1), under UV excitation at 366 nm (2).

TLC provides an unambiguous identification of the product, and the behavior of the product in the selected eluent gives a structural indication about the possible prototropic form assumed from the dye in the conjugate. The left panel of Figure 18 shows the TLC plates used for monitoring the composition of mono(6-deoxy-6-spirolactam-rhodamine B)-β-CD (Rho-β-CD) **(6)** crude at different development stages. The right panel in Figure 18 shows the effectiveness of the selective precipitation/filtration during the work-up, and in particular, it reveals that the unreacted dye can be separated from the product while the unreacted NH_2-β-CD and the nonfluorescent ByP_1-β-CD are more challenging to remove. In the left panel of Figure 18, the unreacted dye (Rho) is clearly detectable at any stage of the development, while the product (Rho-β-CD) is detectable only after heating the TLC plate and appears as a slight pink spot (TLC-2 in Figure 18). This spot is colored, strongly UV active, nonfluorescent and charrable (TLC-2, -3, -4 and -5, respectively in Figure 18). The presence of color and the charrability indicates that the compound contains both the chromophore and the CD scaffold.

The strong UV activity and the nonfluorescence suggest that the chromophore is prevalently in lactam form[149]. As it is also known that β-CD can preferably complex the cyclic form of Rho[150], complexation may play a role in the stabilization of the lactam form of the RhoB-appended CD derivative. All this information taken together confirms the presence of the product/conjugate and add to the structural elucidation of the system.

Concerning the reaction work-up, the first part consists of the removal of the unreacted dye with acetone. As shown in Figure 18, after selective precipitation/filtration with acetone, most of the unreacted dye and ByP_2-β-CD remain in the mother liquor. At this stage, the crude already has acceptable purity (>90% based on TLC), but flash chromatography with ACN/H_2O gradient elution permits the removal of the remaining CD-related by-products and further increases the purity. After this additional purification step, compound **(6)**, has been extensively characterized by NMR spectroscopy.

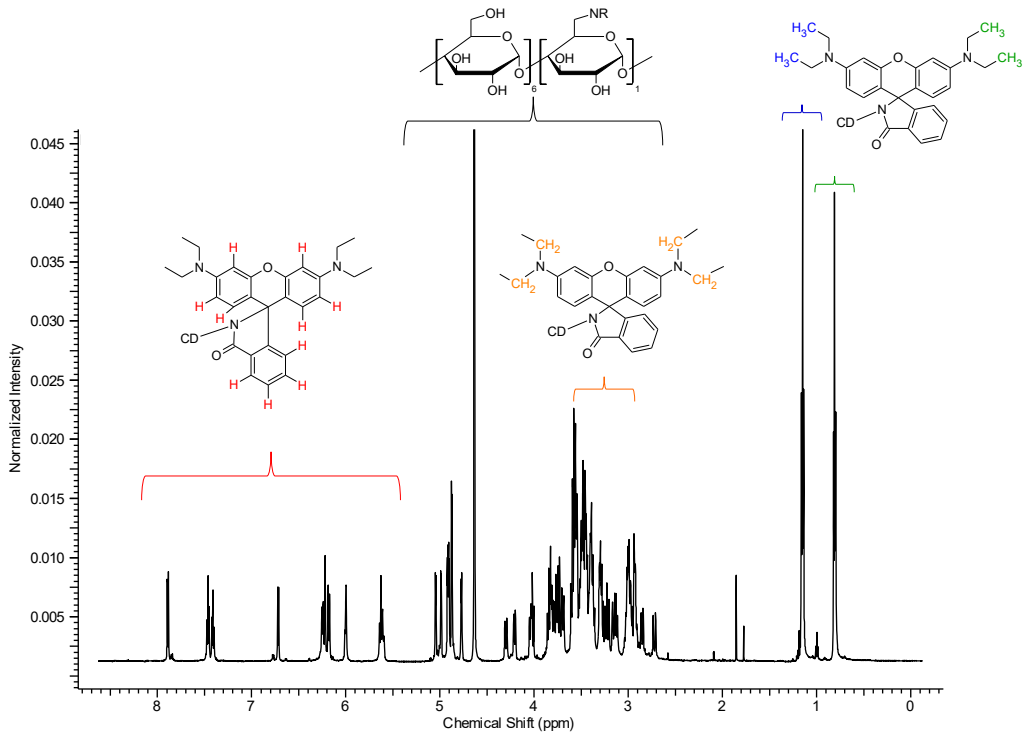

Figure 19. ^{1}H-NMR spectrum of Rho-β-CD with partial assignments (D_2O, 600 MHz, 25 °C).

The proton NMR spectrum shown in Figure 19 is a typical spectrum of an asymmetric CD. The two constituent parts of the molecule can be easily recognized: the signals in the aromatic (between 5.5-8.0 ppm) and aliphatic regions (between 0.5-1.5 ppm) belong to the Rho moiety while the set of signals between 2.5-5.5 ppm belongs to the CD and also includes the methylene units of the fluorophore. The integration of the signals fits perfectly the theoretical values for a monosubstituted Rho-β-CD derivative as also confirmed by the found value of the pseudo-molecular ion during the electrospray ionization mass spectrometry (ESI-MS) analysis. The signals in the aromatic regions are well resolved, the multiplicity of the signals can be clearly determined, and this is not an obvious characteristic for Rho-based CD derivatives since usually the aromatic signals of these compounds are represented by very broad peaks.

The presence of broad signals is characteristic for compounds randomly substituted as the NMR signals are made from the frequencies of all the isomers composing the mixture. An incomplete fluorescent tagging of the starting single-isomer β-CD (or inadequate purification), as well as aggregation of the compound, can cause broadening of the peaks[151]. In the proton spectrum in Figure 19, it can also be appreciated the good resolution of the anomeric region; several doublets can be clearly identified. The separation of the anomeric doublets is a fundamental requisite for the total assignment of an asymmetric molecule[146].

The core of the CD region between 2.5-5.5 ppm is rather crowded and cannot be elucidated without the use of 2D techniques. On the other hand, the two signals in the aliphatic region can be easily assigned to the alkyl side-chains of the Rho moiety. Another important set of information that can be deduced/extrapolated from the careful analysis of the spectrum in Figure 19 concerns the asymmetry of the Rho in the molecule. The proton spectrum of the Rho both in lactone and HCl form shows only one kind of signal for the alkyl groups and for the aromatic protons of the xanthene moiety as well, irrespectively of the symmetry of the molecule, being the lactone a symmetric molecule and the acid form of Rho an asymmetric one. This means that the differentiation in multiple NMR signals in the Rho-β-CD conjugate is strictly related to the presence of the CD scaffold. The CD moiety allows the formation of a local asymmetric environment that permits the differentiation/resolution of otherwise indistinguishable signals of the fluorophore, in particular, this phenomenon is based on the (intermolecular) partial complexation of the fluorophore inside the cavity. These data supported by the results of 2D ROESY measurements and by the findings of Wang and co-workers about the crystal structure of Rho in lactone form[152], allowed us to propose the model shown in Figure 20 for the intermolecular inclusion mode of Rho-β-CD. This model for the supramolecular assembly is also in agreement with previous data about the inclusion complexation of organic dyes with β-CD dimers[153].

Figure 20. Cartoon models for the possible intermolecular inclusion mode of Rho-β-CD in solution.

The analysis of the DEPT-ed-HSQC spectrum (Figure 21) gives further information on the product. The compound is unambiguously substituted on the primary side. The signals at 40 ppm (*C*-6_{sub} in Figure 21) correspond to the methylene moiety of the glucose unit that bears the fluorophore. The two *C*-6_{sub} signals in the DEPT-ed-HSQC spectrum have identical carbon but different proton frequencies, since the two protons of the substituted methylene unit are not magnetically equivalent – one of them is pointing inward the cavity, while the other one is oriented outwards. These resonances of the two magnetically non-equivalent protons (*H*-6a and *H*-6b), are typical for primary-side monosubstituted CDs[146].

It is also possible to distinguish the two signals of the methylene units of side-chains of the Rho (around 47 ppm (F1 Chemical Shift in Figure 21)) from the unsubstituted methylene moiety of the glucose units (*C*-6_{unsub} around 65 ppm (F1 Chemical Shift) in Figure 21).

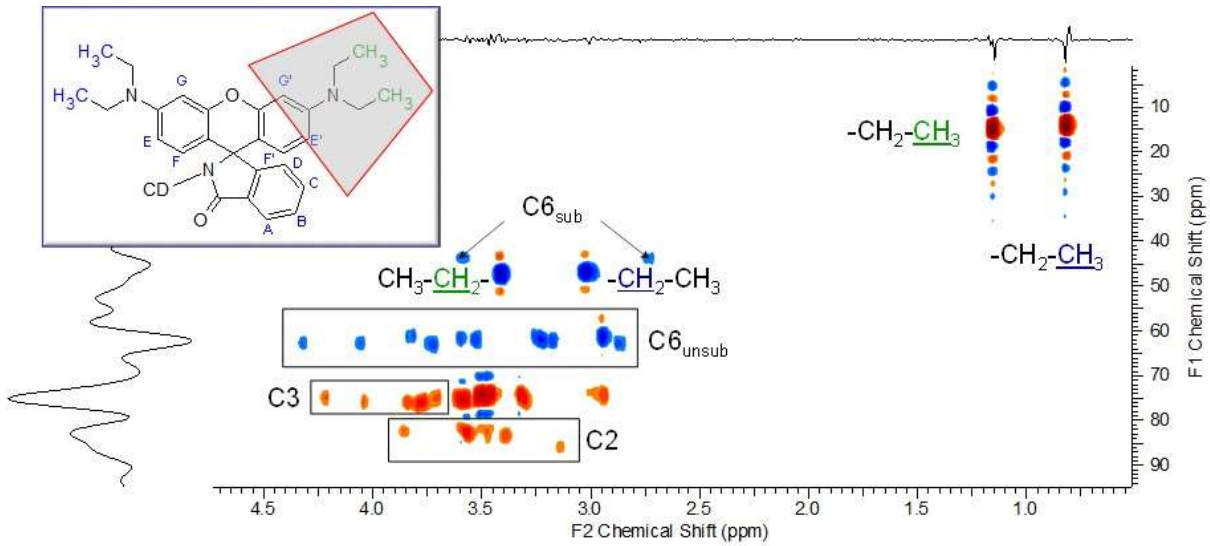

Figure 21. Expansion of DEPT-ed-HSQC spectrum of Rho-β-CD with partial assignments (D_2O, 600 MHz, 25 °C).

4.3.2 Fluorescein-appended β-CD

Fluorescein (Flu) disodium salt was purchased in high purity allowing the formation of the product, but with moderate yield. For this reaction, several Flu-related by-products could be detected by TLC, and the starting NH_3Cl-β-CD could be only partially converted to mono(6-fluoresceinyl-carboxamido-6-deoxy)-β-cyclodextrin (Flu-β-CD) **(7)** (20–30% conversion based on TLC). Although different attempts were made to enhance the conversion (such as tuning the pH of the reaction, using NH_3Cl-β-CD in free base form as starting

material, replacing the base NMM with NaOH and reacting the lactone form of the fluorophore instead of the sodium salt), the improvements were not substantial.

The reason for the partial conversion under the selected alkaline conditions can be related to the appearance of several dye-related by-products. Under the selected aqueous alkaline conditions, the phenol moiety of the Flu is mainly deprotonated and as phenolate can participate in the formation of Flu-based acyl derivatives (such as esters or anhydride). The formation of these by-products could lead to depletion of the coupling agent by conversion to 2-hydroxy-4,6-dimethoxy-1,3,5-triazine (DMM-OH) and could explain the moderate conversion of the starting material. The removal of the unreacted dye, as well as the dye-related by-products, can be achieved by selective precipitation/filtration with acetone. Flash chromatography using ACN/H_2O/(25% aq.NH_3) 10/5/1 eluent mixture permits the removal of the unreacted NH_2-β-CD-related impurities. At this stage, compound **7**, has been extensively characterized by spectroscopic techniques.

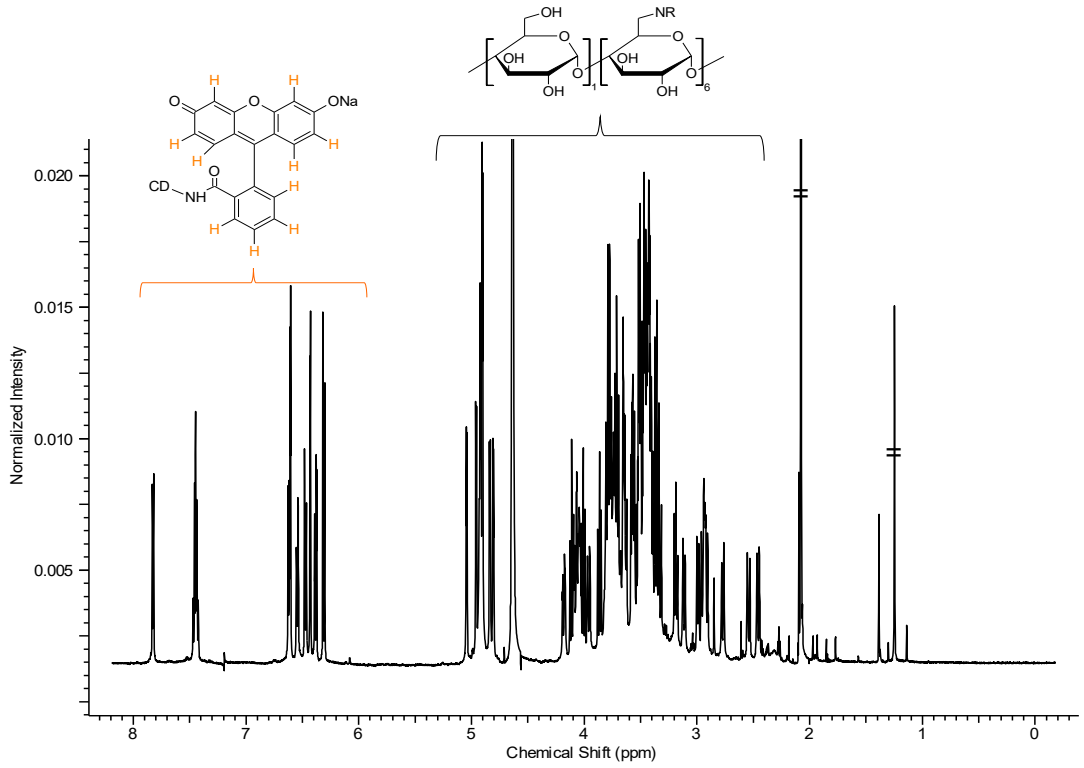

Figure 22. ^{1}H-NMR spectrum of Flu-β-CD **(7)** with partial assignments (D_2O, 600 MHz, 25 °C).

The proton NMR spectrum shown in Figure 22 is a typical spectrum of an asymmetric CD. The two constituent parts of the molecule can be recognized. The signals in the aromatic region (between 6.0-8.0 ppm) belong to the Flu moiety while the set of signals between 2.2-5.5 ppm belongs to the CD. The integration of the signals perfectly fits the theoretical values for a monosubstituted Flu-β-CD conjugate as also confirmed by the found value of the pseudo-molecular ion during the ESI-MS analysis (see experimental part).

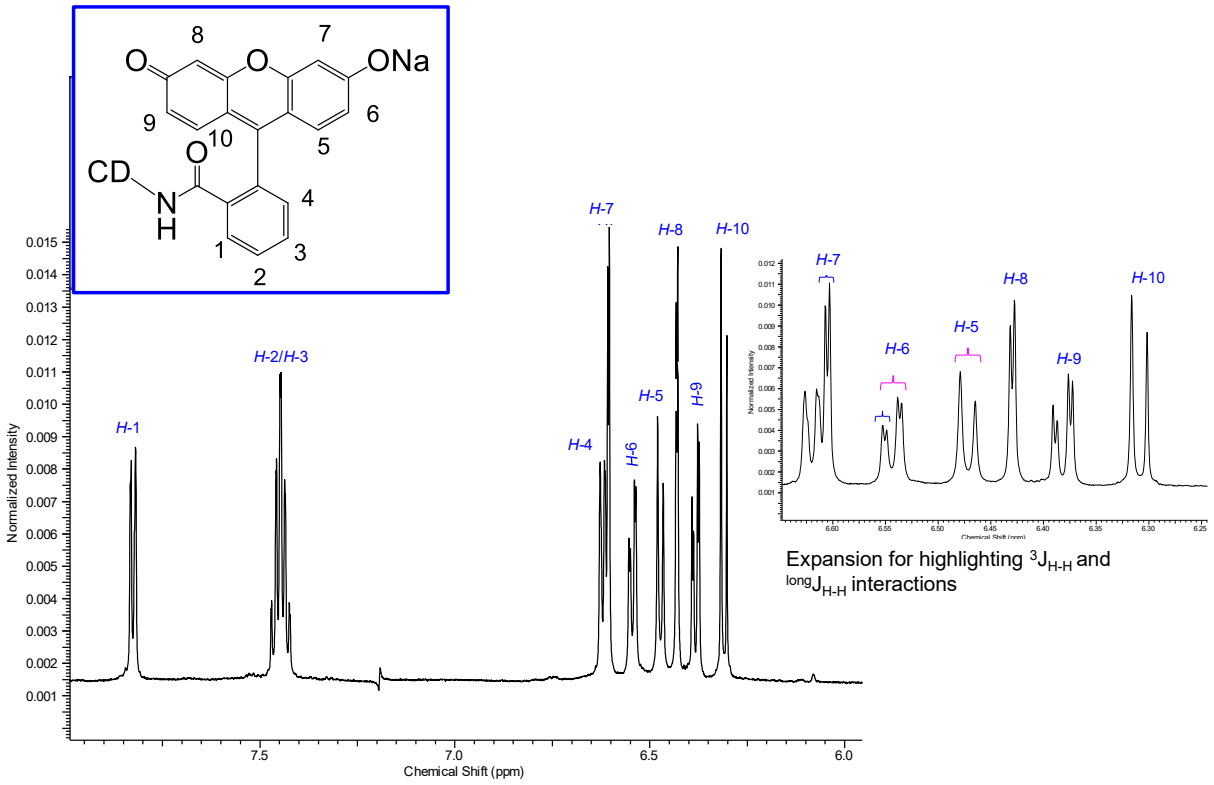

Figure 23. Expansion of the aromatic region of the ^{1}H-NMR spectrum of Flu-β-CD with partial assignments (D_2O, 600 MHz, 25 °C).

In the region between 6.0-8.0 ppm of the ^{1}H-NMR spectrum of Flu-β-CD (Figure 23), two different kinds of aromatic couplings can be detected. The different values of the $^{3}J_{H\text{-}H}$ and $^{long}J_{H\text{-}H}$ couplings permit the unambiguous assignment of the couples of protons *H*-5/*H*-7 and *H*-8/*H*-10. In the proton spectrum in Figure 22, it can also be appreciated the good resolution of the anomeric region; several doublets can be clearly identified. The core of the CD region between 2.2-5.5 ppm (Figure 22) is rather crowded and cannot be easily elucidated without the use of 2D techniques.

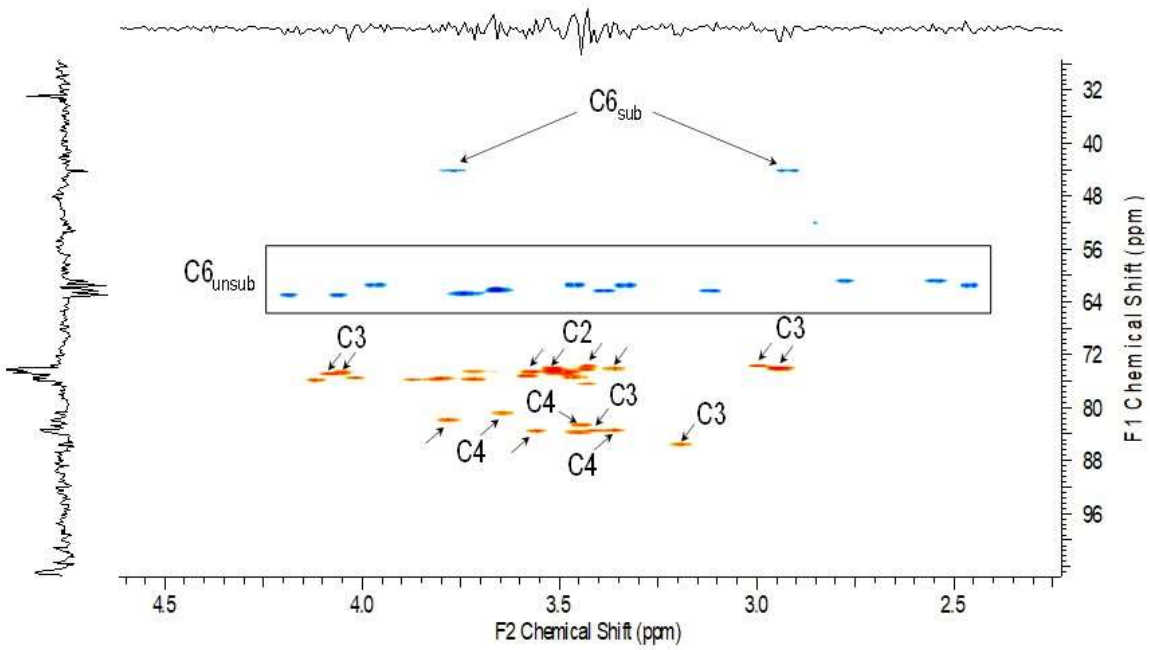

Figure 24. DEPT-ed-HSQC spectrum of Flu-β-CD with partial assignments. Assignments are based on a combination of COSY, TOCSY, and HMBC measurements[106].

The analysis of the DEPT-ed-HSQC spectrum gives further information on the product. The compound is unambiguously substituted on the primary side. The frequencies at around 44 ppm (*C*-6_{sub} in Figure 24) belong to the methylene moiety of the glucose unit that bears the fluorophore. As in the case of Rho-β-CD the two *C*-6_{sub} signals have identical carbon frequency, but different protons since the two protons of the methylene unit are not magnetically equivalent (*C*-6_{sub} in Figure 24). The signals of the CD core and the partial assignments of the *C*-2, *C*-3, and *C*-4 are based on a combination of COSY, DEPT-ed-HSQC, HMBC, and TOCSY measurements[106].

4.3.3 Eosin-appended β-CDs

The purity of the commercially available dyes, EoY **(8)** and EoB **(10)**, purchased from different providers (two different sources for each dye were tested) was not suitable for the preparation of the β-CD conjugates. Therefore, both dyes were freshly synthesized starting from Flu. Although the described synthetic procedures for the preparation of eosin dyes commonly use Br_2[154,155,156], herein the less hazardous *N*-bromosuccinimide (NBS) was used as the source of bromine. Thus, compound **8** was prepared in a single step from Flu-Na in ethanol (EtOH) in the presence of NBS (Figure 25).

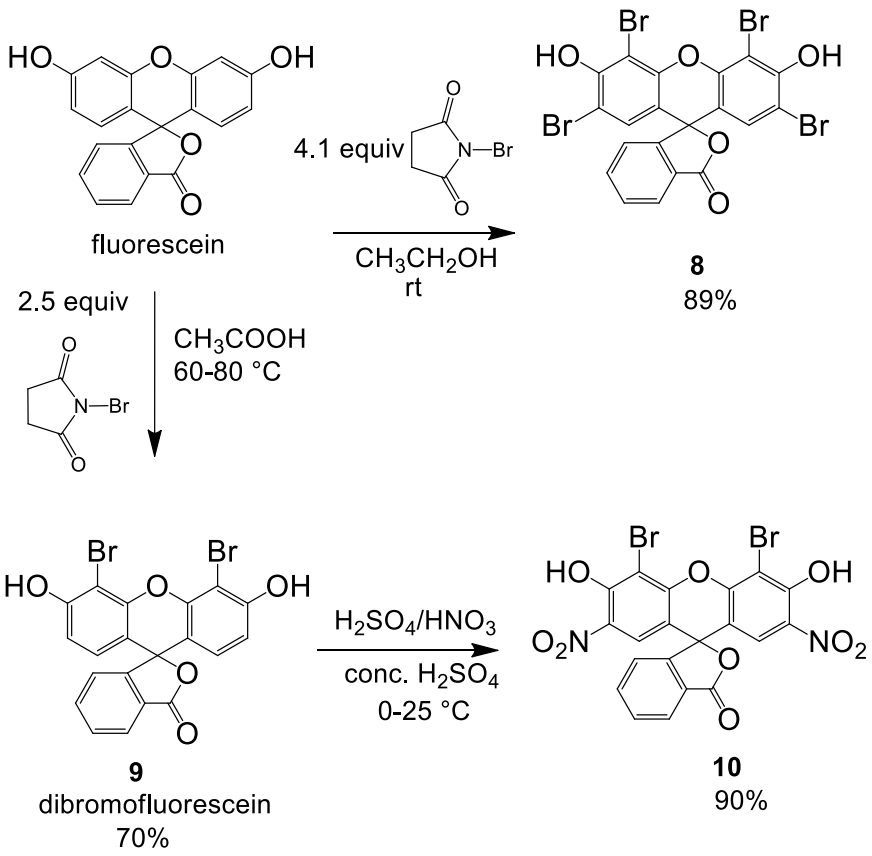

Figure 25. Reaction scheme for the synthesis of eosin Y (**8**) and eosin B (**10**).

The synthesis of compound **10** was performed in two steps: first, dibromofluorescein **(9)** was synthesized through partial bromination of Flu with NBS in acetic acid (Figure 25). However, under the selected reaction conditions, a three-component mixture of mono-, di-, and tribromofluorescein was obtained, and the isolation of the targeted dibrominated product from this crude was extremely laborious and low yielding. On the other hand, when using NBS in a slight excess (2.5-fold molar excess with respect to Flu) only a two-component mixture of di- and tribromofluorescein was formed. The isolation of **9** from this crude was easily achieved through direct-phase silica gel column chromatography with isocratic chloroform/MeOH elution. Herewith the over brominated by-product was permanently immobilized on the silica gel column, and only the targeted dibromofluorescein was eluted. In the following step, dibrominated fluorescein was nitrated using standard nitration conditions to obtain the desired dye EoB **(10)**.

After the successful synthesis and in-depth NMR characterization of the two eosin dyes, they were subjected to the condensation reaction with NH_2-β-CD. In both cases, the coupling proceeded at room temperature within 3 h for EoY and 12 h in case of EoB. TLC analysis of the crude reaction mixture gave the first unambiguous evidence for the successful

conjugate formation as the formed products have a R_F value distinct from those of the other starting materials. Additionally, the products show intensive absorbance after excitation at 254 nm and 366 nm, and they are carbonizable. Thus the products exhibit the expected characteristics of a fluorescent CD conjugate (Figure 26).

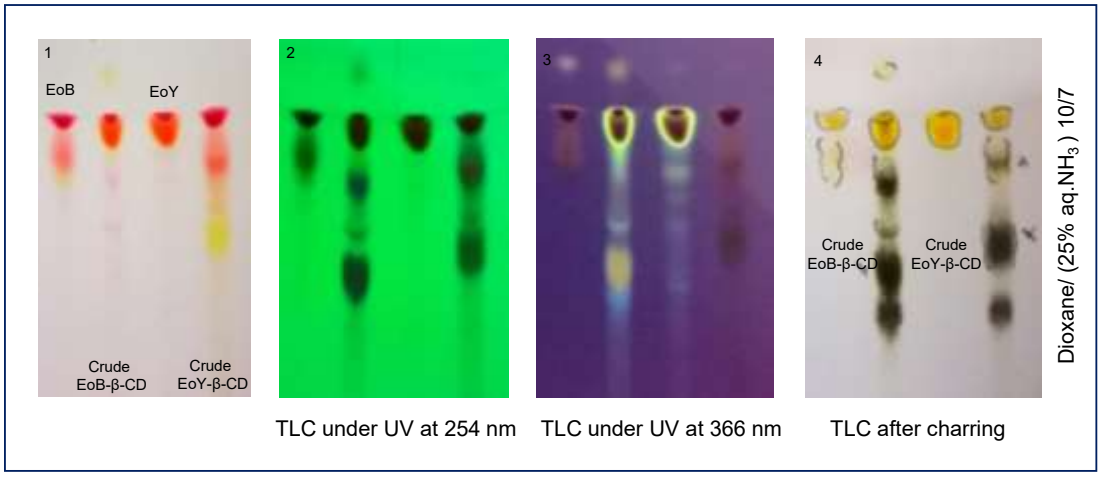

Figure 26. TLC monitoring of the composition of EoB- and EoY-β-CD crudes (**11** and **12**).

Work-up of the reactions included the concentration of the reaction mixtures and selective precipitation of the CD-related compounds (conjugate and unreacted starting material) with acetone. To separate the target conjugates from unreacted NH_2-β-CD (5–10% based on TLC evaluation, see Figure 26), the precipitate was subjected to direct-phase column chromatography using an ACN/H_2O/(25% aq.NH_3) elution mixture, in which the faster-eluting component is the conjugate and the slower is the unreacted NH_2-β-CD which can be eventually recovered.

4.4 Spectroscopic and supramolecular characterization of xanthene-modified β-CDs

4.4.1 IR and UV-Vis spectroscopic characterization of rhodamine B-appended β-CD

In Figure 27, the IR spectra of Rho-β-CD, rhodamine B in acidic form (Rho HCl), and Rho-β-CD in lactone form (Rho Lactone) are shown. The analysis of the spectra unambiguously proved that the fluorophore in Rho-β-CD is in lactam form. The frequency at 1755.9 cm^{-1} in the IR spectrum of Rho Lactone belongs to the carbonyl stretching of the γ-lactone moiety of the dye[157], and this value is very similar to the one found in the carbonyl

region of the IR spectrum of Rho-β-CD at 1755.4 cm^{-1} (Figure 27). This last frequency is typical for the carbonyl stretching of a γ-lactam ring, thus demonstrating that the fluorophore in Rho-β-CD (if isolated according to the procedure reported in the experimental part) is in a non-fluorescent cyclic form.

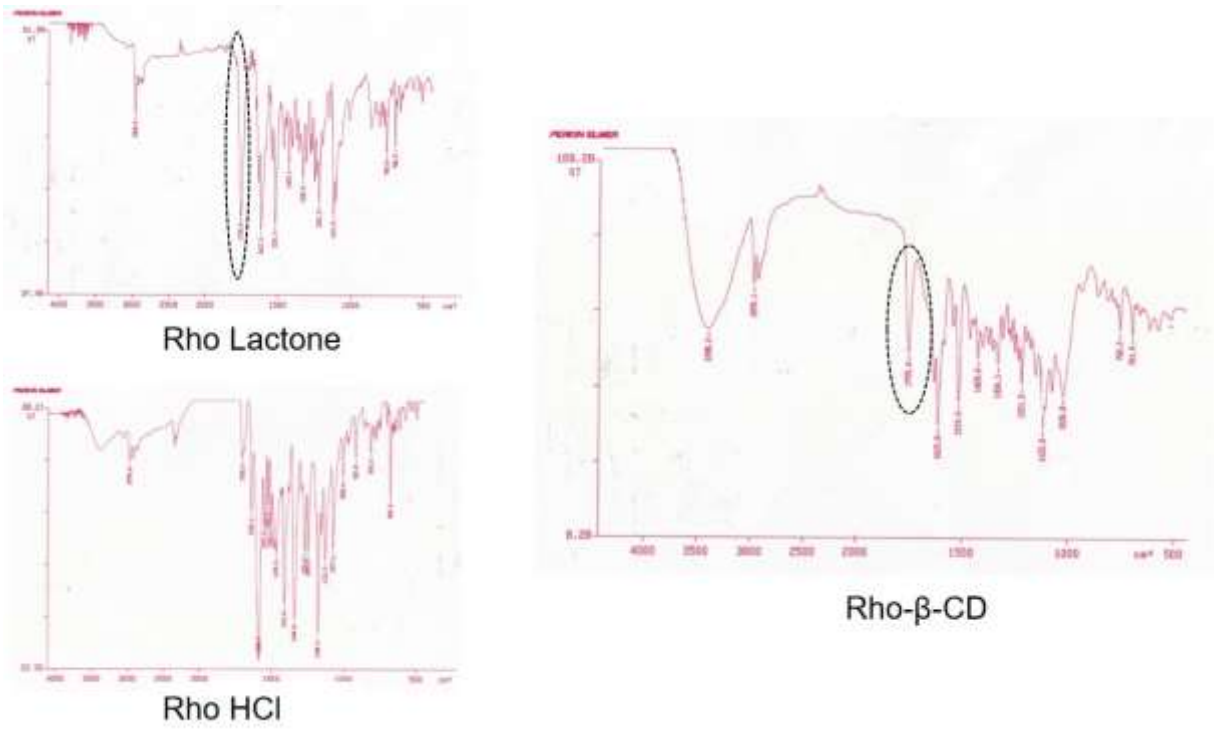

Figure 27. IR spectra of rhodamine B-appended β-CD (Rho-β-CD), rhodamine B in acidic form (Rho HCl), and rhodamine B in lactone form (Rho Lactone).

The same conclusion can also be reached through the analysis of the UV-Vis spectra (Figure 28).

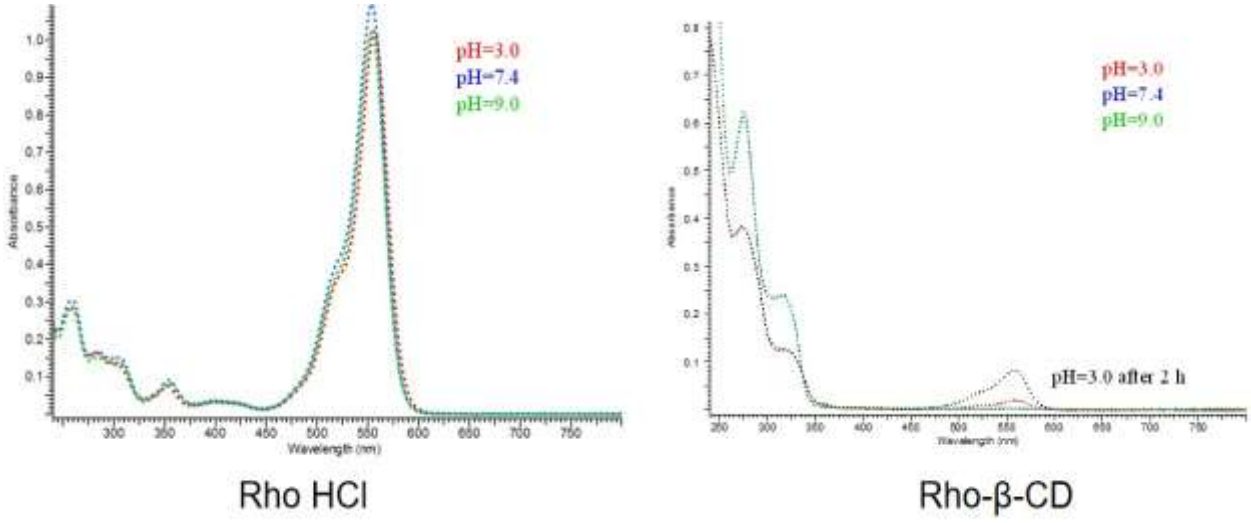

Figure 28. UV-Vis spectra of rhodamine B in acidic form (Rho HCl) and rhodamine B-appended β-CD (Rho-β-CD) at various pH values at the same concentration ($c_{RhoHCl} = c_{Rho\text{-}\beta\text{-}CD} = 0.001$ mM).

The UV-Vis spectra of Rho-β-CD vary according to the pH of the solution differently compared to the free Rho. The free fluorophore shows a strong absorbance at around 550 nm and maintains its fluorescence at any of the examined pH. In the case of Rho-β-CD, this peak is completely suppressed at alkaline and neutral pH and in these conditions the compound is not fluorescent. For the xanthene-appended derivative the peak at around 550 nm only appears at pH=3 (the absorbance of it increasing by time), and in these conditions, Rho-β-CD is a fluorescent compound. The phenomenon can be easily explained based on the change of the isomeric form of the fluorophore according to the pH. The opening of the lactam ring is catalyzed by acidic conditions thus switching the equilibrium of the prototropic forms of the dye towards the fluorescent amide form[158].

4.4.2 UV-Vis spectroscopic characterization of fluorescein-appended β-CD

The UV-Vis spectra of Flu disodium salt and Flu-β-CD are shown in Figure 29.

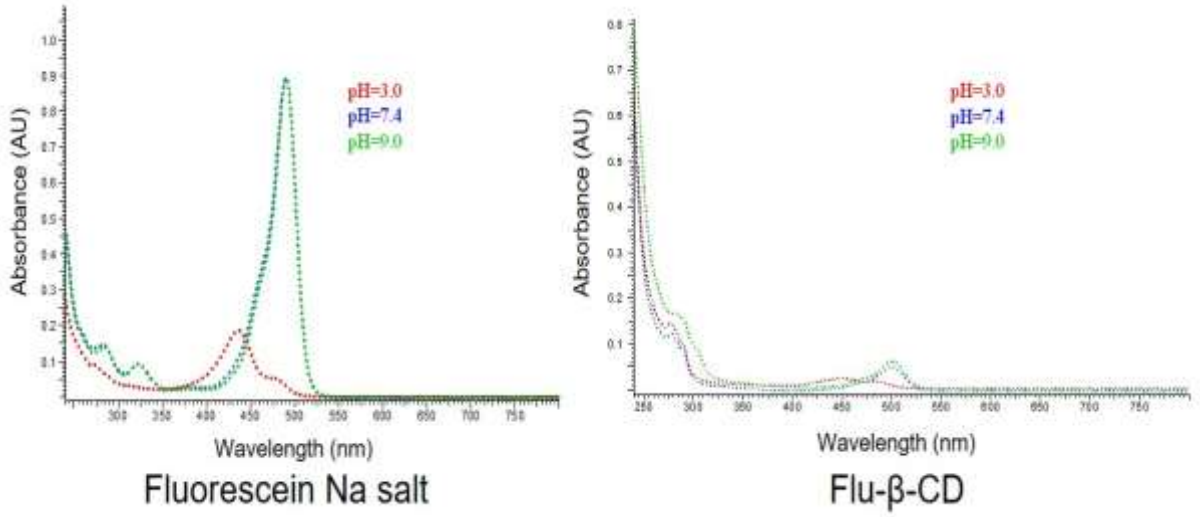

Figure 29. UV-Vis spectra of fluorescein disodium salt and fluorescein-appended β-CD at various pH values at the same concentration (c_{Flu} = $c_{Flu\text{-}\beta\text{-}CD}$ = 0.001 mM).

In acidic conditions (at pH=3) the UV-Vis spectrum of the free dye changes remarkably as well as its fluorescence. In particular, the peak at around 490 nm is almost completely suppressed, and the fluorescence under irradiation at 366 nm decreases substantially. This behavior is in agreement with the formation of the non-fluorescent lactone form of the Flu in acidic conditions[159]. The lactone formation is mainly responsible for the fluorescence quenching of the dye. The UV-Vis spectra of Flu-β-CD resemble those of Flu-

Na, and the fluorescence of the compound is heavily quenched at pH=3. By taking into consideration these data, it can reasonably be assumed that the Flu moiety of Flu-β-CD is mainly in the open amide form (at neutral and alkaline pH) and that the compound acts as a complementary molecular switch to Rho-β-CD. While Rho-β-CD exhibits fluorescence at acidic pH, Flu-β-CD shows fluorescence at neutral and alkaline pH.

4.4.3 Aggregation behavior of Eo-β-CD conjugates

For the aggregation investigation, Eo-β-CD solutions prepared with distilled water were studied. Eo-β-CDs were applied in 1 mM solution to obtain reliably high scattered intensity for the characterization by DLS. Figure 30 indicates that the aggregation behavior of mono(6-deoxy-6-eosinyl B-carboxamido)-β-CD (EoB-β-CD) and mono(6-deoxy-6-eosinyl Y-carboxamido)-β-CD (EoY-β-CD) samples significantly differs. The size distribution of EoY-β-CD shows that the sample is essentially monodisperse with a peak at around 5 nm. On the other hand, EoB-β-CD is more likely to form large aggregates, most probably due to the higher affinity of EoB (aromatic nitro compound) for the β-CD cavity. Aggregate populations sized approx. 100-300 nm, as well as 5000-6000 nm, were found for EoB-β-CD.

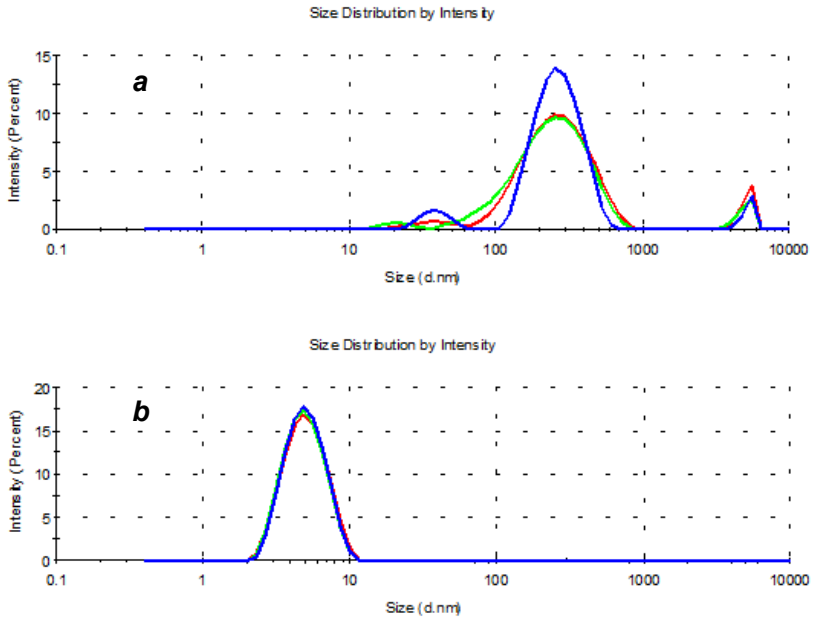

Figure 30. Size distributions of 1 mM aqueous EoB-β-CD (***a***) and EoY-β-CD (***b***) solution at 25.0 °C (pH=7) by intensity (three parallel measurements: blue, green and red lines).

The strong aggregation character of EoB-β-CD can remarkably influence the spectroscopic and photophysical properties of the conjugate.

4.4.4 Spectroscopic and photophysical properties of Eo-β-CD conjugates

Preliminary spectroscopic investigations on the conjugates were carried out in aqueous solutions. Figure 31 shows the absorption and fluorescence emission spectra of EoY-β-CD and for comparison of EoY. Apart from a slight red shift of the absorption maximum, the absorption spectral profile in the visible region of the conjugate is similar to that of the free dye, ruling out any relevant aggregation phenomena. This hypothesis was well confirmed by the fluorescence emission spectrum, which exhibits an intense band maximum at 550 nm. The fluorescence quantum yield was $\Phi_f = 0.20$, the very same value reported for the free EoY[160].

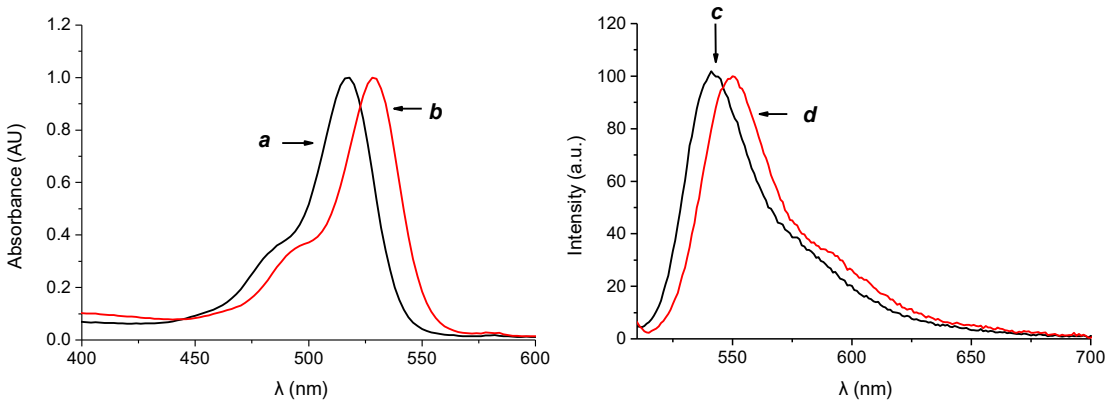

Figure 31. Normalized absorption spectra of aqueous solutions of eosin Y (*a*) and eosin Y-appended β-CD (*b*) and fluorescence emission spectra of optically matched aqueous solutions of eosin Y (*c*) and eosin Y-tagged β-CD (*d*) ($\lambda_{exc} = 490$ nm).

On the other hand, the fluorescence decay of the conjugate was different from the free, unconjugated EoY. Figure 32 illustrates the fluorescence decay traces observed in both cases.

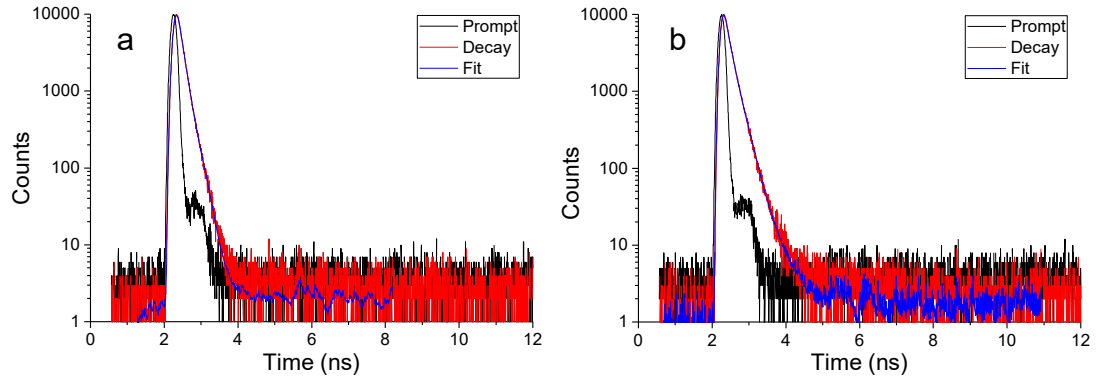

Figure 32. Time-resolved fluorescence observed for aqueous solutions of eosin Y (a) and eosin Y-tagged β-CD (b) ($\lambda_{exc} = 455$ nm; $\lambda_{em} = 570$ nm).

The analysis of the fluorescence decay in the case of EoY was fitted by a bi-exponential kinetic with a longer, dominant lifetime of 1.44 ns (83%) and a minor shorter component of 0.48 ns (17%). The decay of the EoY-β-CD conjugate was more complex and fitted by a tri-exponential fit with lifetimes of 4.26 ns (3%), 1.77 ns (45%) and below 0.2 ns (52%). This behavior may tentatively be attributed to populations of fluorophores probably interacting differently with the CD cavity.

As outlined in section 3.4.2., $^1O_2$ is the key species involved in PDT, and it is generated by energy transfer from the excited triplet state of a PS and the nearby molecular oxygen. Although several indirect methodologies based on suitable chemical traps are known to detect $^1O_2$ formation, the best experimental methodology to prove and quantify its production is its direct detection. It is based on the monitoring of the typical phosphorescence of $^1O_2$ in the near-IR spectral window[161]. As shown in Figure 33, excitation of the conjugate with visible green light led to the appearance of the characteristic luminescence signals with a maximum at *ca*. 1270 nm analogously to what observed for EoY. $^1O_2$ quantum yield of Φ_Δ = 0.47 was obtained, that is similar to that of the free dye in the same solvent (Φ_Δ = 0.49)[162]. This finding rules out any significant intra- or inter-encapsulation of the excited triplet state of the dye within the β-CD. If this was the case, the reduced quenching by oxygen due to steric hindrance would have resulted in a much smaller value for Φ_Δ.

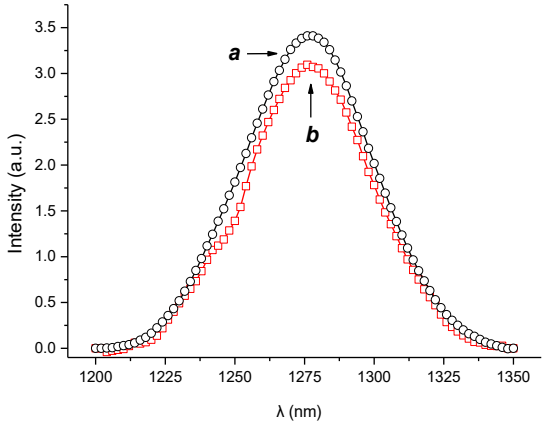

Figure 33. $^1O_2$ luminescence detected upon 528 nm light excitation of optically matched D_2O solutions of EoY (*a*) and EoY-β-CD (*b*).

The EoB-β-CD did not show either detectable fluorescence emission or $^1O_2$ photogeneration. This is not surprising in light of the massive aggregation of this derivative in an aqueous medium (see Figure 30). Studies in progress are addressed to clarify this point better and to design strategies to circumvent this drawback.

4.5 Synthesis of per(2,3-di-*O*-methyl-6-*O*-carboxymethyl)-CDs

Based on the numerous application sites of CDs peralkylated on their secondary side and percarboxymethylated on their primary rim, it is obvious that the development of a reliable and straightforward synthetic procedure, offering a high purity of the final compounds, is of significant importance.

The synthetic strategy towards this family of persubstituted compounds is shown in Figure 34. The first step aimed the protection of the primary hydroxyl groups; therefore heptakis(6-*O*-*tert*-butyldimethylsilyl)-β-CD (TBDMSi-β-CD) **(13)** and octakis(6-*O*-*tert*-butyldimethylsilyl)-γ-CD (TBDMSi-γ-CD) **(17)** were prepared according to a modified procedure of Fügedi *et al*[52].

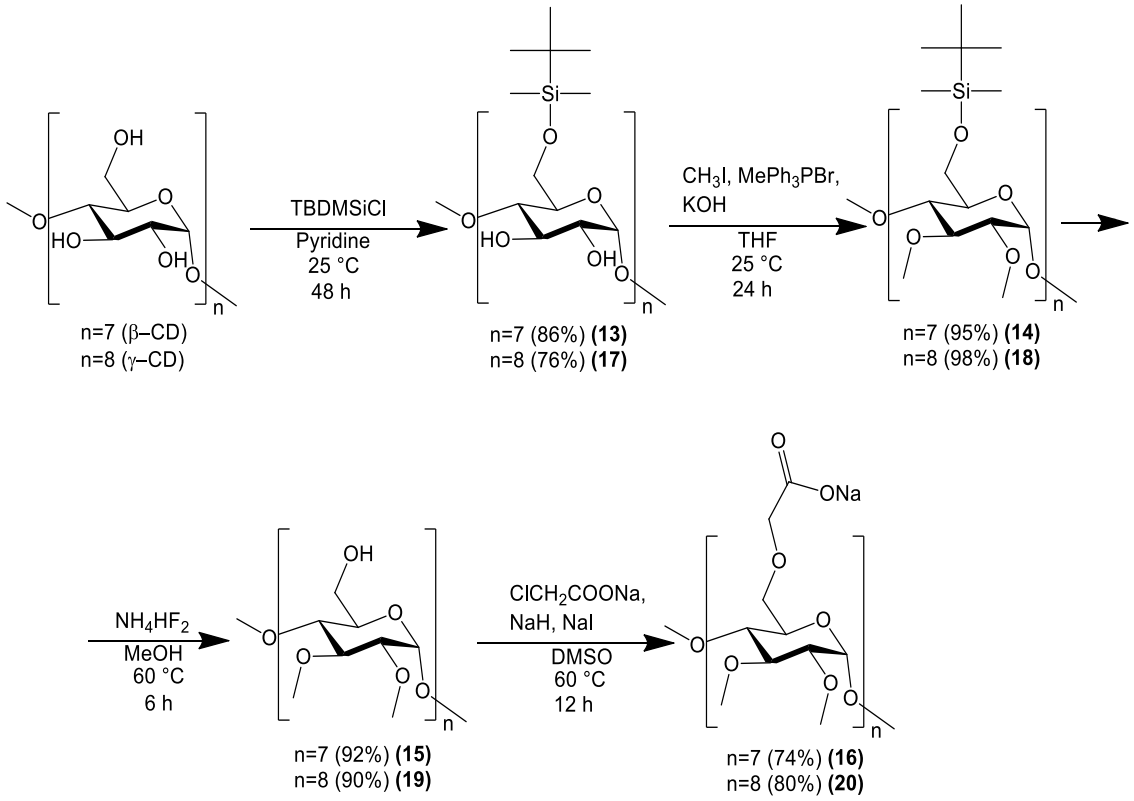

Figure 34. Synthesis scheme for the preparation of heptakis(2,3-di-*O*-methyl-6-*O*-carboxymethyl)-β-CD **(16)** and of octakis(2,3-di-*O*-methyl-6-*O*-carboxymethyl)-γ-CD **(20)**.

The changes respect to the established procedures in both cases were concerning the amount of silylating agent related to the amount of CD and the development of a rapid and reproducible purification methods. As first, the original procedure was modified in order to reduce the number of by-products. Upon addition of a small excess of *tert*-butyldimethylsilyl-chloride (TBDMSiCl) (1.1 equiv per OH-6 group in the case of β-CD and γ-CD) the TLC and the HPLC (Figure 35) monitoring showed the formation of the main products, the expected TBDMSi-β-CD and TBDMSi-γ-CD, respectively along with two by-products.

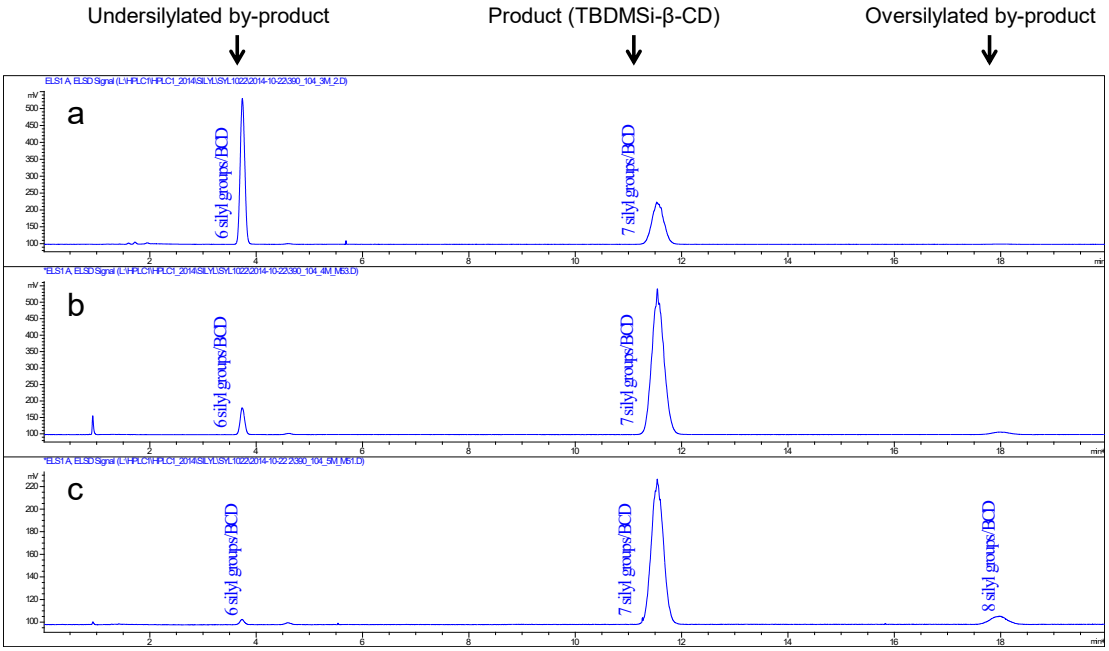

Figure 35. Reaction monitoring of silylation of β-CD by HPLC-ELSD: a) 1.0 equiv of TBDMSi-Cl per *OH*-6 group, b) 1.10 equiv of TBDMSi-Cl per *OH*-6 group, c) 1.25 equiv of TBDMSi-Cl per *OH*-6 group.

For β-CD the TLC (EtOAc/96%EtOH/H_2O 30/5/4 eluent mixture, direct-phase silica plate) showed three spots having R_f = 0.7, 0.6 and 0.3 for the oversilylated by-product, for the TBDMSi-β-CD product and for the undersilylated by-product, respectively. HPLC analysis (MeOH/EtOAc 78/22 mobile phase, isocratic, flow rate 1.8 mL/min, C18 stationary phase) with ELS detection showed the same amount of components with comparable intensity ratios. At this point, in order to simplify the purification, a small excess of TBDMSiCl (0.15 equiv per *OH*-6 group) was added until the most polar spot was no longer detectable by TLC neither by HPLC (Figure 35c). The separation of the two remaining components, the more polar product and the less polar oversilylated impurity, was easily performed by elution from a short pad of silica gel using quaternary mixtures of solvents. The dichloromethane

(DCM)/ACN/96%EtOH/(30%aq.NH_3) 40/40/20/4 mixture elutes exclusively the oversilylated species, while the target product stays immobilized at the top of the pad. Subsequently, TBDMSi-β-CD was recovered from the silica gel pad by changing the eluent to DCM/ACN/96%EtOH/H_2O 40/40/20/4 quaternary mixture. This procedure can be efficiently used for the purification of TBDMSi-β-CD, instead of the previously reported fractional crystallization methods, since it gives the consistently TLC and HPLC pure TBDMSi-β-CD in fairly good 86% yield[163].

By slight modification of this purification protocol, the persilylated γ-derivative could also be purified from its oversilylated by-product. Excess of TBDMSiCl (1.4 equiv per OH-6 group in total) was added until a two-component mixture was obtained. The crude product was immobilized on a short silica gel pad, and the less polar component was eluted with DCM/MeOH/96%EtOH/(30%aq.NH_3) 10/10/10/1 mixture. After a complete removal of the by-product, the targeted TBDMSi-γ-CD was eluted with the three-component mixture of DCM/MeOH/H_2O 10/5/1 as eluent. TBDMSi-γ-CD was recovered in 76% yield with 94% purity as determined by HPLC. It is worth to mention that the preparation of highly pure persilylated intermediates is the key factor of the entire single-isomer synthesis. If high purity is achieved at this first reaction step, due to the high yielding nature of the following reactions, the time-consuming column chromatographic purifications can be omitted.

The silylated intermediates TBDMSi-β-CD and TBDMSi-γ-CD were exhaustively methylated on their secondary sides by phase-transfer catalysis resulting in compounds heptakis(2,3-di-*O*-methyl-6-*O*-*tert*-butyldimethylsilyl)-β-CD **(14)** and octakis(2,3-di-*O*-methyl-6-*O*-*tert*-butyldimethylsilyl)-γ-CD **(18)**, respectively. The removal of the *tert*-butyldimethylsilyl protecting groups was carried out according to the protocol of Zhang *et al.*[164] yielding the per-2,3-dimethylated intermediates at a conversion rate of 92% and 90% for heptakis(2,3-di-*O*-methyl)-β-CD (HDM-β-CD) **(15)** and for octakis(2,3-di-*O*-methyl)-γ-CD (ODM-γ-CD) **(19)**, respectively.

HDM-β-CD and ODM-γ-CD are very versatile molecular scaffolds since they show high solubility in organic as well as in aqueous solvent mixtures[165]. Furthermore, they allow selective manipulation with the primary OH groups of CDs[69]. The ability of HDM-β-CD to separate enantiomers was tested in non-aqueous CE conditions, but it showed no enantiorecognition properties under the studied conditions[24]. The lack of enantioselectivity may arise from the absence of ionic interactions which would give oriented interactions with analytes, but also from the elimination of the hydrogen bond circle from the secondary side. It is well known from the literature that methylation of the secondary hydroxyl groups of CDs

eliminates the very strong network of H-bonds that keeps the CD cavity rigid and hence confers considerable flexibility on the macrocycle[166].

As the last step towards per-6-carboxymethylated CDs, the dimethylated intermediates were carboxymethylated on their primary side in DMSO using NaH as a base, NaI as a catalyst and sodium chloroacetate as an alkylating agent. The target product, the heptakis(2,3-di-*O*-methyl-6-*O*-carboxymethyl)-β-CD sodium salt (HDMCM-β-CD) **(16)** was recovered with a 74% yield while octakis(2,3-di-*O*-methyl-6-*O*-carboxymethyl)-γ-CD sodium salt (ODMCM-γ-CD) **(20)** was formed with a conversion rate of 80%. NaI catalyst plays a crucial role in these reactions since it *in situ* generates the iodoacetate alkylating agent which is readily soluble in DMSO and more reactive than the sodium chloroacetate counterpart. Both parameters, the high solubility (excess of alkylating agent in the reaction mixture) and electrophilicity are of significant importance as the multiple alkylation is occurring in close spatial proximities making the full substitution difficult to achieve. The reaction monitoring and the determination of the isomeric purity of the final product are similarly important and necessitate sophisticated chromatography. As the crude products of the carboxymethylation reactions are mixtures of structurally related polyanionic compounds, a stationary phase with weak anion-exchange and inclusion complex forming capacity was an optimal choice for the separation. Taking into account that the core structures of these polyanions are methylated CDs, the CD-Screen-IEC column was applied. This type of chromatography separates CD derivatives based on their ability to form inclusion complexes and ion pairs with ((4-dimethylamino)aryl)alkyl-carbamidesilyl silica gel and this stationary phase was constructed and optimized for analysis of negatively ionizable cyclodextrins[167]. The HPLC method using CD-Screen-IEC stationary phase was suitable for the separation of the impurities possessing a different degree of carboxymethylation.

In Figure 36 the HPLC monitoring of the carboxymethylation of ODM-γ-CD is depicted in the absence (a) and in the presence (b) of NaI as a catalyst. The purity of HDMCM-β-CD and ODMCM-γ-CD final products determined by CD-Screen-IEC chromatography with ELS detection was found to be 97.1% and 95.5%, respectively.

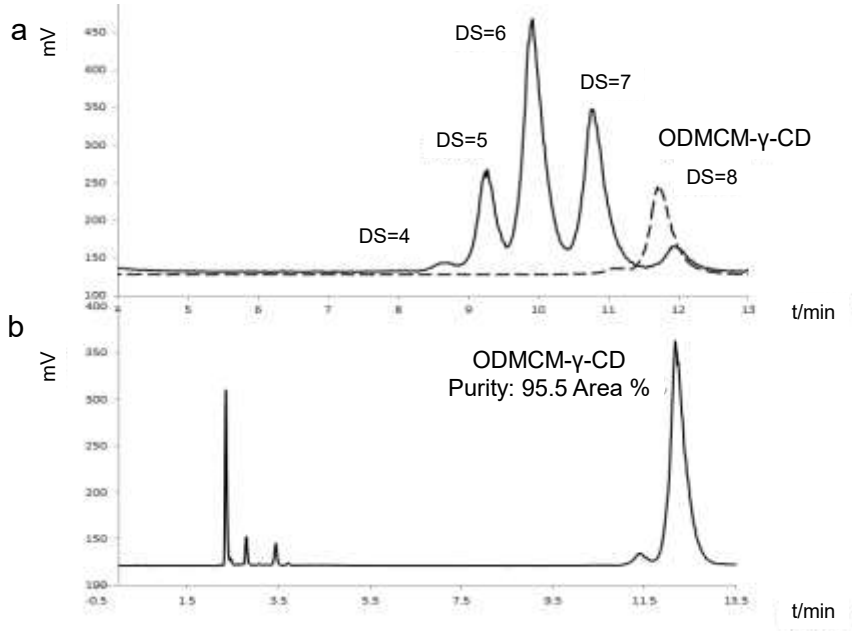

Figure 36. Chromatograms for the CD-Screen-IEC analysis of a) carboxymethylation of the ODM-γ-CD performed in the absence (solid line) and in the presence (dashed line) of NaI as catalyst (DS = degree of substitution for CM groups) b) the synthesized single-isomer ODMCM-γ-CD.

4.6 Characterization and application of per(2,3-di-O-methyl-6-O-carboxymethyl)-CDs in chiral capillary electrophoresis

HDMCM-β-CD and ODMCM-γ-CD are typical representatives of persubstituted carboxymethyl SIDs, but their application as chiral resolving agents has not been described to date. After the successful preparation and characterization of these compounds, the objective of our investigations has been to apply them in enantioseparations and to investigate the effect of their ionization states on the enantioseparation of various analytes. The single-isomer persubstituted HDMCM-β-CD contains seven CM substituents giving rise to a wide variety of differently charged forms depending on the pH. The predicted pK_a values of HDMCM-β-CD are as follows: pK_{a1}=2.37; pK_{a2}=2.73; pK_{a3}=2.99; pK_{a4}=3.21; pK_{a5}=3.43; pK_{a6}=3.69; pK_{a7}=4.06. The pK_a prediction in the case of multiprotic systems can often be misleading as

the interaction between the protonation sites could not be accurately predicted. This is why, in the case of the structurally related ODMCM-γ-CD, the pH-dependent ^{1}H NMR spectra were measured in order to highlight the limitation of the prediction.

Significant pH-dependent chemical shift changes (> 0.25 ppm) can be observed for the protons of the methylene moiety located in the proximity of the carboxylate (Figure 37). This resonance exhibits the expected downfield shift upon protonation, thereby being a good probe of local electron density and thus, carboxylate-specific ionization can be deduced. The ^{1}H NMR-titration curve of this resonance indicates that the overlapping protonation of the eight carboxylates occurs in the pH range of 2.04-7.70; consequently, ODMCM-γ-CD exists predominantly in octa-anionic form at pH 7.0, while the minute anionic character can be rendered to the host at pH 2.5.

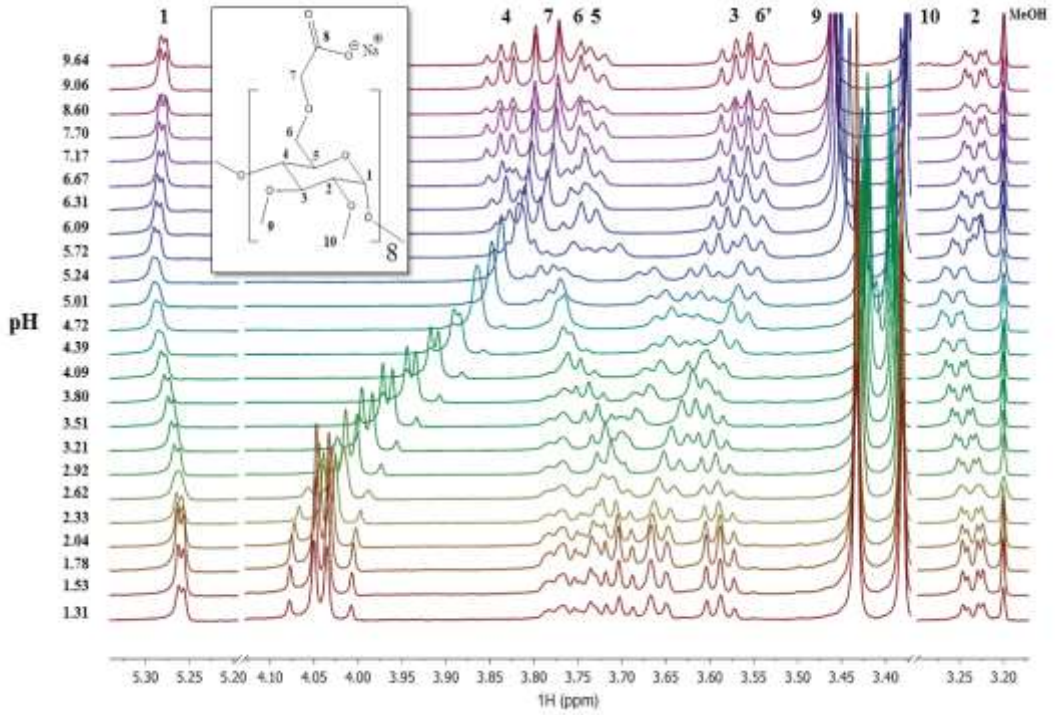

Figure 37. The NMR-pH titration of ODMCM-γ-CD (25.0 °C, 600 MHz).

Taking these data into consideration, the pH-dependent enantioselective features of these selectors were studied in a matrix of four CD concentrations (1, 2.5, 5, and 7.5 mM) and pH levels 2.5, 4.5 and 7.0. The chosen pH values represent three different forms of the chiral hosts: at pH 2.5 the majority of the carboxylates are protonated, HDMCM-β-CD and ODMCM-γ-CD being a slightly negatively charged selector, while at pH 7.0 almost all the carboxylates are deprotonated and therefore they behave as a hepta- and octa-anionic species,

respectively. Carboxymethylated CDs usually separate the enantiomers effectively in the pH range where the carboxylates are partially protonated[168,169,170,171,172], therefore HDMCM-β-CD was also tested at pH 4.5. At pH 2.5 the hydrogen bonds could be responsible for the enantioselective complex formation, while at pH 7.0 ionic interactions could be the main type of interactions due to the multianionic charge of the selector, which can drive the complex formation and increase the complex stability.

Tadalafil, a marketed drug for the treatment of erectile dysfunction (Cialis®) and pulmonary arterial hypertension (Adcirca®), contains two chiral centers, thus giving rise to four stereoisomers, among which the *RR*-tadalafil is in clinical use[173]. At pH 2.5 HDMCM-β-CD showed no enantiorecognition for none of the enantiomer pairs, while at pH 4.5 the *SS*-*RR* pair could be separated with the *SS, RR, SR, RS* stereoisomer migration order. Further increase in the pH resulted in resolution enhancement and at pH 7.0 all the four non-charged tadalafil stereoisomers could be baseline separated (with 3.3; 5.6 and 2.4 resolution factor (R_S) values, between the first-second, second third and third-fourth migrating stereoisomer, respectively) with the *SR, SS, RR, RS* migration order (Figure 38).

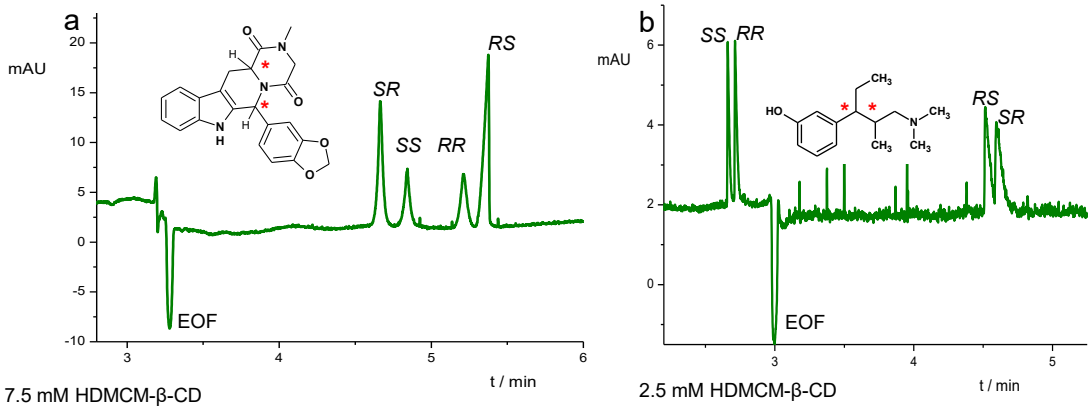

Figure 38. Representative aqueous chiral CE electropherograms applying HDMCM-β-CD at pH=7.0 for the separation of tadalafil (a) and tapentadol (b) enantiomers.

Tapentadol is an opioid analgesic with four stereoisomers, but the commercial preparations contain only the *RR* stereoisomer, which is the weakest isomer in terms of opioid activity[174]. By using HDMCM-β-CD as a chiral selector, the *SS, RR* enantiomers of tapentadol were not separated at pH 2.5. Increasing the BGE pH to 4.5 these isomers showed partial separation with an R_S value of 1.1 at 7.5 mM selector concentration. Unfortunately, at this pH the other enantiomeric pair (*RS, SR*) co-migrates with the EOF at 5 and 7.5 mM

selector concentrations. Resolution enhancement was observed for the *RR-SS* enantiomer pair while the *RS-SR* resolution deteriorated in the BGE of pH 7.0. The outstanding resolution and the distinct complexation behavior between the *SS/RR* and the *RS/SR* isomers manifested in a significant difference between their migration times: while *SS/RR* pair migrated as an apparent cationic associate (before the EOF), the *RS/SR* pair reached the detector after the electroosmotic flow (forming an apparent anionic complex with HDMCM-β-CD, Figure 38 b). Furthermore, due to the optimal *SS, RR* enantiomer migration order, this HDMCM-β-CD based CCE method could serve as a basis of a further chiral purity profiling method for the determination of *SS*-tapentadol in excess of the eutomer.

Dapoxetine, a selective serotonin reuptake inhibitor, marketed as Priligy® and Westoxetin®, is the first compound developed specially for the treatment of premature ejaculation[175]. As the eutomer (*S*)-dapoxetine is 3.5 times more effective than (*R*)-dapoxetine a fast and reliable enantioseparating method is essential for the analysis of the compound[176]. Using ODMCM-γ-CD as a chiral selector at pH 2.5 dapoxetine and its two metabolites exhibited remarkable enantioresolution in a selector concentration-dependent manner. Dapoxetine and demethyl-dapoxetine exhibited enantioseparation using 5 mM ODMCM-γ-CD, while the enantiomers of didemethyl-dapoxetine could be resolved by applying as low as 1 mM CD concentration. As the NMR titration (Figure 37) revealed, at this low pH value the selector is practically electroneutral, while the dapoxetine derivatives, being tertiary, secondary and primary amines respectively bearing a positive charge. Furthermore, increasing the ODMCM-γ-CD concentration in the BGE the migration times increased, indicating the strong interaction between the positively charged dapoxetines and the practically neutral host. Despite the absence of strong electrostatic interactions between host and the guest, enantiorecognition occurred which highlights the importance of other underestimated interactions (hydrogen bonding, ion-dipole interactions) what such well defined carboxymethylated selector as ODMCM-γ-CD can offer.

At pH 7.0 all the dapoxetine derivatives are protonated, existing in monocationic form while ODMCM-γ-CD exists as an octaanionic species, therefore the ionic interaction between the oppositely charged species is preferred. Enantiorecognition occurred in the case of all the studied dapoxetine metabolites, but the increase in ODMCM-γ-CD concentration resulted in a pronounced increase in migration time; thus the evaluation of these electropherograms are neglected due to peak distortions or extremely long analysis time (see Figure 39 c and 39 d).

Contrary to that, the migration times at pH 2.5 are significantly shorter allowing reduced analysis times and providing improved peak shapes (see Figure 39 a and b). Therefore, fine-tuning the pH of the BGE could be a key parameter in method developments.

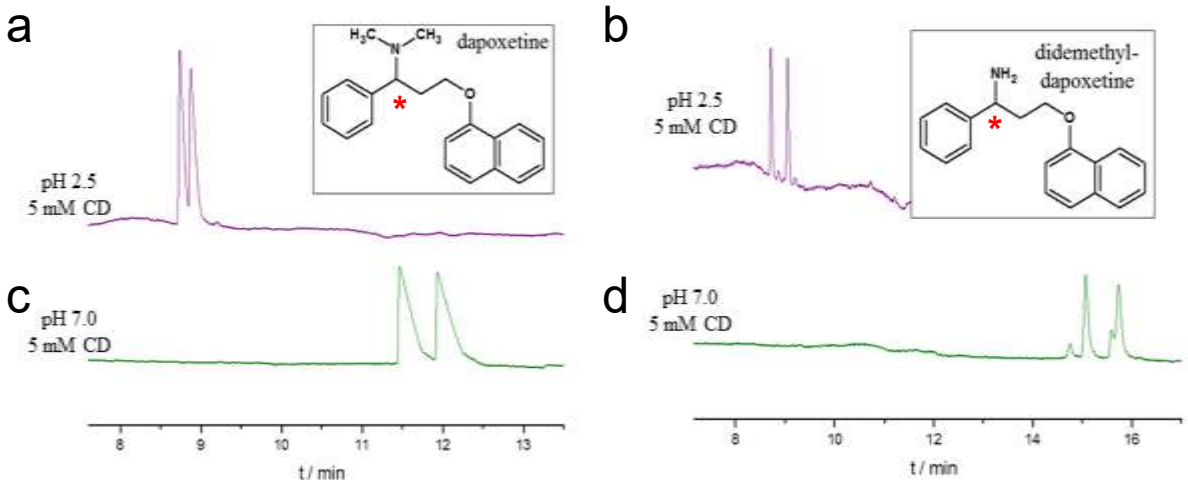

Figure 39. Representative chiral CE electropherograms applying ODMCM-γ-CD demonstrating the dependency on the pH of the BGE.

In order to characterize the host-guest interaction at a molecular level and to get a deeper insight into the discrimination of dapoxetine enantiomers observed by CCE method, NMR spectroscopic methods were applied. Similarly to the CCE experiments, the enantioselectivity of ODMCM-γ-CD by NMR was also monitored at two pH values (pH 2.5 and at pH 7.0) with racemic dapoxetine.

In the ^{1}H NMR spectra, complexation induced chemical shift changes of the individual enantiomers could be observed at both pH values (Figure 40).

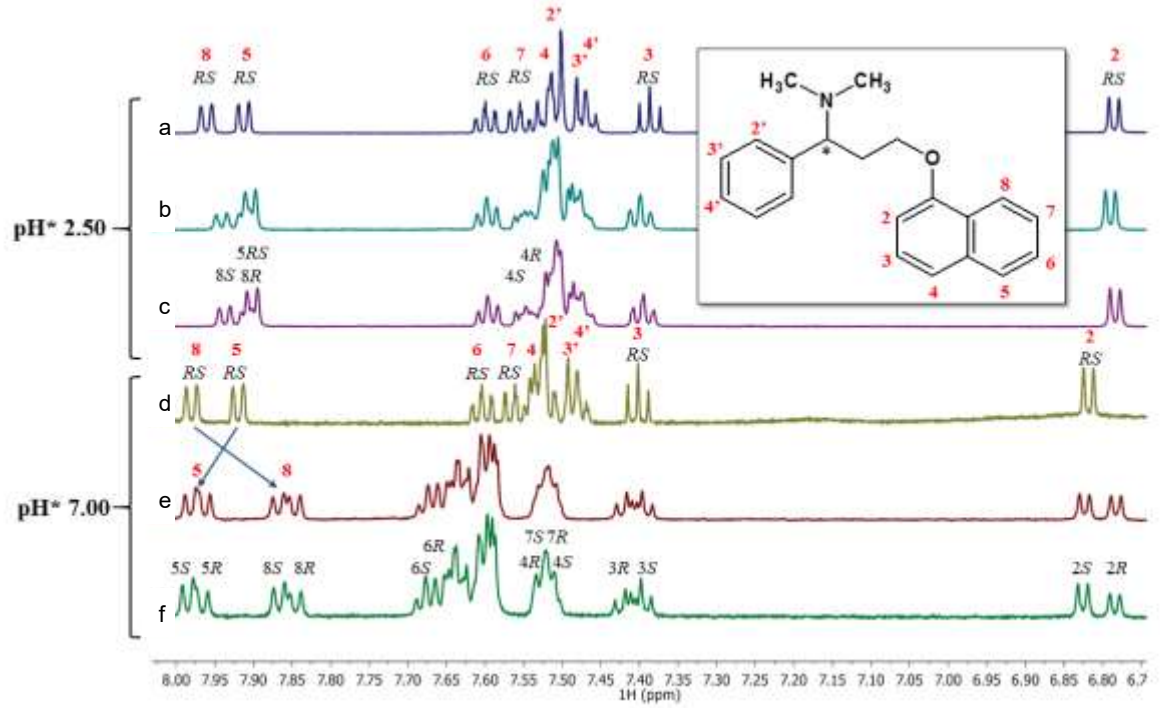

Figure 40. The ^{1}H NMR spectra of a) racemic dapoxetine, b) racemic dapoxetine and ODMCM-γ-CD, c) racemic dapoxetine and ODMCM-γ-CD system spiked with (*S)*-dapoxetine at pH 2.5, d) racemic dapoxetine, e) racemic dapoxetine and ODMCM-γ-CD, f) racemic dapoxetine and ODMCM-γ-CD system spiked with (*S)*-dapoxetine at pH 7.0.

By spiking the dapoxetine-ODMCM-γ-CD system with enantiopure (*S)*-dapoxetine, the ^{1}H NMR resonances of the enantiomers could be assigned. Comparing the ^{1}H NMR spectra of the dapoxetine-ODMCM-γ-CD system at two pHs, significant differences could be observed. While at pH 2.5, only the *H*-8 resonance of the naphthyl moiety shows remarkable enantiomeric splitting. Contrary to that, significant enantiomeric splitting can be observed in the case of all resonances (*H*-2, *H*-3, *H*-4, *H*-5, *H*-6, *H*-7 and *H*-8) of the naphthyl moiety of dapoxetine at pH 7.0 (where dapoxetine is in monocationic- and ODMCM-γ-CD in polyanionic form, respectively). More pronounced complexation-induced chemical shift changes ($\Delta\delta$) can also be observed at pH 7.0 compared to pH 2.5: *H*-8 exhibits an upfield shift of $\Delta\delta > 0.1$ ppm, *H*-7 reflects an upfield shift of $\Delta\delta = 0.05$ ppm, while both *H*-6 and *H*-5 resonances shifted downfield (see Figure 40) upon complexation. Both $\Delta\delta$ values and the number of enantiomeric splittings observed suggest, that ODMCM-γ-CD shows

enantioselective recognition of dapoxetine isomers at pH 2.5 and also at pH 7.0, however, this effect is more pronounced and more observable by NMR at pH 7.0, while pH 2.5 can be beneficial for the development of a rapid CCE method.

5. Conclusions

The main objective of this thesis was the preparation of well defined single-isomer CD derivatives applicable in analytical and pharmaceutical sciences where the isomeric purity of CDs is of relevant importance as it might influence the proposed application.

Cinnamylated α-CDs were prepared as potential pseudostationary phases for capillary electrophoresis where their self-assembling and chiral character is intended to improve analytical separations[43]. The three monosubstituted regioisomers were synthesized using a straightforward approach which allowed the gram-scale isolation of the compounds of interest. The unequivocal characterization and identification of the three regioisomers was performed with the aid of 1D and 2D NMR measurements. Interestingly, the three isomers showed distinct physico-chemical properties which most probably originates from their different intermolecular interactions. 6-*O*-Cin-α-CD was found to be sparingly soluble in water, whereas the 2-*O*- and 3-*O*-isomer showed very high aqueous solubility; therefore the mechanism of the self-assembly of these two derivatives was further investigated and compared. NMR and DLS studies revealed, that 2-*O*-Cin-α-CD and 3-*O*-Cin-α-CD form supramolecular aggregates through intermolecular host-guest interactions and the size of these assemblies can be controlled by external stimuli, such as temperature or addition of suitably sized guest molecules. The possibility of using these two derivatives as background electrolyte additives in capillary separation techniques is currently under investigation but other applications, where a tunable size of highly-ordered structures is needed, can also benefit from these supramolecular structures.

With the aim to prepare fluorophore-tagged β-CDs, a new synthetic methodology was developed based on a coupling reaction between NH_2-β-CD, commercially available coupling agent and unmodified xanthene dyes[106]. This method is superior to the previously used one based on isothiocyanate coupling, as it does not require the laborious isothiocyanate premodification of the dyes and can be performed under mild reaction conditions in aqueous solvents. The versatility of the method was demonstrated by the preparation of 4 different xanthene-β-CD conjugates. Eo-β-CD derivatives were investigated as potential

photosensitizing agents, while Flu-β-CD and Rho-β-CD were studied as pH-sensitive chemosensors[106,107].

The second part of the thesis is focused on the synthesis of selectively persubstituted β- and γ-CDs[67]. Previously described procedures for synthesis of key intermediates (TBDMSi-β-CD, TBDMSi-γ-CD, HDM-β-CD, ODM-γ-CD) were optimized to afford products in highest possible yields and isomeric purity. From these synthons, single-isomer carboxymethylated β-CD (HDMCM-β-CD) and γ-CD (ODMCM-γ-CD) were prepared, completely methylated on their secondary side and fully carboxymethylated on their primary rim. The enantioresolution power of these chiral selectors was studied on pharmaceutically relevant racemates such as the selective serotonin reuptake inhibitor dapoxetine, the analgesic tapentadol or the phosphodiesterase type 5 inhibitor tadalafil. As the ionic character of these derivatives is pH dependent, great emphasis was laid on the understanding, how the ionization state of the selector influences the enantiorecognition process.

Throughout this work, several mono- and persubstituted single-isomer CDs were prepared as final products or as key intermediates for further synthesis. The fact that many of these compounds have been already successfully used in different analytical[67,24] and pharmaceutical applications[68,145], indicates the growing interest for selectively substituted CDs and underlines the importance of the recent study. Furthermore, fluorophore-tagged CD derivatives and selectively persubstituted derivatives developed in this thesis appeared in the fine chemical product portfolio of the world's only all-around cyclodextrins company (CycloLab Cyclodextrin Research and Development Laboratory, Budapest, Hungary), showing also the interest of the private sector.

6. Experimental part

6.1 Details of analytical measurements

Acetonitrile (HiPerSolv for HPLC-SuperGradient) used for HPLC measurements was the product of VWR International (Radnor, PA, USA). Triethylamine, formic acid and ammonia solution used for preparation of HPLC buffers, as well as benzoic acid and Tris, used for the preparation of CE buffer solutions were of analytical grade and purchased from commercial suppliers. All reagents were used without further purification. Purified water (Millipore-Synergy) was used throughout the capillary electrophoretic study. D_2O, $CDCl_3$, CD_3OD and DMSO-d_6 was purchased from Merck KGaA.

Melting points were determined in an open capillary using Büchi MP B-545 equipment.

Silica gel coated TLC aluminum sheets were from Merck (Art. No.:1.05554). Plates were developed in a saturated chamber. Visualization of TLC plates was achieved under UV light at 254/366 nm and by charring with a solution of 96%-EtOH/96%-H_2SO_4 9/1 by heating at 105-110 °C. Quantitative analysis of TLC plates was performed with the software JustQuantify Free.

^{1}H-, ^{13}C- NMR spectra and DEPT-ed-HSQC, HMBC, TOCSY, COSY and ROESY spectra were recorded in D_2O on a Varian VXR-600 at 600 MHz at 25 °C.

Mass spectra were obtained on Bruker ESQUIRE 3000 ES-ion trap instrument with electrospray ionization (ESI) in negative and positive mode.

CE experiments were conducted on an Agilent 7100 Capillary Electrophoresis System equipped with Diode Array Detector (Waldbronn, Germany). The free dye content of the xanthene-modified CD derivatives was measured by CE in 30 mM NaH_2PO_4 buffer of pH set to 6.1. The samples were run in uncoated fused silica capillaries of 25 cm effective length at 20 kV applied voltage and introduced hydrodynamically at 200 mbar·s. On each day, before a set of measurements the capillary was washed with H_2O for one minute, followed by 1 M NaOH for ten minutes, 0.1 M NaOH for three minutes and again water for one minute. Between the runs, the capillary was flushed with 0.1 M NaOH-water-0.1 M NaOH for 1 minute each and with the operating buffer for 2.5 minutes. A series of calibration solutions corresponding to 5-0.2% of free dye in the product were applied for quantification.

Infrared spectroscopy was performed on Thermo Nicolet AVATAR 370 FT-IR instrument.

UV/Vis absorption and fluorescence spectra were recorded with a Jasco V 650 spectrophotometer and a Fluorolog-2 (Model, F111) spectrofluorimeter, respectively. The total fluorescent dye content was evaluated by UV-Vis spectroscopy. The estimation of the chromophore was performed based on a calibration curve using as standard the starting fluorescent dye (Rho B, Flu disodium salt, EoY or EoB).

Fluorescence lifetimes were recorded with Fluorolog-2 (Model, F111) spectrofluorimeter equipped with a TCSPC Triple Illuminator. The samples were irradiated by a pulsed diode excitation source Nanoled at 455 nm. The kinetic was monitored at 545 nm and each solution itself was used to register the prompt at 455 nm. The system allowed measurement of fluorescence lifetimes from 200 ps.

$^1O_2$ emission was registered with the same spectrofluorimeter equipped with a NIR-sensitive liquid nitrogen cooled photomultiplier, exciting the air-equilibrated samples in D_2O solution at 528 nm with the fluorimeter lamp. The fluorescence and $^1O_2$ quantum yields of Eo-β-CD conjugates were calculated by using EoY as a reference.

The aggregate size measurements were carried out using a Malvern Zetasizer Nano ZS instrument (Malvern Instruments Ltd, United Kingdom) equipped with the manufacturer's standard 633 nm laser source. The samples were analyzed at 25 ºC having the solutions filled inside a quartz cuvette of 1.00 × 1.00 cm dimensions. The particle sizes were obtained from the autocorrelation functions recorded and processed by Zetasizer Software version 6.2.

Agilent 1100 HPLC system equipped with refractive index (RI) detector or evaporative light scattering detector (ELSD, Alltech 3300, Grace, MD, USA) was used to determine the purity of all CD derivatives. TBDMSi-β-CD and TBDMSi-γ-CD were analyzed applying a non-aqueous reversed-phase HPLC method based on the method developed by Busby *et al*[177]. Luna C18 analytical column (250 mm × 4.6 mm, 5 µm, Phenomenex Inc., Torrance, CA, USA) was used with MeOH/EtOAc 78/22 mobile phase at a flow rate of 1.8 mL/min and refractive index detection. Kinetex C18 (100 mm × 4.6 mm, 2.6 µm, Phenomenex Inc., Torrance, CA, USA) stationary phase with a mobile phase of IPA(isopropyl alcohol)/MeOH/H_2O 7/41/52 at a flow rate 0.5 mL/min and RI (refractive index) detector was used for the purity assesment of HDM-β-CD and ODM-γ-CD. HDMCM-β-CD and ODMCM-γ-CD were characterized by an anion-exchange inclusion assisted HPLC method using a 250 mm × 4.6 mm analytical column packed with a 5 µm CD-Screen-IEC stationary phase (Bio-Sol-Dex Ltd, Kecskemét, Hungary) with a solvent gradient of 1.5% triethylamine formate buffer (pH 4.0) with ACN (0 min 15%, 15 min 40%) for HDMCM-β-CD and with a solvent gradient of 36 mM ammonium acetate buffer (pH 4.0) with ACN (0 min 20%, 20 min 40%). Flow rate for HDMCM-β-CD analysis was set to 1.1 mL/min while for ODMCM-γ-CD separation was set to 1.0 mL/min. ELS detection was used in both cases.

CE experiments for the purity assessment of the final HDMCM-β-CD and ODMCM-γ-CD products were carried out on an Agilent 7100 instrument (Agilent Technologies, Waldbronn, Germany), equipped with a photodiode array detector and the Chemstation software for data handling. Untreated fused silica capillaries (33.5 cm total, 25 cm effective length, 50 µm id, Agilent) were used. The temperature of the capillary was set to 25 °C. During measurements 20 kV voltage was applied in positive polarity mode. Indirect UV detection was performed at 350 nm/200 nm. The running buffer contained 30 mM benzoic acid and 100 mM Tris, pH 8.2.

Aqueous CCE measurements were carried on an HP CE3D instrument, nonaqueous capillary electrophoretic measurements on an Agilent 7100 instrument (Agilent Technologies, Waldbronn, Germany), both equipped with a photo-DAD and the Chemstation software for data handling. Untreated fused silica capillaries were used (58.5 cm total, 50 cm effective length, 50 μm id for aqueous; 33.5 cm total and 25.0 cm effective length and 50 μm id for NACE tests from Agilent). In both setups, the temperature of the capillaries was set to 20 °C, during the measurements 30 kV voltage was applied, UV detection was performed at 200 nm. Samples were injected hydrodynamically (40 mbar 3 s for aqueous CE, 50 mbar 4 s for NACE).

6.2 Reagents and chemicals

α-, β- and γ-CD were the products of Wacker Chemie AG (Munchen, Germany). Anhydrous DMF was prepared by distillation with P_2O_5 at reduced pressure and was stored over molecular sieves 3 Å under argon atmosphere. Anhydrous pyridine was prepared by standing over KOH for several days and subsequent distillation from CaH_2 under atmosphere of Ar. Molecular sieves were activated at 280 °C for 8 h under reduced pressure (1 Pa). Cinnamyl bromide (97% purity), *trans*-cinnamic acid, adamantane-1-carboxylic acid, sodium hydride (60% dispersion in mineral oil), fluorescein disodium salt (Flu-Na, 98.5-100.5%), 4-(4,6-dimethoxy-1,3,5-triazin-2-yl)-4-methylmorpholinium chloride (DMT-MM-Cl, >96%), 4-methylmorpholine (NMM, 99%), *N*-bromosuccinimide (ReagentPlus, 99%,), eosin Y disodium salt (dye content ≥85%, Source 1), eosin B (Dye content 90%, Source 1) Rhodamine B HCl salt (Rho-B·HCl, ≥95%), rhodamine B base (Rho-B Lactone, dye content >97%), *N*,*N*′-dicyclohexylcarbodiimide (DCC, 99%) and 1-hydroxybenzotriazole hydrate (HOBt, ≥99%), ammonium hydrogen difluoride ($(NH_4)HF_2$ 98.5%), *tert*-butyldimethylsilyl chloride (97%), sodium chloroacetate (98%), potassium hydroxide (KOH, 85%), sodium iodide (NaI, 99%), triethylamine (99.5%), tosyl chloride (99%), and hydrazine monohydrate (98%) were sourced from Sigma-Aldrich (St. Louis, MO, USA). Eosin Yellowish (Lot: 10187074, Source 2) and Eosin B (Lot: 10184683, Source 2) were sourced from Alfa Aesar. Methyltriphenylphosphonium bromide (98%), iodomethane (CH_3I, 99%) and palladium/charcoal activated (10% Pd or 5% Pd content) were purchased from Merck KGaA (Darmstadt, Germany). Syntheses solvents and solvents for TLC eluents such as pyridine, THF, DMSO, DMF, MeOH, EtOH, 1-propanol, ACN, $CHCl_3$, DCM, NH_4OH (25% and 30%

NH_3 in H_2O) were of reagent grade and were sourced from Molar Chemicals (Halásztelek, Hungary).

6.3 Synthesis of compounds

6.3.1 Synthesis of monosubstituted cinnamyl-α-cyclodextrins

Mono-2-*O*-cinnamyl-α-cyclodextrin (1a) (2-*O*-Cin-α-CD) and mono-3-*O*-cinnamyl-α-cyclodextrin (1b) (3-*O*-Cin-α-CD)

Dried α-CD (5 g, 5.14 mmol) was dissolved in dry DMSO (50 mL), and sodium hydride (60% dispersion in mineral oil) was added (0.148 g, 6.16 mmol) to the solution. The reaction mixture was stirred under argon atmosphere for 3 h, then cinnamyl bromide (1.21 g, 6.16 mmol) was added to the reaction mixture. The reaction was monitored by direct-phase TLC (1-propanol/H_2O/EtOAc/(25%aq.NH_3) 6/3/1/1) and by reversed-phase TLC (H_2O/MeOH 1/1) and was determined as finished after 3 h when no significant increase in monosubstituted derivatives was observed. The reaction mixture was neutralized with HCl and then concentrated under reduced pressure at 70 °C. Addition of acetone (500 mL) to the concentrated DMSO solution yielded a white precipitate that was filtered out and washed with acetone (3 × 50 mL). Direct-phase TLC showed that the precipitate consisted of a mixture of unreacted α-CD, monosubstituted α-CD, and disubstituted α-CD, while the mother liquor contained only the unreacted cinnamyl bromide. The precipitate was dissolved in DMF (30% solution) and injected into the preparative reversed-phase chromatographic column. The unreacted α-CD, the pure isomers of the mono-Cin-α-CD and the fraction of di-Cin-α-CD derivatives were eluted separately from the column using a gradient of H_2O/MeOH (from H_2O/MeOH 100/0 to H_2O/MeOH 50/50) elution mixture. Fractions with H_2O/MeOH 90/10 eluent were concentrated to give the compound **1b** in (1.05 g, 21% yield).

Mono-3-*O*-cinnamyl-α-cyclodextrin (1b) (3-*O*-Cin-α-CD)

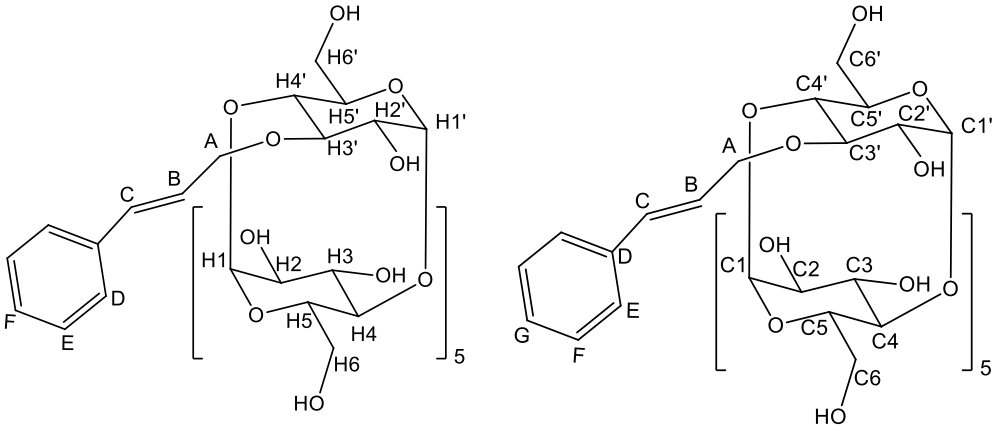

^{1}H NMR (600 MHz, D_2O) δ (ppm): 7.63 (d, *J*=7.6 Hz, 2H, D), 7.57 (dd, 2H, E), 7.50 (t, *J*=7.3 Hz, 1H, F), 6.77 (d, *J*=15.8 Hz, 1H, C), 6.48 – 6.40 (1H, B), 5.15 – 4.98 (6H, *H*-1, *H*-1'), 4.57 – 4.40 (m, 2H, A), 4.02 – 3.53 (m, 36H, *H*-2, *H*-3, *H*-4, *H*-5, *H*-6, *H*-2', *H*-3', *H*-4', *H*-5', *H*-6').

^{13}C NMR (150 MHz, D_2O) δ (ppm): 138.98 (D), 138.44 (C), 131.64 (F), 130.94 (G), 129.16 (E), 127.22 (B), 104.72 – 103.49 (*C*-1', *C*-1), 84.31 – 83.65 (*C*-4, *C*-4'), 82.09 (*C*-2'), 79.82 – 79.60 (*C*-3'), 76.16 (A), 76.61 – 73.88 (*C*-2, *C*-3, *C*-5', *C*-5), 63.02-62.79 (*C*-6, *C*-6').

ESI-MS *m/z* found: 1111.4 $[M + Na]^+$, calculated $C_{45}H_{68}O_{30}Na$ $[M + Na]^+$: 1111.3688.

Evaporation of fractions with the H_2O/MeOH 70/30 elution mixture afforded compound **1a** (0.45 g, 9% yield).

Mono-2-*O*-cinnamyl-α-cyclodextrin (1a) (2-*O*-Cin-α-CD)

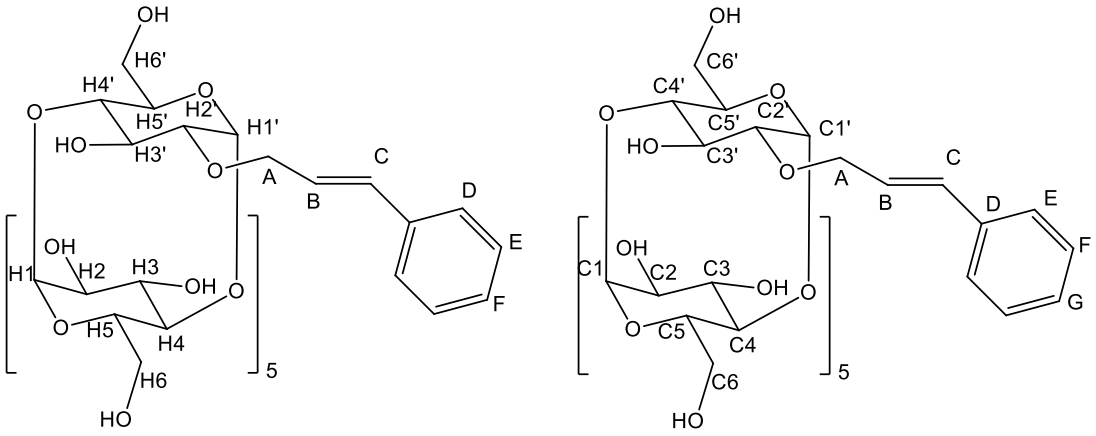

^{1}H NMR (600 MHz, D_2O) δ (ppm): 7.62 (d, *J*=7.5 Hz, 2H, D), 7.50 (dd, *J*=7.3 Hz, 2H, E), 7.41 (t, *J*=7.5 Hz, 1H, F), 6.83 (d, *J*=15.9 Hz, 1H, C), 6.50-6.42 (m, 1H, B), 5.22 (s, 1H, *H*-1'), 5.12-4.99 (5H, *H*-1), 4.47 (m, 2H, A), 4.05 (t,1H, *H*-3'), 4.09-3.57 (m, 35H, *H*-2, *H*-3, *H*-4, *H*-5, *H*-6, *H*-2', *H*-4', *H*-5', *H*-6').

^{13}C NMR (150 MHz, D_2O) δ (ppm): 138.95 (D), 136.35 (C), 131.49 (F), 130.68 (G), 129.26 (E), 127.80 (B), 104.27–103.90 (C1), 102.16 (*C*-1'), 84.55 – 73.90 (*C*-2, *C*-3, *C*-4, *C*-5, *C*-2', *C*-3', *C*-4', *C*-5'), 75.21 (*C*-3'), 74.82 (A), 63.11-62.79 (*C*-6), 63.00 (*C*-6').

ESI-MS *m*/*z* found: 1111.4 $[M + Na]^+$, calculated $C_{45}H_{68}O_{30}Na$ $[M + Na]^+$: 1111.3688.

Regioisomeric analysis was carried out by cross-linking the data of ^{1}H NMR, ^{13}C NMR, correlation spectroscopy NMR (COSY), total correlated spectroscopy NMR (TOCSY), distortionless enhanced polarization transfer edited heteronuclear single quantum correlation NMR (DEPT-edited-HSQC) and heteronuclear multiple bond coherence NMR (HMBC).

As an example, the elucidation of compound **1a** is discussed in section 4.1. The 2D NMR spectra used for the identification of compound **1b** can be found in our published article[43].

Mono-6-*O*-cinnamyl-α-cyclodextrin (2) (6-*O*-Cin-α-CD)

The compound **2** was prepared according to the procedure published in literature[42]. α-CD (5 g, 5.14 mmol) was dissolved in a solution of NaOH (8.8 g, 221 mmol) in H_2O (28 mL). The solution was cooled to 0 °C, and cinnamyl bromide (1.14 mL, 7.7 mmol) was added dropwise with stirring. The mixture was then stirred for three days at room temperature. The reaction was quenched with 50% H_2SO_4, adjusted to neutral pH, and the reaction mixture was evaporated in vacuo. The residue was adsorbed on silica gel (20 g), and separation by chromatography on silica gel column (1-propanol/H_2O/(25%aq.NH_3) 6/3/1) afforded title compound as a white powder (0.346 g, 6% yield).

Mono-6-*O*-cinnamyl-α-cyclodextrin (2) (6-*O*-Cin-α-CD)

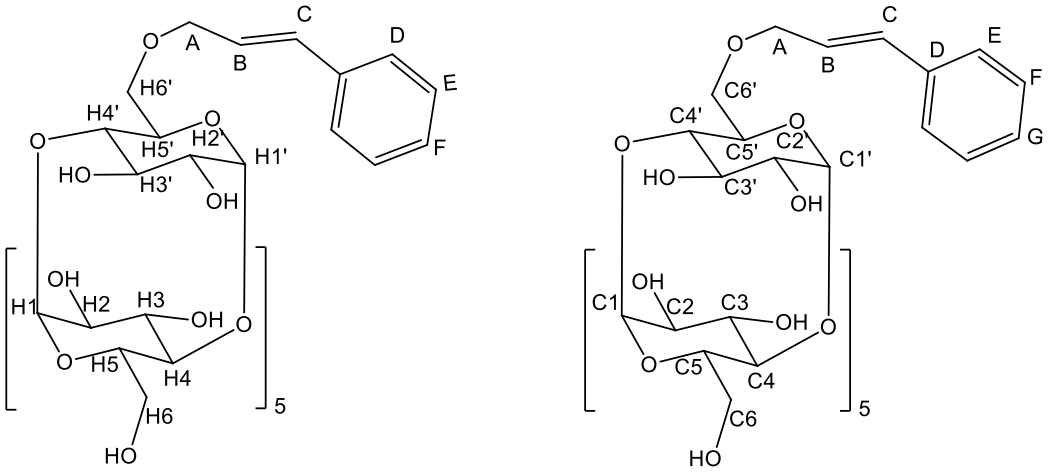

^{1}H NMR (600 MHz, 1:1 CD_3OD–D_2O) δ (ppm): 7.46 (d, *J*=7.6 Hz, 2 H, D), 7.40 (dd, *J*= 7.5 Hz, 2 H, E), 7.33 (t, *J*=7.3 Hz, 1 H, F), 6.72 (d, *J*=15.9 Hz, 1 H, C), 6.41 (dt, 1 H, *J*=15.8 Hz, B), 5.03–4.98 (m, 6 H, *H*-1, *H*-1'), 4.24 (d, *J*=6.0 Hz, 2 H, A), 3.96–3.51 (m, 36H, *H*-2, *H*-3, *H*-4, *H*-5, *H*-6, *H*-2', *H*-3', *H*-4', *H*-5', *H*-6').

^{13}C NMR (150 MHz, 1:1 CD_3OD–D_2O) δ (ppm): 137.49 (D), 134.01 (C), 129.72 (F), 129.01 (G), 127.43 (E), 126.44 (B), 103.02 – 102.08 (*C*-1, *C*-1'), 82.69 – 72.18 (*C*-2, *C*-3, *C*-4, *C*-5, *C*-2', *C*-3', *C*-4', *C*-5'), 72.87 (A), 69.47 (*C*-6'), 64.56 – 61.27 (*C*-6).

ESI-MS *m*/*z* found: 1111.4 $[M + Na]^+$, calculated $C_{45}H_{68}O_{30}Na$ $[M + Na]^+$: 1111.3688.

6.3.2 Synthesis of monosubstituted β-CD scaffolds for fluorophore labeling

Mono-6-*O*-tosyl-β-cyclodextrin (3) (Ts-β-CD)

Compound **3** was prepared according to the published procedure[33] which was modified.

β-CD (22.6 g, 20 mmol) was dissolved in hot water (250 mL), a solution of copper(II) sulfate (15 g, 60 mmol) in water (150 mL) and a solution of sodium hydroxide (12 g, 300 mmol) in water (150 mL) were added in sequence. The addition of the sodium hydroxide solution resulted in a color change of the solution from light green to deep blue. The reaction mixture was stirred at room temperature for 10 min, and then a solution of tosyl chloride (4.8 g, 25 mmol) in ACN (25 mL) was added drop-wise over a period of 2 h. The reaction was monitored by direct-phase TLC (1,4-dioxane/(25%aq.NH_3)/1-propanol 10/7/3) and was determined as finished after 5 h, when no significant increase in monotosylated derivative was observed (R_F = 0.3). The dark blue solution was neutralized using H^+ ion exchange resin. The

blue color of the solution disappeared during the resin treatment. Filtration of the resin resulted in a colorless, transparent solution (pH=7), which was concentrated under reduced pressure (10 mbar) at 40 °C to a 1/500 of its volume and was poured into acetone (400 mL). A white precipitate was obtained which was filtered out, washed with acetone (3 × 50 mL) and dried to constant weight in a vacuum drying box in the presence of P_2O_5 and KOH. The crude product contained unsubstituted β-CD, target product Ts-β-CD, and multiply tosylated derivatives. Compound **3** (6.76 g, 5.24 mmol) from this mixture was obtained after repeated crystallization in 10-fold excess (m/v) of 50% MeOH as white solid material (8.52 g, 6.6 mmol, 33%).

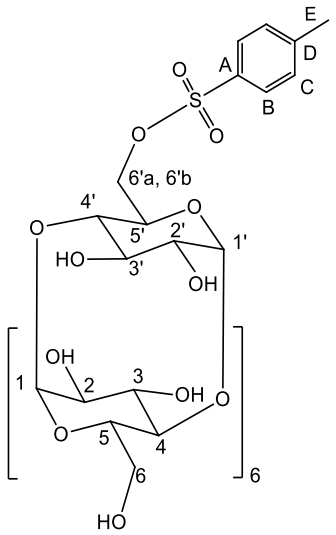

^{1}H NMR (DMSO-*d*$_6$ 600 MHz) δ (ppm): 7.75 (d, *J*=8.1 Hz, 2H, B), 7.43 (d, *J*=8.1 Hz, 2H, C), 5.81-5.63 (m, 14H, *OH*-2, *OH*-3), 4.84-4.76 (m, 7H, *H*-1, *H*-1'), 4.49-4.34 (m, 6H, *OH*-6), 4.43 (d, *J* = 10.3 Hz, 1H, *H*-6'a), 4.19 (dd, *J* =11.0 Hz, *J*=6.4 Hz, 1H, *H*-6'b), 3.71-3.20 (m, 40H, *H*-2, *H*-3, *H*-4, *H*-5, *H*-6, *H*-2', *H*-3', *H*-4', *H*-5'), 2.43 (s, 3H, E).

^{13}C NMR (DMSO-*d*$_6$ 150 MHz) δ (ppm): 144.78 (D), 132.65 (A), 129.86 (C), 127.56 (B), 102.21-101.26 (*C*-1, *C*-1'), 81.48-80.75 (*C*-4, *C*-4'), 73.03-71.85 (*C*-2, *C*-3, *C*-5, *C*-2', *C*-3'), 69.68 (*C*-6'), 68.88 (*C*-5'), 59.88-59.24 (*C*-6), 21.18 (E).

ESI-MS *m*/*z* found: 1311.4 $[M + Na]^+$, calculated $C_{45}H_{68}O_{30}Na$ $[M + Na]^+$: 1311.37.

Mono(6-deoxy-6-azido)-β-cyclodextrin (4) (N_3-β-CD)

Compound **4** was prepared according to the published procedure[35] whith slight modification concerning the work-up of the reaction. Compound **3** (50.0 g, 38 mmol) was dissolved in dry

DMF (300 mL), and sodium azide (3.0 g, 46 mmol) was added. The reaction mixture was heated to 105 °C, and stirred for 1 h at this temperature. The clear solution was concentrated to the half of its initial volume and poured to acetone (1 L) at room temperature. White crystalline precipitate was instantly formed. The crude product was recrystallized from H_2O/acetone 1/10 mixture, followed by intensive washing of the the precipitate with this solvent mixture (500 mL) in order to remove any residue of NaN_3. After this purification step compound **4** was recovered as white solid material (42.8 g, 36.9 mmol 97%) and was dried to constant weight under reduced pressure (10 mbar) overnight in the presence of P_2O_5 and KOH.

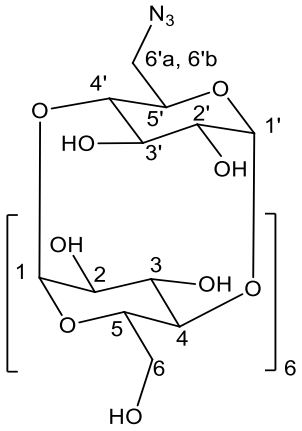

^{1}H NMR (D_2O, 500 MHz) δ(ppm): 5.035-4.987 (m, 7H, *H*-1, *H*-1'), 3.956 – 3.713 (m, 28 H, *H*-3, *H*-5, *H*-6, *H*-3', *H*-5',*H*-6'a, *H*- 6'b), 3.630-3.454 (m, 14H, *H*-2, *H*-4, *H*-2', *H*-4').

^{13}C NMR (D_2O, 125 MHz) δ(ppm): 101.839, 101.617 (*C*-1, *C*-1'), 82.030, 81.352, 81.257, 81.208, 81.128 (*C*-4, *C*-4'), 73.060, 73.029, 72.996, 72.969, 72.811, 72.788, 72.035, 71.937, 71.872, 71.794, 71.755, 70.521 (*C*-3, *C*-5, *C*-2, *C*-3', *C*-5', *C*-2'), 60.465, 60.350, 60.308, 60.280 (*C*-6), 51.050 (*C*-6').

ESI-MS *m/z* found: 1182.4 $[M + Na]^+$, calculated $C_{42}H_{69}O_{34}N_3Na$ $[M + Na]^+$: 1182.37.
NMR spectra are in agreement with literature[35].

Mono(6-deoxy-6-amino)-β-cyclodextrin hydrochloride (5) (NH_2-β-CD)

Compound **5** was prepared according to the procedure published in literature[35], directly from compound **4**.

NMR spectra are in agreement with literature[35] and ESI-MS is consistent with the structure.

6.3.3 Synthesis of xanthene-modified β-CDs

(6-Spirolactam rhodamine B-6-deoxy)-β-cyclodextrin (6) (Rho-β-CD): Rhodamine B (160 mg, 0.3 mmol) was dissolved in H2O (6 mL) and NMM (132 µL, 1.2 mmol), compound 5 (350 mg, 0.3 mmol), DMT-MM-Cl (83 mg, 0.3 mmol) were added in sequence to the pink solution. The mixture was stirred at r.t. for 3 h, concentrated under reduced pressure to half of the volume and precipitated with acetone (100 mL). The precipitate was filtered and washed with acetone (3 × 5 mL) in order to remove the unreacted dye. The crude (360 mg) was purified by chromatography (gradient elution from ACN/H2O 8/2 to ACN/H2O 7/3, 6 g of silica gel per 50 mg of crude), the fractions were concentrated under reduced pressure and addition of acetone (50 mL) yielded a pink precipitate. The solid was filtered, washed with acetone (3 × 2 mL) and drying at 60 °C under reduced pressure (10 mbar) overnight in the presence of P_2O_5 and KOH yielded compound **6** as a slight pink powder (350 mg, 72%).

^{1}H NMR (D_2O, 600 MHz) δ (ppm): δ 7.90-7.88 (d, 1H), 7.48-7.45 (t, 1H), 7.42-7.40 (t, 1H), 6.72-6.71 (d, 1H), 6.25-6.24 (d, 1H), 6.22 (s, 1H), 6.19-6.17 (d, 1H), 6.00 (s, 1H), 5.64-5.63 (d, 1H), 5.61-5.60 (d, 1H), 5.05-5.04 (d, 1H), 4.99 (d, 1H), 4.92 (d, 1H), 4.91-4.90 (d, 1H), 4.88-4.87 (d, 2H), 4.78-4.77 (d, 1H), 4.31-2.71 (m, 50H), 1.16-1.14 (t, 6H), 0.82-0.80 (t, 6H) (partial assignments as shown in Figures 19, 21).

^{13}C NMR (D_2O, 150 MHz) δ (ppm): 172.62, 156.22, 155.54, 154.97, 152.42, 151.11, 136.08, 132.80, 132.12, 131.80, 130.60, 125.69, 125.47, 112.60, 111.27, 107.21, 105.68, 105.29, 105.20, 104.88, 104.61, 104.46, 103.80, 101.56, 100.23, 85.94, 83.40, 83.07, 82.99, 82.29, 80.87, 76.40, 76.33, 75.96, 75.88, 75.71, 75.54, 75.06, 74.93, 74.70, 74.66, 74.60, 74.29, 74.15, 74.09, 74.05, 73.90, 73.79, 62.91, 62.78, 62.19, 61.91, 61.29, 61.09, 47.33, 46.87, 43.76, 15.02, 14.20.

ESI-MS *m*/*z* found 1559.3960 $[M+H]^+$, calculated $C_{70}H_{100}O_{36}N_3$ $[M+H]^+$: 1559.6154;
m/*z* found 1581.3973 $[M+Na]^+$ calculated $C_{70}H_{100}O_{36}N_3Na$ $[M+Na]^+$: 1582.5307.

IR (KBr) ν/cm^{-1}: 3398 (O-H), 2970 (C-H), 1755 (γ-lactam ring, C=O stretching), 1616, 1519, 1429, 1334, 1221, 1122, 1027, 760, 701.

Free rhodamine content based on TLC: <0.1% (w/v).

Free rhodamine content based on CE: <0.1% (w/v).

Mono(6-deoxy-6-fluoresceinyl-carboxamido)-β-cyclodextrin (7) (Flu-β-CD): Fluorescein disodium salt (110 mg, 0.3 mmol) was dissolved in H_2O (6 mL) and NMM (132 µL, 1.2 mmol), compound 5 (350 mg, 0.3 mmol), DMT-MM-Cl (83 mg, 0.3 mmol) were added in

sequence to the yellow solution. The mixture was stirred at room temperature for 3 h, concentrated under reduced pressure to half of the volume and precipitated with acetone (100 mL). The precipitate was filtered and washed with acetone (3 × 5 mL) in order to remove the dye-related by-products. The crude (390 mg) was purified by chromatography (eluent: ACN/H2O/(25%aq.NH_3) 10/5/1, 10 g of silica gel per 50 mg of crude), the fractions were concentrated under reduced pressure and addition of acetone (50 mL) yielded an orange precipitate. The solid was filtered, washed with acetone (3 × 2 mL) and drying at 60 °C under reduced pressure (10 mbar) overnight in the presence of P_2O_5 and KOH yielded compound **7** as a slight orange powder (154 mg, 35%).

^{1}H NMR (D_2O, 600 MHz) δ (ppm): 7.83-7.82 (d, 1H), 7.47-7.42 (dt, 2H), 6.63.-6.61 (d, 1H), 6.61-6.60 (d, 1H), 6.55-6,53 (dd, 1H), 6.48-6.46 (d, 1H), 6.43 (d, 1H), 6.39-6.37 (dd, 1H), 6.32-6.30 (d, 1H), (aromatic region, for partial assignment see Figure 23) 5.05-5.04 (d, 1H), 4.96 (d, 1H) 4.92-4.90 (m, 3H), 4.84-4.83 (d, 1H), 4.81-4.80 (d, 1H), 4.19-2.45 (m, 42H) (partial assignments as shown in Figure 22 - 24).
^{13}C NMR (D_2O, 150 MHz) δ (ppm): 174.07, 161.09, 160.01, 156.50, 155.05, 154.40, 136.56, 131.99, 131.92, 130.56, 130.36, 125.84, 125.24, 115.70, 114.19, 112.09, 111.49, 106.02, 105.06, 104.98, 104.81, 104.40, 104.30, 103.29, 101.14, 85.50, 83.69, 83.65, 83.52, 83.42, 83.26, 82.58, 81.77, 80.75, 76.37, 75.92, 75.81, 75.64, 75.40, 75.33, 75.24, 75.13, 74.91, 74.77, 74.64, 74.56, 74.37, 74.21, 74.09, 74.04, 73.65, 73.50, 62.93, 62.33, 62.08, 61.49, 61.46, 60.89, 44.16.
ESI-MS m/z found: 1449.1524 $[M+H]^+$, calculated $C_{62}H_{81}O_{38}N$ $[M+H]^+$:1448.2904.
Free fluorescein content based on TLC: <0.1% (w/v).
Free fluorescein content based on CE: <0.1% (w/v).

Eosin Y (8) (EoY)

Compound **8** was prepared according to the published procedure[154] whith modification concerning the type and the amount of the brominating agent. Fluorescein (Flu) (1.1 g, 3.3 mmol) was suspended in EtOH (50 mL) then *N*- bromosuccinimide (NBS) in solid form was added in two portions (2 × 1.2 g, 2 × 6.6 mmol). After the addition of the first portion, the precipitate of Flu disappeared as the formed dibromofluorescein was readily soluble in EtOH. During the addition of the second portion of NBS gradually crystals of EoY were formed. In order to complete the reaction, the mixture was stirred further at r.t. for 30 minutes and then allowed to crystallize for 24 h. The pure product of EoY was recovered by filtration on a glass filter and washing the crystals with EtOH (3 × 5 mL). Overnight drying of the crystals at 105

°C under reduced pressure (10 mbar) in the presence of P_2O_5 and KOH yielded compound **8** as a deep purple crystalline material (1.9 g, 89% yield).

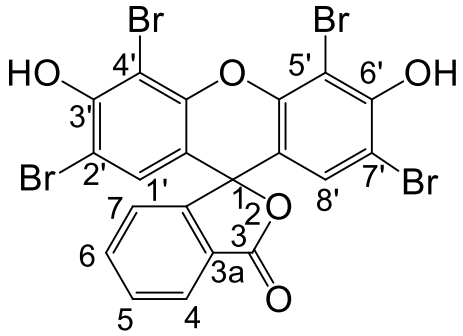

^{1}H NMR (DMSO-d$_6$ 600 MHz) δ (ppm): 8.076 (d, *J*=7.4 Hz, 1H, *H*-4), 7.555 (m, 1H, *H*-5), 7.517 (m, 1H, *H*-6), 7.158 (d, *J*=7.1 Hz, 1H, *H*-7). 6.978 (s, 2H, *H*-1'- *H*-8').

^{13}C NMR (DMSO-d$_6$ 151 MHz) *δ* (ppm): 171.20 (*C*-3), 156.06, 135.78, 133.43 (*C*-4), 133.17 (*C*-1'- *C*-8'), 131.83 (*C*-5 - *C*-6), 131.82 (*C*-7), 120.80, 112.79, 102.01.

ESI-MS *m/z* found: 669.7 $[M + Na]^+$, calculated $C_{20}H_7NaBr_2O_5$ $[M + Na]^+$: 669.87.

Dibromofluorescein (9)

Compound **9** was prepared according to the published procedure[155] whith modification concerning the type and the amount of the used brominating agent and the final chromatographic purification. Flu (1 g, 3 mmol) was suspended in acetic acid (400 mL), and the deep red suspension was heated to 60 °C. NBS (1.25 g, 7 mmol) was dissolved separately in 100 mL acetic acid at room temperature and added to the heated suspension of Flu. Addition of the NBS solution caused immediate dissolution of Flu. The obtained solution with an intensive red color was stirred at 80 °C under reflux for additional 2 hours, concentrated under reduced pressure and precipitated with H_2O. The orange precipitate was recovered by filtration on a glass filter and by washing the solid with H_2O (3 x 100 mL). The precipitate was dried overnight at 105 °C under reduced pressure (10 mbar) in the presence of P_2O_5 and KOH. The targeted compound **9** was obtained after column chromatographic purification on direct-phase silica gel using $CHCl_3$/acetone 1/1 isocratic elution in 1.02 g (70% yield).

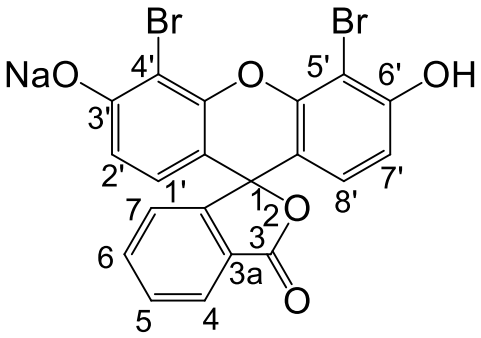

^{1}H NMR (DMSO-d$_6$ 600 MHz) δ (ppm): 8.164 (d, *J*=7.6 Hz, 1H, *H*-4), 7.906 (m, 1H, *H*-6), 7.835 (m, 1H, *H*-5), 7.373 (d, *J*=7.6 Hz, 1H, *H*-7), 6.836 (d, *J*=8.6 Hz, 2H, *H*-2'-*H*-7'), 6.733 (d, *J*=9.0 Hz, 2H, *H*-1'-*H*-8').

^{13}C NMR (DMSO-d$_6$ 150 MHz) δ (ppm): 172.55 (*C*-3), 152.25 (*C*-3'–*C*-6'), 137.96 (*C*-6), 132.67 (*C*-5), 129.66 (*C*-1'- *C*-8'), 127.71 (*C*-4), 126.94 (*C*-7), 115.24 (*C*-2'-*C*-7'), 113.93 (*C*-4'-*C*-5').

ESI-MS *m*/*z* found: 511.9 $[M + Na]^+$, calculated $C_{20}H_9NaBr_2O_5$ $[M + Na]^+$: 512.08.

Eosin B (10) (EoB)

Compound **10** was prepared according to the published procedure[155] which was modified.

Compound **9** (300 mg, 0.612 mmol) was dissolved in concentrated sulphuric acid (15 mL) and cooled down to 0 °C. A mixture of 0.210 mL of nitric acid and 0.600 mL of sulfuric acid was added dropwise under rigorous stirring and cooling of the reaction mixture. The proceeding of the reaction was monitored by direct-phase TLC using EtOAc/MeOH/(25%aq.NH_3) 8/2/1 elution mixture. After 12 hours of stirring at room temperature, when TLC monitoring showed complete conversion of starting material, reaction mixture was poured on to crushed ice, which resulted in a yellow precipitate formation. The precipitate was filtered, washed with H_2O (3 × 10 mL) and dried to constant weight at 105 °C under reduced pressure (10 mbar) in the presence of P_2O_5 and KOH. The final product – compound **10** - obtained after drying is a yellow solid material. Yield 345 mg (90%).

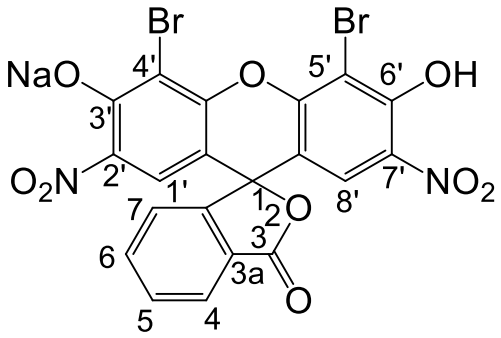

^{1}H NMR (DMSO-d$_6$ 600 MHz) δ (ppm): 7.977 (d, *J*=7.3 Hz, 1H, *H*-4), 7.865 (t, *J*=7.2 x (2) Hz, 1H, *H*-6), 7.756 (t, *J*=7.3 x (2) Hz, 1H, *H*-5), 7.492 (d, *J*=7.3 Hz, 1H, *H*-7), 7.041 (s, 2H, *H*-1'-*H*-8').

^{13}C NMR (DMSO-d$_6$ 150 MHz) δ (ppm): 171.49 (*C*-3), 168.42, 155.73, 152.54, 138.56 (*C*-6), 137.21, 133.59 (*C*-5), 130.79, 127.97 (*C*-4), 127.87 (*C*-1'-*C*-8'), 127.74 (*C*-7), 109.82, 104.95.

ESI-MS *m*/*z* found: 601.9 $[M + Na]^+$, calculated $C_{20}H_7N_2NaBr_2O_9$ $[M + Na]^+$: 601.84.

Mono(6-deoxy-6-eosinyl B-carboxamido)-β-cyclodextrin (11) (EoB-β-CD): Freshly prepared compound **10** (186 mg, 0.32 mmol) was dissolved in H_2O (20 mL) and NMM (105 µL, 97 mg, 0.96 mmol), NH_2-β-CD hydrochloride (374 mg, 0.32 mmol), DMT-MM-Cl (88 mg, 0.32 mmol) were added in sequence to the orange solution. The mixture was stirred at r.t. for 3 h, concentrated under reduced pressure to half of the volume and precipitated with acetone (100 mL). The precipitate was filtered and washed with acetone (3 × 5 mL) in order to remove the unreacted dye. The crude (350 mg) was dissolved in the minimum amount of H_2O and purified by column chromatography (ACN/(25%aq.NH_3)/H_2O 10/5/2, 10 g of silica gel per 50 mg of crude), the fractions were concentrated under reduced pressure and addition of acetone (50 mL) yielded an orange precipitate. The solid was filtered, washed with acetone (3 × 2 mL) and drying at 60 °C under reduced pressure (10 mbar) overnight in the presence of P_2O_5 and KOH yielded compound **11** as a dark orange powder (357 mg, 65%).

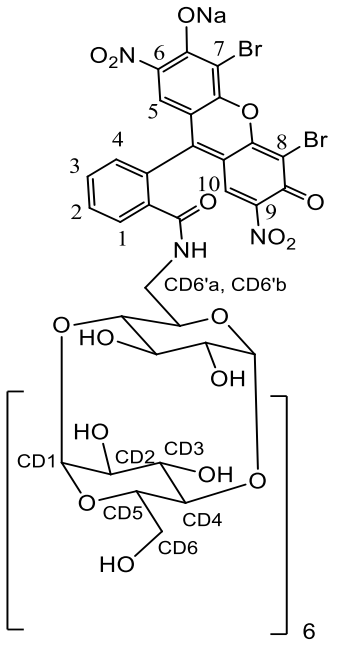

^{1}H NMR (DMSO-d$_6$, 600 MHz) δ (ppm): 7.771 (d, *J*=6.9 Hz, 1H, *H*-1), 7.531 -7.450 (m, 2H, *H*-2 – *H*-3), 7.443 (s, 1H, *H*-5), 7.068 (d, *J*=6.9 Hz, 1H, *H*-4), 7.030 (s, 1H, *H*-10), 5.920 – 5.520 (m, 14H, CD-*OH*-2/CD-*OH*-3), 4.855-4785 (m, 7H, CD-*H*-1), 4.470 – 4.330 (m, 6H, CD-*OH*-6), 3.855 – 2.970 (m, 42H, CD-*H*-2, CD-*H*-3, CD-*H*-4, CD-*H*-5, CD-*H*-6, 42H).

^{13}C NMR (DMSO-d$_6$, 150 MHz) δ (ppm): 168.28, 153.44, 152.57, 152.20, 134.50, 134.21, 132.92 (*C*-3), 129.34, 128.36 (*C*-2), 126.34 (*C*-5), 123.67 (*C*-10), 122.97 (*C*-1), 122.90 (*C*-4), 102.00 - 101.50 (CD-*C*-1), 84.98, 82.25, 81.82, 81.63, 81.48, 81.07, 80.01, 73.36, 72.94, 72.56, 72.17, 71.92, 66.69, 65.47, 60.42 - 59.31 (CD-*C*-6), 42.68 (CD-*C*-6'a, CD-*C*-6'b).

ESI-MS *m*/*z* found 1695.19 $[M-H]^-$, calculated $C_{62}H_{78}Br_2N_3O_{42}$ $[M-H]^-$:1696.08; *m*/*z* found 1730.10 $[M+Cl]^-$ calculated $C_{62}H_{77}Br_2ClN_3O_{42}$ $[M+Cl]^-$: 1731.53; *m*/*z* found 847.70 $[M-2H]^{2-}$, calculated $C_{62}H_{77}Br_2N_3O_{42}$ $[M-2H]^{2-}$: 848.04.

Mono(6-deoxy-6-eosinyl Y-carboxamido)-β-cyclodextrin (12) (EoY-β-CD):

Freshly prepared compound **8** (600 mg, 0.93 mmol) was dissolved in H_2O (30 mL) and NMM (135 µL, 124 mg, 1.22 mmol), NH_2-β-CD free base (1 g, 0.88 mmol), DMT-MM-Cl (250 mg, 0.9 mmol) were added in sequence to the yellow solution. The mixture was stirred at r.t. for 1 day, concentrated under reduced pressure to half of the volume and precipitated with acetone (200 mL). The precipitate was filtered and washed with acetone (3 × 5 mL) in order to remove the unreacted dye. The crude (1.3 g) was dissolved in the minimum amount of H_2O and purified by chromatography (eluent: ACN/(25%aq.NH_3)/H_2O 10/3/1, 10 g of silica gel per 50 mg of crude), the fractions were concentrated under reduced pressure and addition of acetone (50 mL) yielded a yellow precipitate. The solid was filtered, washed with acetone

(3 × 10 mL) and drying at 60 °C under reduced pressure (10 mbar) overnight in the presence of P_2O_5 and KOH yielded compound **12** as a yellow powder (1.05 g, 67%).

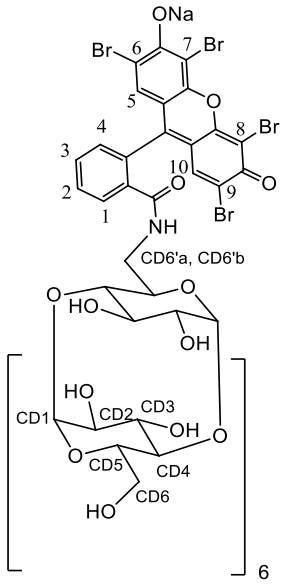

^{1}H NMR (DMSO-d$_6$, 600 MHz) δ (ppm): 7.751 (d, *J*=6.2 Hz, 1H, *H*-1), 7.468 (m, 2H, *H*-2 - *H*-3), 6.963 (d, *J*=6.5 Hz, 1H, *H*-4), 6.351 (s, 2H, *H*-5 - *H*-10), 5.950 – 5.505 (m, 14H, CD-*OH*-2/CD-*OH*-3), 4.870 – 4.551 (m, 7H, CD-*H*-1), 4.510 – 4.370 (m, 6H, CD-*OH*-6), 3.840 – 2.740 (m, 42H, CD-*H*-2, CD-*H*-3, CD-*H*-4, CD-*H*-5, CD-*H*-6).

^{13}C NMR (DMSO-d$_6$, 150 MHz) δ (ppm): 168.12, 153.64, 148.78, 148.44, 132.69 (*C*-3), 129.50, 128.22 (*C*-2), 126.86 (*C*-5 - *C*-10), 123.14 (*C*-4), 122.59 (*C*-1), 102.02 - 99.61 (CD-*C*-1), 85.19, 81.82, 81.50, 81.09, 79.86, 73.35, 72.96, 72.58, 72.20, 71.94, 66.50, 65.92, 60.28 - 59.40 (CD-*C*-6), 42.56 (CD-*C*-6'a, CD-*C*-6'b).

ESI-MS *m*/*z* found 1763.09 $[M-H]^-$, calculated for $C_{62}H_{78}Br_4NO_{38}$ 1763.87; *m*/*z* found: 881.30 $[M-2H]^{2-}$, calculated $C_{62}H_{77}Br_4NO_{38}$ $[M-2H]^{2-}$: 881.935.

6.3.4 Synthesis of persubstituted CDs

Heptakis(6-*O*-*tert*-butyldimethylsilyl)-β-cyclodextrin (13) (TBDMSi-β-CD)

Compound **13** was prepared according to the published procedure[52] whith modification concerning the purification of the final product. β-Cyclodextrin (5 g, 4.405 mmol) was suspended in dry pyridine (80 mL) under nitrogen atmosphere and stirred for 30 minutes until a clear solution formed. *tert*-Butyldimethylsilyl chloride (TBDMSiCl) (5.57 g, 37.0 mmol) was added in one portion, and the resulting suspension was stirred at room temperature for 12 h. The reaction was followed by TLC (EtOAc/96%-EtOH/H_2O 30/5/4) which showed three spots at R_F = 0.7, 0.6 and 0.3. Portions of TBDMSiCl (0.66 g, 4.40 mmol) were added each 12

h until the most polar product was consumed. The mixture was poured into H_2O (500 mL) and filtered. The solid was washed with H_2O (250 mL) and dried by co-evaporation with toluene (3 × 50 mL). The crude product was solved in DCM (50 mL), mixed with silica gel (20 g), concentrated until a homogeneous powder was obtained and loaded onto a short (5 × 6 cm) pad of silica gel which was first eluted with DCM/ACN/96%-EtOH/(30%aq.NH_3) 40/40/20/4, until the TLC spot at R_F = 0.7 (R_t (retention time) = 18 min, see Figure 38.) completely eluted (1.5 L). The eluent was changed to DCM/ACN/96%-EtOH/H_2O 40/40/20/4 (2.5 L) to yield pure compound **13** as a white powder which was dried at 50 ºC under reduced pressure (10 mbar) in the presence of P_2O_5 and KOH until constant weight (7.3 g, 3.78 mmol, 86%), R_F = 0.6 (EtOAc/96%-EtOH/H_2O 30/5/4), R_t = 11.5 min (78/22 MeOH/EtOAc mobile phase, isocratic, flow rate 1.8 mL/min, C18 stationary phase), m.p. 299-302 ºC (dec.).

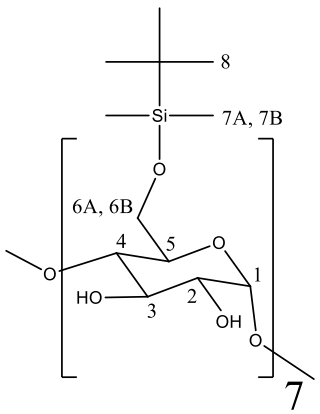

^{1}H NMR (CDCl$_3$, 600 MHz) δ (ppm): 6.74 (bs, OH, *C*-2/*C*-3-OH), 5.27 (bs, OH, *C*-2/*C*-3-OH), 4.89 (d, *J*=3.5 Hz, 7H, *H*-1), 4.04 (t, *J*=9.2 Hz, 7H, *H*-3), 3.90 (dd, *J*=11.3 Hz, *J*=2.9 Hz, *H*-6A), 3.71 (bd, *J*=10.5 Hz, 7H, *H*-6B), 3.64 (dd, *J*=9.6 Hz, *J*=3.5 Hz, 7H, *H*-2), 3.62 (bs, 7H, *H*-5), 3.56 (t, *J*=9.2 Hz, 7H, *H*-4,), 0.87 (s, 63H, *H*-8), 0.04 (s, 21H, *H*-7A), 0.03 (s, 21H, *H*-7B)

^{13}C NMR (CDCl$_3$, 150 MHz) δ (ppm): 102.1 (*C*-1), 81.9 (*C*-4), 73.7 (*C*-2), 73.5 (*C*-3), 72.7 (*C*-5), 61.8 (*C*-6), 26.0 (*C*-8), 18.4 ($SiC(CH_3)_3$), -4.9 (*C*-7A), -5.0 (*C*-7B).

NMR spectra are in agreement with literature[52].

MALDI-TOF *m/z* found: 1956.9 $[M + Na]^+$, calculated $C_{84}H_{168}O_{35}Si_7Na$ $[M + Na]^+$: 1956.9;

Heptakis(2,3-di-*O*-methyl-6-*O*-*tert*-butyldimethylsilyl)-β-cyclodextrin (14) (HDMTBDMSi-β-CD)

Freshly dried compound **13** (40 g, 0.020 mol) was dissolved in THF (400 mL) at room temperature. KOH (109 g 1.94 mol) was added followed by the addition of the phase transfer catalyst - Ph_3MePBr (2.43 g, 0.0068 mol). MeI (23.34 mL, 53.2 g, 0.3749 mol) was added as last, and the heterogeneous reaction mixture was stirred at room temperature for 12 h. When the TLC and HPLC reaction monitoring showed complete substitution and no more partially methylated components (R_F<0.5 (DCM/MeOH 96/4) were present in the reaction mixture, the reaction was quenched by filtration on a glass filter. Filtration resulted in a white solid material and a pale yellow mother liquor. The filtrate was concentrated *in vacuo*, the complete removal of THF was achieved by azeotropic distillation/co-evaporation with H_2O. White residue was obtained after complete solvent evaporation (45 g) which was re-suspended in H_2O (100 mL), filtered on a glass filter and repeatedly washed with H_2O (500 mL) and with MeOH (100 mL) in order to remove the catalyst. Upon catalyst removal, the pure compound **14** was dried at 80 ºC under reduced pressure (10 mbar) in the presence of P_2O_5 and KOH until constant weight (41.7 g, 19.57 mmol, 95%), R_F = 0.5 (DCM/MeOH 96/4).

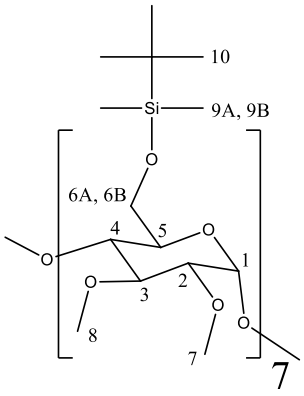

^{1}H NMR ($CDCl_3$, 600 MHz) δ (ppm): 5.21 (d, *J*= 3.4 Hz, 7H, *H*-1), 4.13 (d, *J*=9.2 Hz, 7H, *H*-6A), 3.79 (7H, *H*-4), 3.66 (d, *J*=9.2 Hz, 7H, *H*-6B), 3.63 (14H, *H*-5/*H*-3), 3.59 (s, 21H, *H*-8 (*C*-3-*O*-Me)), 3.52 (s, 21H, *H*-7 (*C*-2-*O*-Me)), 3.38-3.36 (dd, *J*=9.5 Hz, *J*=3.4 Hz, 7H, *H*-2), 0.87 (s, 63H, *H*-10) 0.07 (s, 21H, *H*-9A), 0.06 (s, 21H, *H*-9B)

^{13}C NMR ($CDCl_3$, 150 MHz) δ (ppm): 102.1 (*C*-1), 81.9 (*C*-4), 73.7 (*C*-2), 73.5 (*C*-3), 72.7 (*C*-5), 61.8 (*C*-6), 26.0 (*C*-10), 18.4 ($SiC(CH_3)_3$), -4.9 (*C*-9A), -5.0 (*C*-9B)

MALDI-TOF *m/z* found: 2130.2 $[M + H]^+$, calculated $C_{98}H_{197}O_{35}Si_7$ $[M + H]^+$: 2130.2

Heptakis(2,3-di-*O*-methyl)-β-cyclodextrin (15) (HDM-β-CD)

Compound **15** was prepared by applying the published desilylation procedure[164] on compound **14.** Compound **14** (40 g, 0.01876 mol) was suspended in MeOH (200 mL) resulting in a stirrable white suspension. Ammonium hydrogen difluoride $(NH_4)HF_2$ (7.49 g, 0.1314 mol) was added to the suspension and temperature was elevated to 60 °C (reflux). The reaction mixture was stirred under methanol reflux for 2 hours and at 25 °C for 12 hours. The proceeding of the reaction was monitored by direct-phase TLC ($CHCl_3$/MeOH/H_2O 50/10/1) and by reversed-phase HPLC (Kinetex C-18 (Phenomenex), isopropanol(IPA)/MeOH/H_2O 7/41/52 isocratic elution, 0.5 mL/min flow rate, RI detection). After 6 hours of vigorous stirring, HPLC and TLC analysis showed complete consumption of silylated species. The reaction mixture was concentrated on a rotary evaporator at 40 °C. White residue, obtained after evaporation (44 g) was taken up in DCM (100 mL) and extracted with H_2O (3 × 100 mL) in order to extract the product into the aqueous phase and hence to purify the crude from water-insoluble organic impurities. Aqueous layers after extraction were combined and concentrated on a rotary evaporator at 40 °C to one-third of their initial volume (100 mL). NaCl (25 g) was added, and the salinated aqueous solution was extracted with $CHCl_3$ (2 × 400 mL) in order to purify the target compound from inorganic impurities, insoluble in $CHCl_3$. Organic fractions after the last extraction were combined, dried over anhydrous Na_2SO_4 and evaporated to dryness resulting in pure compound **15** (17.3 mmol, 22.98 g, 92%).

R_F = 0.5 ($CHCl_3$/MeOH/H_2O 50/10/1), R_t = 37 min (IPA/MeOH/H_2O 7/41/52 mobile phase, isocratic, flow rate 1.8 mL/min, C18 stationary phase).

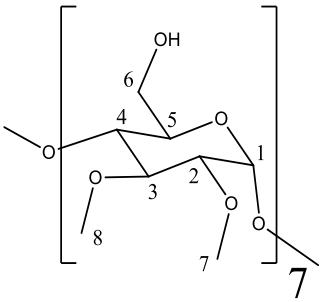

^{1}H NMR (D_2O, 600 MHz) δ (ppm): 5.30 (d, *J*=3.7 Hz, 7H, *H*-1), 3.90 (7H, *H*-4), 3.86 (14H, *H*-6), 3.77-3.69 (14H, *H*-3, *H*-5), 3.67 (s, 21H, *H*-7 (*C*-3-*O*-Me)), 3.52 (s, 21H, *H*-8 (*C*-2-*O*-Me)) 3.37 (dd, 7H, *J*=9.1 Hz, *J*=3.6 Hz, *H*-2)

^{13}C NMR (D_2O, 150 MHz) δ (ppm): 97.18 (*C*-1), 80.98 (*C*-3), 80.06 (*C*-2), 77.13 (*C*-5), 71.65 (*C*-4), 60.53 (*C*-6), 59.81 (*C*-7(*C*-3-*O*-Me)), 58.09 (*C*-8(*C*-2-*O*-Me)).

ESI-MS *m/z* found: 1354.0 $[M + Na]^+$, calculated $C_{56}H_{98}O_{35}Na$ $[M + Na]^+$: 1353.58

Heptakis(2,3-di-*O*-methyl-6-*O*-carboxymethyl)-β-cyclodextrin sodium salt (16) (HDMCM-β-CD)

Freshly dried compound **15** (3 g, 2.25 mmol) was dissolved in dry DMSO (500 mL), and sodium chloroacetate (7.35 g, 18 mmol) was suspended in this solution. NaI (9.45 g, 63.1 mmol) and 60% mineral oil dispersion of NaH (0.756 g, 31.5 mmol) was added as next, resulting in an intensive gas evolution from the reaction mixture. After the foaming was stopped, the formed gray suspension was heated to 60 °C and stirred at this temperature for additional 12 h. The proceeding of the reaction was followed by direct-phase TLC (1,4-dioxane/(25%aq.NH_3) 1/1.2) and by HPLC (CD-Screen-IEC stationary phase and ELS detector). As the conversion completed and no more partially carboxymethylated derivatives (R_F > 0.4, (1,4-dioxane/(25%aq.NH_3) 1/1.2), R_t < 11.0 min (CD-Screen-IEC stationary phase, solvent gradient of 1.5% triethylamine formate buffer (pH 4.0) with ACN (0 min 15%, 15 min 40%) were present, the reaction was quenched with MeOH (50 mL), neutralized with 1M HCl and then concentrated under reduced pressure at 70 °C. Addition of acetone (500 mL) to the concentrated DMSO solution (50 ml) yielded a white precipitate that was filtered out and washed with acetone (3 × 50 mL). Precipitated crude product (5 g) was dissolved in H_2O (100 mL) and further purified by repeated extraction with $CHCl_3$ (3 × 100 mL) to remove water-insoluble organic impurities. Aqueous phase after extraction was titrated to pH 2 with 1 M HCl and extracted again with $CHCl_3$ (3 × 100 mL) to remove water-soluble impurities. HDMCM-β-CD in acidic form was obtained after the evaporation of the combined organic layers of the second extraction as white solid material. The material was redissolved in H_2O and titrated to pH 9 with 1 M NaOH to obtain the sodium salt of HDMCM-β-CD (compound **16**). In order to remove any solvent residues the final compound was dialyzed against doubly distilled water for 3 days followed by freeze-drying to obtain the final sodium salt of compound **16** as a white powder (3.15 g, 1.67 mmol, 74%), R_F = 0.4 (1,4-dioxane/(25%aq.NH_3) 1/1.2), R_t < 11.0 min (CD-Screen-IEC stationary phase, solvent gradient of 1.5% triethylamine formate buffer (pH 4.0) with ACN (0 min 15%, 15 min 40%).

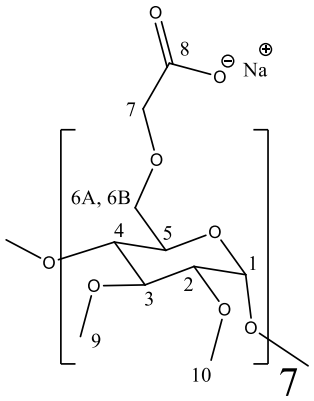

7

^{1}H NMR ($CDCl_3$, 600 MHz) δ (ppm): 5.26 (d, *J*=3.4 Hz, 7H, *H*-1), 3.86-3.77 (m, 14H, *H*-7), 3.74 (m, 7H, *H*-5), 3.86 (m, 7H, *H*-4), 3.83 (d, *J*=9.8 Hz, 7H, *H*-6A), 3.58 (t, *J*=10.1 Hz, 7H, *H*-3), 3.58 (d, *J*=10.2 Hz, 7H, *H*-6B), 3.38 (s, 21H, *H*-10 (*C*-2-*O*-Me)), 3.48 (s, 21 H, *H*-9 (*C*-3-*O*-Me)), 3.22 (7H, dd, *J*=10.1, *J*=3.4 Hz, *H*-2)

^{13}C NMR ($CDCl_3$, 150 MHz) δ (ppm): 180.1 (*C*-8), 99.9 (*C*-1), 83.4 (*C*-3), 82.60 (*C*-2), 79.8 (*C*-4), 73.6 (*C*-5), 73.0 (*C*-7), 71.4 (*C*-6), 62.2 (*C*-9), 60.6 (*C*-10).

ESI-MS negative mode *m/z* found: 1735.6 $[M]^-$ and 867.00 $[M]^{2-}$, calculated $C_{70}H_{111}O_{49}$ $[M]^-$ 1735,62 and $C_{70}H_{110}O_{49}$ $[M]^{2-}$ 867.31.

Octakis(6-*O*-*tert*-butyldimethylsilyl)-γ-cyclodextrin (17) (TBDMSi-γ-CD)

Compound **17** was prepared according to the published procedure[52] whith modification concerning the purification of the final product. γ-cyclodextrin (5 g, 3.86 mmol) was suspended in dry pyridine (100 mL) under nitrogen atmosphere and stirred for 30 minutes until a clear solution formed. *tert*-Butyldimethylsilyl chloride (TBDMSiCl) (5.5 g, 36.284 mmol) was added in one portion, and the resulting suspension was stirred at room temperature for 12 h. The reaction was followed by TLC (DCM/MeOH/H_2O 10/5/1) which showed three spots at R_F = 0.9, 0.6 and 0.5. Portions of TBDMSiCl (3 × 970 mg, 3 × 6.43 mmol) were added each 12 h until the most polar product was consumed. The mixture was poured into H_2O (600 mL) and filtered. The solid was washed with H_2O (250 mL) and dried by co-evaporation with toluene (3 × 75 mL). The crude product was solved in DCM (50 mL), mixed with silica gel (20 g), concentrated until a homogeneous powder was obtained and loaded onto a short (5 × 6 cm) pad of silica gel which was first eluted with DCM/MeOH/96%-EtOH/(30%aq.NH_3) 10/10/10/1, until the TLC spot at R_F = 0.9 (DCM/MeOH/H_2O 10/5/1) completely eluted (2.25 L). The eluent was changed to DCM/ACN/96%-EtOH/H_2O 40/40/20/4 (2.5 L) to yield pure compound **17** as a white solid material which was dried at 50 ºC under reduced pressure (10 mbar) in the presence of P_2O_5 and KOH until constant weight

(6.49 g, 2.934 mmol, 76%), R_F = 0.6 (DCM/MeOH/H_2O 10/5/1), R_t = 11.0 min (78/22 MeOH/EtOAc mobile phase, isocratic, flow rate 1.8 mL/min, C18 stationary phase), m.p. 264.5-267 ºC.

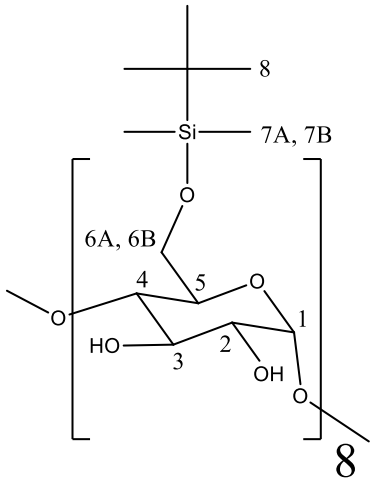

^{1}H NMR ($CDCl_3$, 600 MHz) δ (ppm): 6.74 (bs, OH, *C*-2/*C*-3-OH), 5.32 (d, *J*=3.2 Hz, 8H, *H*-1), 5.27 (bs, OH, *C*-2/*C*-3-OH), 4.04 (t, *J*=9.2 Hz, 8H, *H*-3), 3.90 (dd, *J*=11.3 Hz, *J*=2.9 Hz, *H*-6A) 3.71 (bd, *J* =10.5 Hz, 8H, *H*-6B), 3.64 (dd, *J*=9.2 Hz, *J*=3.2 Hz, 8H, *H*-2), 3.62 (8H, *H*-5), 3.56 (t, *J*=9.2 Hz, 8H, *H*-4), 0.87 (s, 72H, *H*-8), 0.04 (s, 24H, *H*-7A), 0.03 (s, 24H, *H*-7B)

^{13}C NMR ($CDCl_3$, 150 MHz) δ (ppm): 95.5 (*C*-1), 73.9 (*C*-4), 71.6 (*C*-2), 71.5(*C*-3), 70.9 (*C*-5), 61.8 (*C*-6), 25.9 (SiC(CH_3)$_3$), 18.35 (*C*-8), -4.9 (*C*-7A), -5.2 (*C*-7B)

NMR spectra are in agreement with literature[52].

MALDI-TOF *m/z* found: 2234.7 $[M + Na]^+$, calculated $C_{96}H_{192}O_{40}Si_8Na$ $[M + Na]^+$ 2234.11

Octakis(2,3-di-*O*-methyl-6-*O*-*tert*-butyldimethylsilyl)-γ-cyclodextrin (18) (ODMTBDMSi-γ-CD)

Compound **17** (13.5 g, 6.1 mmol) was dissolved in THF (50 mL) resulting in a transparent colorless solution. KOH (36.769 g, 0.6553 mol) was added, followed by the addition of the phase transfer catalyst - Ph_3MePBr (0.8218 g, 2.3 mmol). MeI (7.899 mL, 18.01 g, 0.12688 mol) was added as last, and the heterogeneous reaction mixture was stirred at room temperature overnight. When the TLC and HPLC reaction monitoring showed complete substitution and no more partially methylated components (R_F <0.6 (DCM/MeOH 96/4) were present in the reaction mixture, the reaction was quenched by filtration on a glass filter Filtration resulted in a white solid material and a pale yellow mother liquor. The filtrate was concentrated *in vacuo*, the complete removal of THF was aided by azeotropic distillation/co-

evaporation with H_2O. White residue was obtained after complete solvent evaporation (17 g) which was re-suspended in H_2O (50 mL), filtered on a glass filter and repeatedly washed with H_2O (250 mL) and with MeOH (50 mL) in order to remove the catalyst. Upon catalyst removal, the pure compound **18** was dried at 80 ºC under reduced pressure (10 mbar) in the presence of P_2O_5 and KOH until constant weight (13.5 g, 19.57 mmol, 90.8%), R_F = 0.6 (DCM/MeOH 96/4).

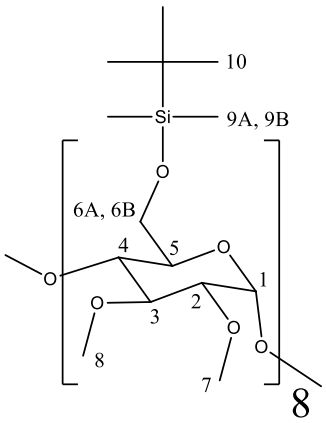

^{1}H NMR ($CDCl_3$, 600 MHz) δ (ppm): 5.32 (d, *J*=3.3 Hz, 8H, *H*-1), 4.04 (t, *J* =9.2 Hz, 8H, *H*-3), 3.90 (dd, *J*=11.3 Hz, *J*=2.9 Hz, 8H, *H*-6A), 3.71 (bd, *J*=10.5 Hz, 8H, *H*-6B), 3.64 (dd, 8H, *J*=9.6 Hz, *J*=3.5 Hz, *H*-2), 3.62 (8H, *H*-5), 3.71 (s, 24H, *H*-8), 3.66 (t, *J* =9.2 Hz, 8H, *H*-4), 3.55 (s, 24H, *H*-7), 0.88 (s, 72 H, *H*-10), 0.04 (s, 24H, *H*-7A), 0.03 (s, 24H, *H*-7B)

^{13}C NMR ($CDCl_3$, 150 MHz) δ (ppm): 97.7 (*C*-1), 82.2, 82.0, 77.9 (*C*-2, *C*-3, *C*-4) 72.35 (*C*-5), 62.35 (*C*-6), 61.5 (*C*-8) 58.07 (*C*-9) 25.95 ($SiC(CH_3)_3$), 18.75 (*C*-8), -4.8 (*C*-7A), -5.1 (*C*-7B)

MALDI-TOF *m/z* found: 2435.7 $[M + H]^+$, calculated $C_{112}H_{224}O_{40}Si_8Na$ $[M + H]^+$ 2435.64

Octakis(2,3-di-*O*-methyl)-γ-cyclodextrin (19) (ODM-γ-CD)

Compound **19** was prepared by applying the published desilylation procedure[164] on compound **18.** Freshly dried compound 18 (13 g, 5.34 mmol) was suspended in MeOH (65 mL) at room temperature resulting in a stirrable white suspension. $(NH_4)HF_2$ (7.49 g, 0.1314 mol) was added, and the reaction mixture was heated up to reflux (60 °C). The reaction mixture was stirred under reflux for 2 hours and at room temperature for 12 hours. The proceeding of the reaction was monitored by direct-phase TLC ($CHCl_3$/MeOH/H_2O 50/10/1) and by reversed-phase HPLC (Kinetex C-18 (Phenomenex), isopropanol(IPA)/MeOH/H_2O 7/41/52 isocratic elution, 0.5 mL/min flow rate, RI detection). After 6 hours of vigorous stirring HPLC and TLC analysis showed complete consumption of silylated species (R_F>0.4 ($CHCl_3$/MeOH/H_2O

50/25/1). The reaction mixture was concentrated on a rotary evaporator at 40 °C. White residue obtained after evaporation (15 g) was taken up in DCM (100 mL) and extracted with H_2O (3 × 100 mL) in order to extract the product into the aqueous phase and hence to purify the crude from water-insoluble organic impurities. Aqueous layers after extraction were combined and concentrated on a rotary evaporator at 40 °C to one third of their initial volume (100 mL). NaCl (30 g) was added and the salinated aqueous solution was extracted with $CHCl_3$ (2 × 100 mL) in order to purify the target compound from inorganic impurities, insoluble in $CHCl_3$. Organic fractions of the last extraction were combined, dried over anhydrous Na_2SO_4 (10 g) and evaporated to dryness resulting in pure compound **19** (7.31 g, 4.8 mmol, 90%). R_F = 0.4 ($CHCl_3$/MeOH/H_2O 50/25/1) R_t = 39 min (IPA/MeOH/H_2O 7/41/52 mobile phase, isocratic, flow rate 1.8 mL/min, C18 stationary phase).

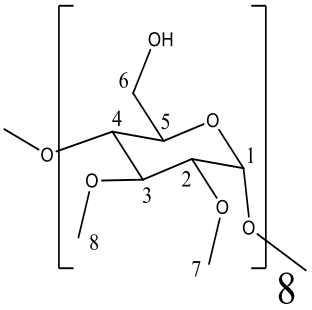

^{1}H NMR (D_2O, 600 MHz) δ (ppm): 5.47 (d, *J*=3.7 Hz, 8H, *H*-1), 3.99 (8H, *H*-4), 3.92 (16H, *H*-6), 3.89–3.80 (16H, *H*-3, *H*-5), 3.67 (s, 24H, *H*-8), 3.62 (s, 24H, *H*-7), 3.48 (dd, *J*=9.2 Hz, *J*=3.3 Hz, 8H, *H*-2).

^{13}C NMR (D_2O, 150 MHz) δ (ppm): 98.62 (*C*-1), 83.44 (*C*-3), 82.77 (*C*-2), 77.07 (*C*-5), 73.36 (*C*-4), 62.84 (*C*-6), 61.40 (*C*-8), 60.90 (*C*-7).

ESI-MS positive mode *m/z* found: 1543.1 $[M+Na]^+$, calculated $C_{64}H_{112}O_{40}Na$ $[M+Na]^+$ 1542.65

Octakis(2,3-di-*O*-methyl-6-*O*-carboxymethyl)-γ-cyclodextrin sodium salt (20) (ODMCM-γ-CD)

Freshly dried compound 19 (5 g, 3.3 mmol) was dissolved in dry DMSO (1000 mL) under Ar atmosphere and sodium chloroacetate (123 g, 1.056 mol), NaI (39.5 g, 0.264 mol) and NaH was added in sequence at room temperature upon which the reaction mixture foamed and a grey suspension was formed. Temperature was increased to 60 ºC upon which homogeneous brown solution was obtained. Reaction mixture was stirred at 60 ºC and monitored by TLC and by HPLC until complete substitution was achieved. As the conversion completed and no

more partially carboxymethylated derivatives (R_F > 0.4, (1,4-dioxane/(25%aq.NH_3) 1/1.2), R_t < 12.0 min (CD-Screen-IEC stationary phase, solvent gradient of 36 mM ammonium acetate buffer (pH 4.0) with ACN (0 min 20%, 20 min 40%) were present, the reaction was quenched with the addition of MeOH (100 mL). The reaction mixture was neutralized with 1M HCl and then concentrated under reduced pressure at 70 °C. Addition of acetone (1000 mL) to the concentrated DMSO solution (50 mL) yielded a white precipitate that was filtered out and washed with acetone (3 × 100 mL). Precipitated crude product (10 g) was dissolved in H_2O (100 mL) and purified by repeated extraction with $CHCl_3$ (3 × 200 mL) to remove water-insoluble organic impurities. Aqueous phase after extraction was titrated to pH 2 with 1 M HCl and extracted again with $CHCl_3$ (3 × 200 mL) to remove water-soluble impurities. ODMCM-γ-CD in acidic form was obtained after the evaporation of the combined organic layers of the second extraction as white solid material. The material was redissolved in H_2O (50 mL) and titrated to pH 9 with 1 M NaOH to obtain the sodium salt of ODMCM-γ-CD (compound **20**). In order to remove any solvent residues the final compound was dialyzed against doubly distilled water for 3 days followed by freeze-drying to obtain the final sodium salt of compound **20** as a white powder (5.68 g, 2.63 mmol, 80%), R_F = 0.4 (1,4-dioxane/(25%aq.NH_3)) 1/1.2), R_t = 12.0 min (CD-Screen-IEC stationary phase, solvent gradient of 36 mM ammonium acetate formate buffer (pH 4.0) with ACN (0 min 20%, 20 min 40%).

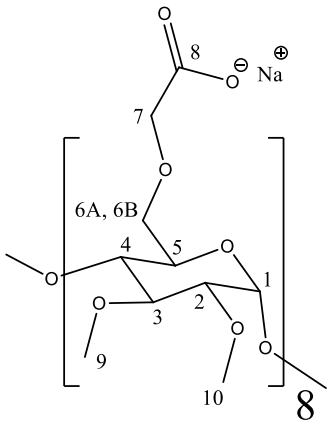

8

^{1}H NMR (D_2O, 600 MHz) δ (ppm): 5.46 (d, *J*=2.8 Hz, 8H, *H*-1), 4.02 (s, 16H, *H*-7), 3.94 (8H, *H*-4 - *H*-5), 3.83 (d, *J*=9.8 Hz, 8H, *H*-6A), 3.78 (8H, *H*-3), 3.73 (d, *J*=10.7 Hz, 8H, *H*-6B), 3.59 (s, 24H, *H*-9), 3.56 (s, 24H, *H*-10), 3.42 (dd, *J*=9.9 Hz, *J*=3.3 Hz, 8H, *H*-2).

^{13}C NMR (D_2O, 150 MHz) δ (ppm):179.13 (*C*-8), 98.62 (*C*-1), 83.31 (*C*-3), 82.70 (*C*-2), 77.12 (*C*-5), 72.61 (*C*-4), 72.34 (*C*-7), 71.71 (*C*-6), 60.98 (*C*-9, *C*-10).

ESI-MS *m/z* found: 2008.5 $[M+Na]^+$ and 1016.1 $[M+2Na]^{2+}$, calculated $C_{80}H_{128}NaO_{56}$ $[M]^+$ 2007.71 and $C_{80}H_{128}Na_2O_{56}$ $[M]^{2-}$ 1015.35.

Experiments performed by external researchers or as collaboration

^1H NMR titration experiment of ODMCM described in section 4.6 was carried by Assoc. Prof. Szabolcs Beni and Andras Darcsi Ph.D. (Department of Pharmacognosy, Semmelweis University, H-1085 Ulloi ut 26)

Fluorescence lifetimes and $^1O_2$ emission discussed in section 4.4.4. were registered in a collaboration with University of Catania. The measurements were carried out by Damien Afonso Ph.D. under the supervison of Prof. Salvatore Sortino (Laboratory of Photochemistry, Department of Drug Sciences, University of Catania, I-95125 Viale A. Doria 6, Italy).

Purity assessment of the four newly prepared xanthene-dye-CD conjugates and the two percarboxymethylated CD derivatives (ODMCM, HDMCM) by capillary electrophoresis and by HPLC were carrid by Erzsebet Varga, Tamas Sohajda Ph.D. and Julianna Szeman Ph.D. (Analytical laboratories of CycloLab, Cyclodextrin R&D Ltd, Budapest, H-1097 Illatos ut 7, Hungary)

7. Acknowledgements

My first acknowledgement goes to my mentor and colleague Milo Malanga Ph.D. for sharing his infinite knowledge about cyclodextrin derivatization and also for being a good boss inside and a good friend outside the laboratory. I am also very thankfull to my supervisors, Eva Fenyvesi Ph.D. from CycloLab and doc. RNDr. Jindrich Jindrich, CSc. from Charles University in Prague because they trusted in me and through my internships a fruitfull collaboration could start between these two institutions.

I express my gratitude to all the research partners, namely the research group of Prof. Antonio Vargas Berenguel from University of Almeria, the group of Prof. Salvatore Sortino from University of Catania, the group of Dr. Konstantina Yannakopoulou from NCSR Demokritos Institute, the group of Assoc. Prof. Szabolcs Beni from Semmelweis University, the group of Assoc. Prof. Marica B. Ericson from University of Gothenburg and the group of

Doc. RNDr. Zuzana Bosáková, CSc. from Charles University in Prague for their continous collaboration and for their creative ideas about the application of cyclodextrin derivatives synthesized during my studies.

I feel very grateful and also lucky for the friendships what I have made with my colleagues during the exploration of cyclodextrin chemistry. The precious company of Giovanna Cutrone, Lorenzo Angiolini, Marco Agnes and Andras Darcsi Ph.D. made the hard times more sufferable and the successes more joyfull.

The most special thanks goes to my family namely to my wife, Eva Benkovics for her support which helped me to accomplish this work and to my daughter, Anna Benkovics for each of her smile which helped me realize the most important things in Life.

8. References

1. Villiers, A. *Compt. Rend.* **1891**, *112*, 536-538.
2. Freudenberg, K.; Cramer, F.; Plieninger, H. Inclusion Compounds of Physiologically Active Organic Compounds. German Patent No. 895,769, **1953**.
3. Crini, G. *Chem. Rev.* **2014**, *114*, 10940-10975.
4. Szejtli, J. *Chem. Rev.* **1998**, *98*, 1743-1754.
5. Bom, A.; Bradley, M.; Cameron, M.; Clark, J.K.; van Egmond, J.; Feilden, H.; MacLean, E.; Muir, A.; Palin, R.; Rees, D.; Zhang, M. Q. *Angew. Chem. Int. Ed*. **2002,** *41*, 265-270.
6. Leclerq, L. *Beilstein J. Org. Chem.* **2016,** *12,* 2644-2662.
7. Liu, L.; Guo, Q-X. *J. Inclusion Phenom. Macrocyclic Chem.* **2002**, *42*, 1-14.
8. Connors, K. A. *Chem. Rev.* **1997**, *97*, 1325-1357.
9. Giordano, F.; Novak, C.; Moyano, J. R. *Thermochim. Acta* **2001**, *380*, 123-151.
10. Bilensoy, E.; Çırpanlı, Y.; Şen, M.; Doğan, A. L.; Çalış, S. *J. Inclusion Phenom. Macrocyclic Chem.* **2007**, *57*, 363-370.
11. Harada, A.; Li, J.; Kamachi, M. *Macromolecules* **1993**, *26*, 5698-5703.
12. De Vries, E. J. C.; Caira, R., M.; Bogdan, M.; Farcas, I. S.; Bogdan, D. *Supramol. Chem.* **2009**, 21, 358-366.
13. Benesi, H. A.; Hildebrand, J. H. *J. Am. Chem. Soc.* **1949**, *71*, 2703-2707.
14. Wachter, H. N.; Fried, V. *J. Chem. Educ.* **1974**, *51*, 798.
15. Fielding, L.. *Tetrahedron* **2000,** *56,* 6151-6170.
16. Schneider, H. J.; Hacket, F.; Rudiger, V.; Ikeda, H. *Chem. Rev.* **1998,** *98*, 1755-1786.
17. Höfler, T.; Wenz, G. *J. Inclusion Phenom. Mol. Recognit. Chem.* **1996**, *25*, 81-84.
18. Zheng, P. J.; Wang, C.; Hu, X.; Tam, K. C.; Li, L. *Macromolecules* **2005,** *38*, 2859-2864.
19. Wallingford, R.A.; Ewing, A.G. *Adv. Chromatogr.* **1989**, *29*, 1–76.
20. Rundlett, K. L.; Armstrong, D. W. *J. Chromatogr. A* **1996,** *721*, 173-186.
21. Kuhn, R.; Hoffstetter-Kuhn, S. *Chromatographia* **1992,** *34*, 505-512.
22. Chankvetadze, B. *Capillary Electrophoresis in Chiral Analysis,* Wiley, Chichester, **1997.**
23. Fanali, S. *J. Chromatogr. A* **2000,** *875*, 89-122.
24. Fejos, I.; Varga, E.; Benkovics, G.; Darcsi, A.; Malanga, M.; Fenyvesi, E.; Sohajda, T.; Szente, L.; Beni, S. *J. Chromatogr. A* **2016,** *1467,* 454-462.

25. Cai, H.; Nguyen, V. T.; Vigh, G. *Anal. Chem.*, 1998**,** *70,* 580-589.
26. Rezanka, P.; Rezankova, K.; Sedlackova, H.; Masek, J.; Rokosova, L.; Blahova, M.; Rezanka, M.; Jindrich, J.; Sykora, D.; Kral, V. *J. Sep. Sci.* **2016***, 39,* 980-985.
27. Khan, A, R.; Forgo, P.; Stine, J. K.; D'Souza, T. V. *Chem. Rev.* **1998**, *98*, 1977-1996
28. Gelb, R.I.; Schwartz, L.M.; Bradshaw, J.J.; Laufer, D.A. *Bioorg. Chem.* **1980,** *9,* 299-304
29. Cornwell, M.J.; Huff, J.B.; Bieniarz, C. *Tetrahedron Lett.* **1995,** *36*, 8371-8374.
30. Rezanka, M. *Eur. J. Org. Chem.* **2016**, 5322-5334.
31. Melton, L. D.; Slessor, K. N. *Carbohydr. Res.* **1971,** *18,* 29-37.
32. Matsui, Y.; Yokoi, T.; Mochida, K. *Chem. Lett.* **1976**, *5*, 1037-1040.
33. Petter, R. C; Salek, J. S.; Sikorski, C. T.; Kumaravel, G.; Fu-Tyan, L. *J. Am. Chem. Soc.* **1990,** 112, 3860-3868.
34. Fujita, K.; Yamamura, H.; Imoto, T.; Tabushi, I. *Chem. Lett.* **1988**, *17*, 543–546.
35. Jicsinszky, L.; Ivanyi, R. *Carbohydr. Polym.* **2001,** *45*, 139-145.
36. Ueno, A.; Moriwaki, F.; Osa, T.; Hamada, F.; Murai, K. *Tetrahedron* **1987**, *43*, 1571-1578.
37. Bednarova, E.; Hybelbauerova, S.; Jindrich J. *Beilstein J. Org. Chem.* **2016**, *12,* 349-352.
38. Fikes, L. E.; Winn, D. T.; Sweger, R. W.; Johnson, M. P.; Czarnik, A. W. *J. Am. Chem. Soc.* **1992**, *114*, 1493-1495.
39. Popr, M.; Hybelbauerova, S.; Jindrich J. *Beilstein J. Org. Chem.* **2014**, *10,* 1390-1396.
40. Martin, K. A., Czarnik, A.W. *Tetrahedron Lett.* **1994**, *35,* 6781-6782.
41. Yoon, J.; Hong, S.; Martin, K. A.; Czarnik, A. W. *J. Org. Chem.* **1995**, *60*, 2792-2795.
42. Rezanka, M.; Jindrich, J. *Carbohydr. Res*. **2012,** *346*, 2374-2379.
43. Benkovics, G. ; Hodek, O. ; Havlikova, M.; Bosakova, Z.; Coufal, P.; Malanga, M.; Fenyvesi, E.; Darcsi, A.; Beni, S.; Jindrich, J. *Beilstein J. Org. Chem.* **2016**, *12*, 97-109.
44. Tomimasu, N.; Kanaya, A.; Takashima, Y.; Hiroyasu, Y.; Harada, A. *J. Am. Chem. Soc.* **2009**, *131*, 12339-12343.
45. Ueno, A.; Breslow, R. *Tetrahedron Lett*. **1982**, *23*, 3451-3454.
46. Cho, E.; Yun, D.; Jeong, D.; Im, J.; Kim, H. Dindulkar, D. S.; Choi, Y.; Jung, S. *Sci. Rep.* **2016**, *6*, 23740 -23750.
47. Jindrich, J.; Tislerova, I. *J. Org. Chem.* **2005,** *70*, 9054-9055.
48. Masurier, N.; Lafont, O.; Le Provost, R.; Lesur, D.; Masson, P.; Djedaıni-Pilard, F.; Estour, F. *Chem. Commun.,* **2009,** 589-591.
49. Sato, T.; Nakamura, H.; Ohno, Y.; Endo, T. *Carbohydr. Res.*, **1990,** *199,* 31-35.
50. Rong, D., D'Souza, V. T., *Tetrahedron Lett.* **1990**, *31*, 4275-4278.
51. Takeo, K., Mitoh, H., Uemura, K. *Carbohydr. Res.* **1989,** *187***,** 203-221.
52. Fügedi, P. *Carbohydr. Res.* **1989**, *192*, 366-369.
53. Aime, S.; Gianolio, E.; Arena, F.; Barge, A.; Martina, K.; Heropoulos, G.; Cravotto, G. *Org. Biomol. Chem.* **2009**, *7*, 370-379.
54. Aime, S.; Gianolio, E.; Robaldo, B.; Barge, A.; Cravotto, G. *Org. Biomol. Chem.* **2006**, *4*, 1124-1130.
55. Tarver, G. J.; Grove, S. J. A.; Buchanan, K.; Bom, A.; Cooke, A.; Rutherford, S. J.; Zhang, M.-Q. *Bioorg. Med. Chem.* **2002**, *10*, 1819-1827.
56. Hanessian, S. Benalil, A.; Laferriere, C. *J. Org. Chem.* **1995**, *60*, 4786-4797.

57. Ward, S.; Calderon, O.; Zhang, P.; Sobchuk, M.; Keller, S. N.; Williams, V. E.; Ling, C.-C. *J. Mat. Chem. C.* **2014**, *2*, 4928-4936.
58. Xia, L.; Lowary, T. L. *J. Org. Chem.* **2013**, *78*, 2863-2880.
59. O'Mahony, A. M.; Ogier, J.; Desgranges, S.; Cryan, J. F.; Darcy, R.; O'Driscoll, C. M. *Org. Biomol. Chem.* **2012**, *10*, 4954-4960.
60. Fulton, D. A.; Stoddart, J. F. *J. Org. Chem.* **2001**, *66*, 8309-8319.
61. Toomari, Y.; Namazi, H.; Entezami, A. A. *Int. J. Biol. Macromoecules* **2015**, *79*, 883-893.
62. Xie, H.; Li, H., Lai, X.; Wu, W.; Zeng, X. *Mater. Lett.* **2015**, *151*, 72-74.
63. Meppen, M.; Wang, Y.; Cheon, H.-W.; Kishi, Y. *J. Org. Chem.* **2007**, *72*, 1941-1950.
64. Badi, N.; Jarroux, N.; Guegan, P. *Tetrahedron Lett.* **2006**, *47*, 8925-8927.
65. Vigh, G. Chiral resolving agents for enantioseparations. US Patent 6,391,862 B1, May 21, **2002.**
66. Kraus, T., Budesinsky, M., Zavada, J. *Carbohydr. Res.* **1997,** *304,* 81-84.
67. Benkovics, G.; Fejos, I.; Darcsi, A.; Varga, E.; Malanga, M.; Fenyvesi, E.; Sohajda, T.; Szente, L.; Beni, S.; Szeman, J. *J. Chromatogr. A* **2016**, *1467*, 445-453.
68. Agnes, M.; Thanassoulas, A.; Stavropoulos, P.; Nounesis, G.; Miliotis, G.; Miriagou, V.; Benkovics, G.; Malanga, M.; Yannakopoulou, K. *Int. J. Pharm.* **2017,** *531,* 480-491.
69. Ashton, P. R.; Koniger, R.; Stoddart, J. F.; Alker, D.; Harding, V. D. *J. Org. Chem.* **1996**, *61*, 903-908.
70. Haynes, I. I. I. J. L., Shamsi, S. A., O'Keefe, F.,Darcey, R., Warner, I. M., *J. Chromatogr. A* **1998**, *803*, 261-271.
71. Baer, H. H.; Berenguel, A. V.; Shu, Y. Y. *Carbohydr. Res*. **1992**, *228*, 307-314.
72. Ashton, P. R.; Ellwood, P.; Staton, I.; Stoddart, J. F. *J. Org. Chem*. **1991**, *56*, 7274-7280.
73. Brunsveld, L.; Folmer, B. J. B.; Meijer, E. W.; Sijbesma, R. P. *Chem. Rev.* **2001**, *101*, 4071-4097.
74. Bosman, A. W.; Sijbesma, R. P.; Meijer, E. W. *Mater. Today* **2014**, *7*, 34-39.
75. Wenz, G.; Han, B.-H.; Müller, A. *Chem. Rev.* **2006**, *106*, 782-817.
76. Harada, A.; Takashima, Y.; Yamaguchi, H. *Chem. Soc. Rev.* **2009**, *38*, 875-882.
77. Tran, N. D.; Colesnic, D.; Adam de Beaumais, S.; Pembouong, G.; Portier, F.; Queijo, A. A.; Tato, J. V.; Zhang, Y.; Menand, M.; Bouteiller, L.; Sollogoub. M. *Org. Chem. Front.* **2014**, *1*, 703-706.
78. Miyauchi, M.; Kawaguchi, Y.; Harada, A. *J. Inclusion Phenom. Macrocyclic Chem.* **2004**, *50*, 57-62.
79. Gonzalez, M. C.; McIntosh, A. R.; Bolton, J. R.; Weedon, A. C. *J. Chem. Soc., Chem. Commun.* **1984,** 1138-1140.
80. Ueno, A.; Suzuki, I.; Osa, T. *J. Chem. Soc., Chem. Commun.* **1988,** *20,* 1373-1374.
81. Fraix, A.; Goncalves, A. R.; Cardile, V.; Graziano, A. C. E.; Theodossiou, T. A.; Yannakopoulou K.; Sortino, S. *Chem. – Asian J.* **2013,** *8*, 2634-2641.
82. Suzuki, I.; Ueno, A.; Osa, T. *Chem. Lett.* **1989,** *18,* 2013-2016.
83. Wang, Y.; Ikeda, T.; Ueno, A.; Toda, F., *Chem. Lett.* **1992,** *21,* 863-866.
84. Wang, Y.; Ikeda, T.; Ikeda, H.; Ueno, A.; Toda, F. *Bull. Chem. Soc. Jpn.* **1994,** *67,* 1598-1607.
85. Chen, X.; Pradhan, T.; Wang, F.; Kim, J. S.; Yoon, J. *Chem. Rev.* **2012,** *112,* 1910-1956.
86. Zheng, H.; Zhan, X.-Q.; Bian, Q.-N.; Zhang, X.-J. *Chem. Commun.* **2013,** *49,* 429-447.

87. Kushida, Y.; Nagano, T.; Hanaoka, K. *Analyst,* **2015,** *140,* 685-695.
88. Seebach, D.; Namoto, K.; Mahajan, Y. R; Bindschadler, P.; Sustmann, R; Kirsch, M.; Ryder, N. S; Weiss, M.; Sauer, M.; Roth, Ch.; Werner, S.; Beer, H.-D.; Munding, C.; Walde, P.; Voser, M. *Chemistry & biodiversity* **2004,** *1,* 65-97.
89. Oplatowska, M.; Elliott, C. T. *Analyst* **2011**, *136*, 2403-2410.
90. Hettegger, H.; Gorfer, M.; Sortino, S.; Fraix, A.; Bandian, D.; Rohrer, C.; Harreither, W.; Potthast, A.; Rosenau, T. *Cellulose,* **2015,** *22,* 3291-3304.
91. Johnson, G., A.; Ellis, E., A.; Kim, H.; Muthukrishnan, N.; Snavely, T.; Pellois, J.-P. *PLOS ONE,* **2014,** *9,* e91220, 1-14.
92. Wang, Y.; Ikeda, T.; Ueno, A.; Toda, F. *Tetrahedron Lett.* **1993,** *34,* 4971-4974.
93. Kitagawa, M.; Hoshi, H.; Sakurai, M.; Inoue, Y.; Chujo, R. *Bull. Chem. Soc. Jpn.* **1988,** *61,* 4225-4229.
94. Hamada, F.; Ishikawa, K.; Higuchi, Y.; Akagami, Y.; Ueno, A. *J. Inclusion. Phenom. Mol. Recognit. Chem.* **1996,** *25*, 283-294.
95. Nishimura, D.; Takashima, Y.; Aoki, H.; Takahashi, T.; Yamaguchi, H.; Ito, S.; Harada, A. *Angew. Chem. Int. Ed.* **2008,** *47,* 6077-6079.
96. Hasegawa, T.; Kondo, Y.; Koizumi, Y.; Sugiyama, T.; Takeda, A.; Ito, S.; Hamada, F. *Bioorg. Med. Chem.* **2009,** *17*, 6015-6019.
97. Nguyen, T.; Francis, B. M. *Org. Lett.* **2003,** *5,* 3245-3248.
98. Srinivasachari, S.; Fichter, M. K.; Reineke, M. T. *J. Am. Chem. Soc.* **2008,** *130*, 4618-4627.
99. Mourtzis, N.; Paravatou, M.; Mavridis, I. M.; Roberts, M. L.; Yannakopoulou, K. *Chem. Eur. J.* **2008,** *14,* 4188-4200.
100. Wenz, G.; Krauter, I.; Sackmann, E. *J. Polym. Sci. A Polym. Chem.* **2009,** *47,* 6223-6230.
101. Kandoth, N.; Malanga, M.; Fraix, A.; Jicsinszky, L.; Fenyvesi, E.; Parisi, T.; Colao, I.; Sciortino, M. T.; Sortino, S. *Chem - Asian J.* **2012,** *7*, 2888-2894.
102. Malanga, M.; Jicsinszky, L.; Fenyvesi, E. *J. Drug Del. Sci. Tech.* **2012,** *22*, 260-265.
103. Agostoni, V.; Horcajada, P.; Noiray, M.; Malanga, M.; Aykaç, A.; Jicsinszky, L.; Vargas-Berenguel, A.; Semiramoth, N.; Daoud-Mahammed, S.; Nicolas, V.; Martineau, C.; Taulelle, F.; Vigneron, J.; Etcheberry, A.; Serre, C.; Gref, R.. *Sci. Rep.* **2015,** *5*, 7925-7932.
104. Fenyvesi, E.; Jicsinszky, L. *Land Contam. Reclam.* **2009,** *17*, 405-412.
105. Malanga, M.; Balint, M.; Puskas, I.; Tuza, K.; Sohajda, T.; Jicsinszky, L.; Szente L.; Fenyvesi, E. *Beilstein J. Org. Chem.* **2014,** *10,* 3007-3018.
106. Malanga, M.; Darcsi, A.; Balint, M.; Benkovics, G.; Beni, S.; Sohajda, T. *Beilstein J. Org. Chem.* **2016,** *12,* 537-548.
107. Benkovics, G.; Alfonso, D.; Darcsi, A.; Beni, S.; Fenyvesi, E.; Szente, L.; Malanga, M.; Sortino, S. *Beilstein J. Org. Chem.* **2017,** *13*, 543-551.
108. Loftsson, T.; Jarho, P.; Masson, M.; Jarvinen, T. *Expert Opin. Drug Deliv.* **2005**, *2,* 335-351.
109. Ren, B.; Gao, H.; Cao, Y.; Jia, L. *J. Hazard. Mater.* **2015,** *285,* 148-156.
110. Kilsdonk, E. P. C.; Yancey, P. G.; Stoudt, G. W.; Bangerter, F. W.; Johnson, W. J.; Philips, M. C.; Rothblat, G. H. *J. Biol. Chem.* **1995,** *270,* 17250-17256.
111. Diaz-Moscoso, A.; Vercauteren, D.; Rejman, J.; Benito, J. M.; Mellet, C. O.; De Smedt, S. C.; García Fernández, J. M. *J. Controlled Release.* **2010,** *146*, 318-325.

112. Plazzo, A. P.; Hofera, C. T.; Jicsinszky, L.; Fenyvesi, E.; Szente, L.; Schiller, J.; Herrmann, A.; Muller, P. *Chem. Phys. Lipids.* **2012***, 165*, 505-511.
113. Fenyvesi, F.; Reti-Nagy, K.; Bacso, Z.; Gutay-Toth, Z.; Malanga, M.; Fenyvesi, E.; Szente, L.; Varadi, J.; Bacskay, I.; Ujhelyi, Z.; Feher, P.; Szabo, G.; Vecsernyes, M. *PLoS ONE.* **2014**, *9*, e84856.
114. Reti-Nagy, K.; Malanga M.; Fenyvesi, E.; Szente, L.; Vamosi, Gy.; Varadi, J.; Bacskay, I.; Feher, P.; Ujhelyi, Z.; Roka, E.; Vecsernyes, M.; Balogh, Gy.; Vasvari, G.; Fenyvesi, F. *Int. J. Pharm.* **2015**, *496*, 509-517.
115. Loftsson, T.; Douchene, D. *Int. J. Pharm.* **2007,** *329*, 1-11.
116. Davis, M. E.; Brewster, M. E. *Nat. Rev. Drug Discov.* **2004,** *3,* 1023-1035.
117. Mazzaglia, A.; Sciortino, M. T.; Kandoth, N.; Sortino, S. *J. Drug Del. Sci. Tec.* **2012,** *22,* 235-242.
118. Bortolus, P.; Monti, S. *Adv. Photochem.* **1996,** *21,* 1-133.
119. Monti, S.; Sortino, S. *Chem. Soc. Rev.* **2002,** *31,* 287-300.
120. Mazzaglia, A.; Micali Monsù, L.; Scolaro L. *Cyclodextrin Materials Photochemistry. Photophysics and Photobiology,* **2006,** Elsevier, pp. 203-222. and ref therein.
121. Yannakopoulou, K.; Jicsinszky, L.; Aggelidou, C.; Mourtzis, N.; Robinson, T. M.; Yohannes, A.; Nestorovich, E. M.; Bezrukov, S.; Karginov, V. A. *Antimicrob. Agents Chemother.* **2011,** *55*, 3594-3597.
122. Castano, A. P.; Mroz, P.; Hamblin, M. R. *Nat. Rev. Cancer* **2006**, *6*, 535-545.
123. Celli, J. P.; Spring, B. Q.; Rizvi, I.; Evans, C. L.; Samkoe, K. S.; Verma, S.; Pogue, B. W.; Hasan, T. *Chem. Rev*. **2010**, *12*, 2795-2838.
124. Hasan, T.; Moor, A. C. E.; Ortel, B. *Cancer Medicine*, 5th ed.; Decker BC, Inc.: Hamilton, Ontario, Canada, **2000.**
125. Kralova, J.; Kejik, Z.; Briza, T.; Pouckova, P.; Kral, A.; Martasek, P.; Kral, V. *J. Med. Chem.* **2010,** *53,* 128-138.
126. Lourenço, L. M. O.; Pereira, P. M. R.; Maciel, E.; Valega, M; Fernando M. J; Domingues, F. M. J.; Domingues, M. R. M.; Neves, M. G. P. M. S.; Cavaleiro, J. A. S.; Fernandes, R.; Tome, J. P. C. *Chem. Commun.* **2014,** *50,* 8363-8366.
127. Benkovics, G.; Alfonso, D.; Darcsi, A.; Beni S.; Fenyvesi, E.; Szente, L.; Malanga, M.; Sortino, S. *Beilstein J. Org. Chem.* **2017**, *13*, 543-551.
128. Kralova, J.; Synytsya, A.; Pouckova, P.; Koc, M.; Dvorak, M.; Kral, V. *Photochem. Photobiol.* **2006,** *82*, 432-438.
129. Rezanka, P.; Navratilova, K.; Rezanka, M.; Kral, V.; Sykora, D. *Electrophoresis* **2014,** *35*, 2701-2721.
130. Escuder-Gilaberta, L.; Martín-Bioscaa, Y.; Medina-Hernándeza, M.J.; Sagrado, S. *J. Chromatogr. A* **2014,** *29*, 2-23.
131. Kalikova, K; Riesova, M; Tesarova, E. *Cent. Eur. J. Chem*. **2012,** *10*, 450-471.
132. Chankvetadze, B. The application of cyclodextrins for enantioseparations. In: Cyclodextrins and Their Complexes, Edited by: Dodziuk, H. Wiley-VCH Verlag GmbH & Co. KGaA: Weinheim, Germany. **2008**, 119-146.
133. Vincent, J. B.; Sokolowski, A. D.; Nguyen, T. V.; Vigh, G. *Anal. Chem.* **1997A,** *69***,** 4226-4233.
134. Vincent, J. B.; Kirby, D. M.; Nguyen, T. V.; Vigh, G. *Anal. Chem.* **1997B,** *69,* 4419-4428.
135. Busby, M. B.; Vigh, G. *Electrophoresis* **2005,** *26,* 1978-1987.
136. Tutu, E.; Vigh, G. *Electrophoresis* **2011,** *32,* 2655-2662.

137. Mavridis, I. M.; Yannakopoulou, K. *Int. J. Pharm.* **2015,** *492,* 275-290.
138. Cucinotta, V.; Contino, A.; Giuffrida, A.; Maccarrone, G.; Messina, M. *J. Chromatogr. A* **2010,** *1217,* 953-967.
139. Williams, B. A.; Vígh, G. *J. Chromatogr. A* **1997,** *777,* 295-309.
140. Wren, S. A. C.; Rowe, R. C. *J. Chromatogr. A* **1992,** *603***,** 235-241.
141. Schmitt, T.; Engelhardt, H. *Chromatographia* **1993,** *37*, 475-481.
142. Akerfeldt, S. K.; DeGrado, F. W. *Tetrahedron Lett.* **1994,** *35,* 4489-4492.
143. Culha M.; Schell, F. M.; Fox, S.; Green, T.; Betts, T.; Sepaniak, M. J., *Carbohydr. Res.* **2004,** *339*, 241-249.
144. Idriss, H.; Estour, F.; Zgani, I.; Barbot, C.; Biscotti, A.; Petit, S.; Galaup, C.; Hubert-Roux, M.; Nicol, L.; Mulderd, P.; Gouhier, G., *RSC Advances*, **2013**, *3,* 4531-4534.
145. Sohajda, T.; Fabian, A.; Tuza, K.; Malanga, M.; Benkovics, G.; Fulesdi, B.; Tassonyi, E.; Szente, L. *Int. J. Pharm.* **2017,** *531,* 512-520.

146. Eliadou, K.; Giastas, P.; Yannakopoulou, K.; Mavridis, M. I. *J. Org. Chem.* **2003,** *68*, 8550-8557.
147. Avram, L.; Cohen, Y. *J. Org. Chem.* **2002**, *67*, 2639-2644.
148. Kaminski Z. J., *Tetrahedron Lett.* **1985**, *26*, 2901-2904.
149. Ramette, R. W.;Sandell, E. B.,*J. Am. Chem. Soc.*, **1956**, *78*, 4872-4878.
150. Bakkialakshmi S.; Menaka, T., *International Journal of ChemTech Research*, **2012**, *4*, 223-231.
151. Jacobsen, N. E; *NMR Hardware and Software, Sample Preparation.* In: NMR Spectroscopy Explained, John Wiley & Sons, Inc., Publication, **2007**.
152. Wang, X.; Song, M.; Long, Y. *J. Solid State Chem.* **2001,** *156,* 325-330.
153. Zhao, Y.; Yang, Y. C.; Shi, H.; Zhu, H. Y.; Huang, R.; Chi, C. M.; Zhao, Y. *Helv. Chim. Acta* **2010,** *93,* 1136-1148.
154. Thorpe, J. F. Thorpe's Dictionary of Applied Chemistry', Vol. IV (edited by J. F. Thorpe, J. F., Whiteby, M. A.), Longmans Green, London **1982**, 316.
155. Gattermann, L. Laboratory Methods of Organic Chemistry (edited by Wieland, H.), Macmillan, London , **1952,** 326.
156. Vasudevan, D.; Anantharaman, P. N. *J.Appl.Electrochem.* **1993** 23, 808-812.
157. Korsunovski, G. A.; Sidorov, A, N. *Zh. Fiz. Khim.* **1968**, 42, 286-289.
158. Mchedlov-Petrosyan, N. O.; Fedorov, L. A.; Sokolovskii, S. A.; Surov, Y. N.; Salinas Maiorga, R., *Bull. Russ. Acad. Sci., Division of chemical science*, **1992**, *41*, 3, 403-409.
159. Bogdanova, L. N.; Mchedlov-Petrossyan, N. O.; Vodolazkaya, N. A.; Lebed, A. V., *Carbohyd. Res.*, **2010**, *345*, 1882-1890.
160. Penzkofer, A.; Beidan, A.; Daiber, M. *J. Lumin.*, **1992**, *51*, 297-314.
161. Wilkinson, F.; Helman, W. P.; Ross, A. B. *J. Phys. Chem. Ref. Data,* **1993**, *22*, 113-262.
162. Redmond, W. R.; Gamlin, N. J. *Photochem. Photobiol.* **1999**, *70*, 391-475.
163. Casas-Solvas, J. M.; Malanga, M.; Vargas-Berenguel, A. *Synthesis of heptakis(6-O-tert-butyldimethylsilyl) Cyclomaltoheptaose,* in Carbohydrate Chemistry: Proven Synthetic Methods, Volume 4, Chapter 26. **2017**
164. Zhang, W.; Robins, M.J. *Tetrahedron Lett.* **1992,** *33*, 1177-1180.
165. Spencer, C. M.; Stoddart, J. F.; Zarzycki, R. *J. ChemSoc. Perkin Trans*. **1987,** *2*, 1323-1336.

166. Makedonopoulou, S.; Yannakopoulou, K.; Mentzafos, D.; Lamzin, V.; Popov, A.; Mavridis, I. M. *Acta Crystallogr. B* **2001,** *57*, 399-409.
167. Szeman, J.; Csabai, K.; Kekesi, K.; Szente, L.; Varga, G. *J. Chromatogr. A* **2006,** *1116,* 76-82.
168. Elbashir, A.A.; Saad, B.; Ali, A.S.M.; Saleh, M.I.; Aboul-Enein, H.Y. *J. Liq. Chromatogr. Related Technol.* **2008,** *31*, 348-360.
169. Li, W.; Liu, C.; Tan, G.; Zhang, X.; Zhu, Z.; Chai, Y. *Int. J. Mol. Sci.* **2012,** *13*, 710-725.
170. Lim, H.K.; Linh, P.T.; Hong, C.H.; Kim, K.H.; Kang, J.S. *J. Chromatogr. B: Biomedical Sciences and Applications.* **2001,** *755*, 259-264.
171. Van Eeckhaut, A.; Detaevernier, M.R.; Michotte, Y. *J. Pharm. Biomed. Anal.* **2004,** *36*, 799-805.
172. Sabah, S.; Scriba, G.K.E. *J. Chromatogr. A.* **1999,** *833*, 261-266.
173. Fejos, I.; Kazsoki, A.; Sohajda, T.; Marvanyos, E.; Volk, B.; Szente, L.; Beni, S. *J. Chromatogr. A.* **2014,** *1363*, 348-355.
174. Fejos, I.; He, Y.; Volgyi, G.; Kazsoki, A.; Sun, J.; Chen, W.; Beni, S. *J. Pharm. Biomed. Anal.* **2014,** *88***,** 594-601.
175. Modi, N.B.; Dresser, M.J.; Simon, M.; Lin, D.; Desai, D.; Gupta, S. *J. Clin. Pharmacol.* **2006,** *46,* 301-309.
176. Neumajer, G.; Sohajda, T.; Darcsi, A.; Toth, G.; Szente, L.; Noszal, B.; Beni, Sz. *J. Pharm. Biomed. Anal.* **2012,** *62*, 42-47.
177. Busby, M.B., Lim, P., Vigh, G., *Electrophoresis.* **2003,** *24*, 351-362.

9. List of author's publications

1. Havlíková, M.; Bosakova, Z.; Benkovics, G.; Jindrich, J.; Popr, M.; Coufal, P.: Use of 6-O-mono-substituted derivatives of β-cyclodextrin-bearing substituent with two permanent positive charges in capillary electrophoresis

Chem. Pap. **2016**, *70* (9), 1144–1154.

Journal impact factor (2016): 1.33.

2. Benkovics, G.; Hodek, O; Havlikova, M.; Bosakova, Z.; Coufal, P; Malanga, M; Fenyvesi, E; Darcsi, A; Beni, S; Jindrich, J.: Supramolecular structures based on regioisomers of cinnamyl-alpha-cyclodextrins

Beilstein J. Org. Chem. **2016,** *12*, 97-109.

Journal impact factor (2016): 2.70.

3. Malanga, M.; Darcsi, A; Balint, M; Benkovics, G; Sohajda, T; Beni; S.: New synthetic strategies for xanthene-dye-appended cyclodextrins
Beilstein J. Org. Chem. **2016,** *12*, 537-548.
Journal impact factor (2016): 2.70.

4. Benkovics, G.; Fejos, I.; Darcsi, A.; Varga, E.; Malanga, M.; Fenyvesi, E.; Sohajda, T.; Szente, L.; Beni, S.; Szeman, J.: Single-isomer carboxymethyl-γ-cyclodextrin as chiral resolving agent for capillary electrophoresis
J. Chromatogr. A **2016,** *1467,* 445-453.
Journal impact factor (2016): 4.03

5. Fejos, I.; Varga, E.; Benkovics, G.; Darcsi, A.; Malanga, M.; Fenyvesi, E.; Sohajda, T.; Szente, L.; Beni, S.: Comparative evaluation of the chiral recognition potential of single-isomer sulfated beta-cyclodextrin synthesis intermediates in non-aqueous capillary electrophoresis
J. Chromatogr. A **2016,** *1467,* 454-462.
Journal impact factor (2016): 4.03

6. Benkovics, G.; Afonso, D.; Darcsi, A.; Beni S.; Fenyvesi, E.; Szente, L.; Malanga, M.; Sortino, S.: Novel β-CD-eosin conjugates
Beilstein J. Org. Chem. **2017,** *13*, 543-551.
Journal impact factor (2016): 2.70.

7. Fejos, I.; Varga, E.; Benkovics, G.; Characterization of a single-isomer carboxymethyl-beta-cyclodextrin in chiral capillary electrophoresis
Electrophoresis **2017,** *38,* 1869-1877.
Journal impact factor (2016): 2.48.

8. Sohajda, T.; Fabian, A.; Tuza, K.; Malanga, M.; Benkovics, G.; Fulesdi, B.; Tassonyi, E.; Szente, L.: Design and evaluation of artificial receptors for the reversal of neuromuscular block
Int. J. Pharm. **2017,** *531,* 512-520.
Journal impact factor (2016): 3.99.

9. Benkovics, G.; Malanga, M. Fenyvesi, E.; The 'Visualized' macrocycles: Chemistry and application of fluorophore tagged cyclodextrins
Int. J. Pharm. **2017,** *531,* 689-700.
Journal impact factor (2016): 3.99.

10. Agnes, M.; Thanassoulas, A.; Stavropoulos, P.; Nounesis, G.; Miliotis, G.; Miriagou, V.; Benkovics, G.; Malanga, M.; Yannakopoulou, K.:
Designed positively charged cyclodextrin hosts with enhanced binding of penicillins as carriers for the delivery of antibiotics: the case of oxacillin
Int. J. Pharm. **2017,** *531(2),* 480-491.
Journal impact factor (2016): 3.99.

11. Benkovics, G.; Perez-Lloret, M.; Afonso, D.; Darcsi, A.; Béni, S.; Fenyvesi, E.; Malanga, M.; Sortino, S.:
A multifunctional β-cyclodextrin-conjugate photodelivering nitric oxide with fluorescence reporting
Int. J. Pharm. **2017,** *531(2)*, 614-620.
Journal impact factor (2016): 3.99.

12. Thomsen, H.; Benkovics, G.; Fenyvesi, É.; Farewell, A.; Malanga, M.; Ericson, B., M.: Delivery of cyclodextrin polymers to bacterial biofilms – an exploratory study using rhodamine labelled cyclodextrins and multiphoton microscopy
Int. J. Pharm. **2017,** *531(2)*, 650-657.
Journal impact factor (2016): 3.99.

13. Stjern, L.; Voittonen, S.; Weldemichel, R.; Thuresson, S.; Agnes, M.; Benkovics, G.; Fenyvesi, É.; Malanga, M.; Yannakopoulou, K.; Feiler, A.; Valetti, S.: Cyclodextrin-mesoporous silica particle composites for controlled antibiotic release. A proof of concept toward colon targeting
Int. J. Pharm. **2017,** *531 (2),* 595-605.
Journal impact factor (2016): 3.99.

14. Wankar, J.; Salzano, G.; Pancani, E.; Benkovics, G.; Malanga, M.; Manoli, F.; Gref, R.; Fenyvesi, E.; Manet, I.: Efficient loading of ethionamide in cyclodextrin-based carriers offers enhanced solubility and inhibition of drug crystallization
Int. J. Pharm. **2017,** *531(2),* 568-576.
Journal impact factor (2016): 3.99.

15. Malanga, M.; Fejos, I.; Varga, E.; Benkovics, G.; Darcsi, A.; Szeman, J.; Beni, S.: Synthesis, analytical characterization and the first capillary electrophoretic use of the single-isomer heptakis-6-O-sulfobutyl-ether-beta-cyclodextrin
J. Chromatogr. A **2017,** *1514,* 127-133.
Journal impact factor (2016): 4.03.

10. List of abbreviations

$^1O_2$ singlet oxygen
Ac acetyl
ACN acetonitrile
AdCOOK potassium adamantane-1-carboxylate
API active pharmaceutical ingredient
BGE background electrolyte
ByP by-product
CCE chiral capillary electrophoresis
CD cyclodextrin
CE capillary electrophoresis
Cin-*α*-CD monocinnamyl-*α*-CD
Cio cinnamoyl
CioOK Potassium-cinnamate
Cio-α-CD monocinnamoyl-α-CD
CM carboxymethyl
COSY correlation spectroscopy
DCC *N,N'*-dicyclohexylcarbodiimide
DEPT - distortionless enhanced polarization transfer
D_h hydrodynamic diameter
DCM dichloromethane
DLS dynamic light scattering
DMF *N,N*-dimethylformamide
DMM-OH 2-hydroxy-4,6-dimethoxy-1,3,5-triazine
DMSO dimethyl sulfoxide
DMT-MM 4-(4,6-dimethoxy-1,3,5-triazin-2-yl)-4-methyl morpholinium chloride
DNA deoxyribonucleic acid
DS degree of substitution
EDA ethylenediamine
EDC 1-ethyl-3-diaminopropyl-carbodiimide
ELSD evaporative light scattering detector
EoB eosin B
EoY eosin Y
EoB-β-CD mono(6-deoxy-6-eosinyl B-carboxamido)-β-cyclodextrin
EoY-β-CD mono(6-deoxy-6-eosinyl Y-carboxamido)-β-cyclodextrin
ESI-MS electrospray ionization mass spectrometry
Et ethyl
FITC fluorescein isothiocyanate
Flu fluorescein
Flu-β-CD mono(6-deoxy-6-fluoresceinyl-carboxamido)-β-cyclodextrin
HDMCM-β-CD heptakis(2,3-di-*O*-methyl-6-*O*-carboxymethyl)-β-cyclodextrin
HDM-β-CD heptakis(2,3-di-*O*-methyl)-β-cyclodextrin
HMBC heteronuclear multiple bond coherence
HOBt *N*-hydroxybenzotriazole

HPLC high performance liquid chromatography
HP-β-CD 2-hydroxypropyl-β-cyclodextrin
HSQC Heteronuclear single quantum correlation
IPA isopropyl alcohol
ITC isothermal titration calorimetry
K_{ass} association constant
Me methyl
N_3-β-CD mono(6-deoxy-6-azido)-β-cyclodextrin
NBS *N*-bromosuccinimide
NH_2-β-CD mono(6-deoxy-6-amino)-β-cyclodextrin
NMM *N*-methylmorpholine
NOE nuclear overhauser effect
NOESY nuclear overhauser effect spectroscopy
ODMCM-γ-CD octakis(2,3-di-*O*-methyl-6-*O*-carboxymethyl)-γ-cyclodextrin
ODM-γ-CD octakis(2,3-di-*O*-methyl)-γ-cyclodextrin
PDT photodynamic therapy
PS photosensitizer
RAMEB randomly methylated β-cyclodextrin
RBITC rhodamine B isothiocyanate
RI refractive index
R_s resolution factor
R_F retardation factor
R_t retention time
Rho Rhodamine B
Rho-β-CD mono(6-deoxy-6-spirolactam-rhodamine B)-β-CD
ROESY rotational nuclear overhauser effect spectroscopy
ROS reactive oxygen species
SBE-β-CD sulfobutylether-β-cyclodextrin
SID single-isomer cyclodextrin derivative
SP supramolecular polymer
TBAF tetra-*n*-butylammonium fluoride
TBDMSiCl *tert*-butyldimethylsilyl chloride
TBDMSi-β-CD heptakis(6-*O*-*tert*-butyldimethylsilyl)-β-cyclodextrin
TBDMSi-γ-CD octakis(6-*O*-*tert*-butyldimethylsilyl)-γ-cyclodextrin
TEPA tetraethylenepentaamine
TLC thin layer chromatography
TOCSY total correlated spectroscopy
Ts *p*-toluenesulfonyl
Ts-β-CD mono-6-*O*-tosyl-β-cyclodextrin